The Natural Ketolides Methymycin and Pikromycin: Binding Sites, Modes of Action, Mechanisms of Resistance

By
Mashal M. Almutairi
Bachelor Degree in Pharmaceutical Sciences
King Saud University, College of Pharmacy, 2006

DISSERTATION
Submitted as partial fulfillment of the requirements for the degree of Doctor of Philosophy in Pharmacognosy in the Graduate College of the University of Illinois at Chicago, 2015
Chicago, Illinois

Committee Members:
Dr. Alexander S. Mankin, Advisor and Chair
Dr. Michael J. Federle, Department of Microbiology and Immunology
Dr. Nancy Freitag, Department of Microbiology and Immunology
Dr. Brian T. Murphy
Dr. Taeok Bae, Indiana University

To my wonderful wife, Eman
For her companionship and encouragement

ACKNOWLEDGEMENTS

First of all, I am profoundly indebted to my supervisor, Dr. Alexander (Shura) Mankin, who was very generous with his time and knowledge and assisted me in each step to complete my Ph.D. journey. He directed and supported me to complete my tasks perfectly. He is not only an excellent researcher but also an amazing teacher. During the last couple of years, he inspired me at professional and personal levels. I am really fortunate to work with him.

I want to thank several members of the Mankin lab for all their insightful discussions and suggestions. Special thanks to Dr. Nora Vázquez-Laslop, for being available for both scientific and personal discussions. I am highly thankful to Dorota Klepacki for teaching me different techniques. I would like to thank Dr. Krishna Kanan for helping me during my preliminary examination and being such a wonderful friend. Last but not least, I am very grateful to the current lab members, Teresa Szal, Shanmugapriya Sothiselvam, James Marks, Sezen Meydan, Tanja Florin, Kollya Aleksashin, Maxim Svetlov, Tonu Margus and Amira kefi. Also I am grateful for the past lab members Dr. Bindiya Kaushal, Dr. Cedric Orelle, Dr. Pulkit Gupta, Dr. Jacqueline M. LaMarre, Dr. Haripriya Ramu and Anna Ochabowicz for their support and friendship and for making the Mankin lab a wonderful place to work.

I thank my committee members Professors Donald Morrison, Michael Federle, Brian Murphy, Taeok Bae and Nancy Freitag for their support and suggestions over the years.

Many thanks to Center for Pharmaceutical Biotechnology administrative staff

previous member Emily Lam and Yi Dong and for the current members Elizabeth Woods and Mary Ann Borjal for their help with all the administrative issues.

Last but not the least, I would like thank all my family and friends (both in US and in Saudi Arabia) for their love and support.

MM

TABLE OF CONTENTS

CHAPTER **PAGE**

TABLE OF CONTENTS (continued)

CHAPTER **PAGE**

LIST OF FIGURES

LIST OF FIGURES (continued)

LIST OF TABLES

LIST OF ABBREVIATIONS

PTC	Peptidyl transferase center
NPET	Nascent peptide exit tunnel
ORF	Open reading frame
uORF	Upstream open reading frame
rRNA	Ribosomal RNA
tRNA	Transfer RNA
mRNA	Messenger RNA
aa-tRNA	Aminoacyl-tRNA
EF	Elongation factor
RRF	Ribosome recycling factor
RF	Release factor
Erm	Erythromycin resistance methyltransferase
PCR	Polymerase chain reaction
LB	Luria-Bertani medium
BHI	Brain heart infusion medium
A600	Absorbance measured at 600 nano meter wavelength
MIC	Minimum inhibitory concentration
C3	Carbon 3
C5	Carbon 5
cDNA	Complementary deoxyribonucleic acid
ATP	Adenosine triphosphate

LIST OF ABBREVIATIONS (continued)

GTP	Guanosine triphosphate
dTTP	Deoxythymidine triphosphate
EDTA	Ethylenediaminetetraacetic acid
ERY	Erythromycin
TEL	Telithromycin
PKM	Pikromycin
MTM	Methymycin
SOL	Solithromycin
CET	Cethromycin
CHL	Chloramphenicol
PDB	Protein data bank
$m^2{}_6$A2058	Dimethylated A2058 at nitrogen 6
m_6A2058	Monomethylated A2058 at nitrogen 6
MLS_B	Macrolide, lincosamide and streptogramin B class of antibiotic
PKS	Polyketide synthase
RT	Reverse transcriptase
DMS	Dimethylsulfate
FIC	Fraction of inhibitory concentration
MDa	megadalton

SUMMARY

The term ‘antibiotics’, which literally means ‘against life’ is used to describe small molecules that are exploited to treat infectious diseases. Different antibiotics are continuously discovered in nature or created by man to solve the antibiotics resistance threats. However, the rate of resistance development by pathogenic bacteria has exceeded all means. The previously seemingly impossible scenario of entering a second pre-antibiotics era is nowadays becoming a reality. In order to resolve the problem, we need not only novel antibiotics but also the understanding of how bacteria become resistant.

When resistance to an antibiotic appears, the efforts are focused to redesign that drug to overcome such resistance. For example, ketolides have been developed to face the increasing resistance against the previous generations of macrolide antibiotics. However, the resistance problems could already exist in nature but are yet to be discovered. Fewer efforts focused on studying the resistance mechanisms in nature. Because the antibiotics-producing bacteria demand resistance mechanisms to avoid committing suicide by their potentially lethal antibiotics, naturally resistance mechanisms are believed to originate from these bacteria. These resistance mechanisms can find their way into pathogenic bacteria under selective pressures, which reflect the importance of studying the resistance genes in their natural niche. In the second chapter, we studied the natural resistance genes from the natural ketolides-producing *Streptomyces venezuelae* ATCC 15439. We discovered that this bacterium has two similar *erm* genes (erythromycin resistance methyltransferase); both Erms modified the same nucleotide, A2058 that resides within the macrolide-binding site in the ribosomal tunnel. However,

they differ by the degree of tunnel modification. The first one monomethylates the ribosomal tunnel, while the other one dimethylates the same nucleotide in the tunnel and further increases the resistance level. We further demonstrated that the monomethylase Erm is constitutively expressed to provide the ketolides-producer with a low level of resistance during the onset of ketolides production. However, the dimethylase Erm is inducible by the naturally produced ketolides to further increase the level of resistance. Our results not only showed how resistances are operated at the natural level, but also, we showed that these resistance mechanisms could find their way into a model of pathogenic bacteria where it makes the cells highly resistant to clinically used ketolide antibiotics. The increasing usage of ketolides is expected to select for these resistance mechanisms and ultimately may curb the clinical value of ketolides.

Bacteria that belong to *Streptomyces* genus are known for their ability to make antibiotics. *S. venezuelae* ATCC 15439 produces two natural ketolide antibiotics, methymycin (MTM) and pikromycin (PKM). All known bacterial ribosome-targeting macrolide antibiotics and their new derivatives, ketolides, bind to the same site within the ribosomal tunnel. Regardless of sharing the same site, ketolide antibiotics are considered the future of macrolides due to their inhibitory activity against not only susceptible strains but also many of macrolide-resistant bacteria. In addition, ketolides are bactericidal against some bacteria. In the third chapter, we studied the natural ketolide antibiotics, MTM and PKM, in regard of their binding site and mode of action. Our results demonstrated that modifications or mutations of ribosomal tunnel nucleotides

render the bacteria highly resistant to MTM and PKM. Furthermore, both MTM and PKM protect the same ribosomal tunnel nucleotides from chemical modifications, which support their binding to the macrolide-binding site. Surprisingly, mutation within peptidyl transferase center (PTC) makes the bacteria specifically resistant to MTM indicating an idiosyncratic binding mode of this antibiotic. The differential binding of MTM to the ribosomal tunnel and the difference in the structures of MTM and PKM results in inhibition of somewhat different spectra of proteins by these antibiotics. Combined with species-specific activity of MTM and PKM, these observations provide rationale for producing two similar but distinct ketolide antibiotics by *S. venezuelae*.

1. BACKGROUNDS AND SIGNIFICANCE

1.1 Bacterial ribosome structure and protein synthesis

Ribosomes are the protein-synthesizing machines in the cell. The bacterial ribosome is a 2.5 megadalton (MDa) macromolecular complex of which two-thirds is comprised of ribosomal RNA (rRNA) and one-third are ribosomal proteins. This complex is made of two subunits: the small 30S subunit and large 50S subunit (Fig. 1.1). The small subunit has the decoding center, which monitors the tRNA and mRNA interactions to ensure the fidelity of translation (1, 2). Three tRNA binding-sites are located at the interface between the two ribosomal subunits: the A-site where the incoming aminoacyl-tRNA (aa-tRNA) enters the ribosome, the P-site where the peptidyl-tRNA is located, and the E-site where the deacylated tRNA can leave the ribosome (3). The large subunit contains the functionally important peptidyl transferase center (PTC) that catalyzes the peptide bond formation (4-7). During active translation, the newly synthesized polypeptide has to snake away from the PTC through a channel in the 50S subunit, where it eventually emerges on the solvent side of 50S subunit. This channel is called the nascent peptide exist tunnel (NPET), which is about 100Å long and 10-20Å wide. The walls of the tunnel are primarily made up of rRNA nucleotides with the exception of L4 and L22 ribosomal protein extensions that create a constriction 30Å away from the PTC (8, 9). The NPET can accommodate up to 30-40 amino acids of an extended polypeptide chain and does not leave much room for the extensive folding of the nascent chain.

Protein synthesis is a process in which the genetic information on the mRNA is translated into a sequence of amino acids. The bacterial translation is comprised of four major steps: initiation, elongation, termination, and recycling (Fig. 1.2). In the initiation step, the small ribosomal subunit associates with mRNA and the initiator fMet-tRNA. During this step, the mRNA start codon, together with the fMet-RNA, accurately positions at the ribosomal P-site and

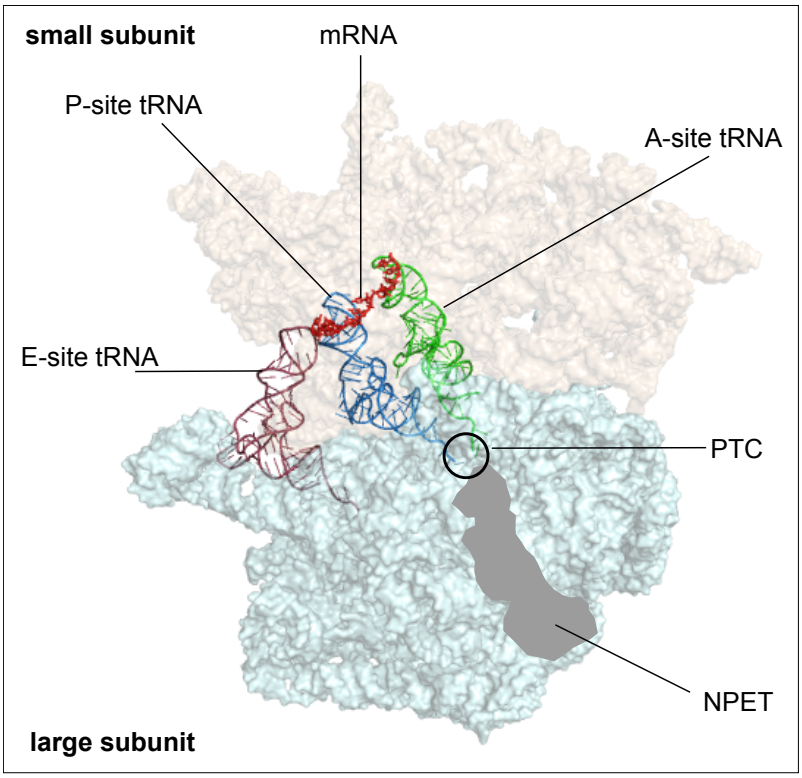

Figure 1.1: The bacterial ribosome. The structure of the ribosome bound by mRNA, aminoacyl-tRNA (A-site), peptidyl-tRNA (P-site), and deacylated-tRNA (E-site). The PTC and NPET are marked.

leads to formation of 30S initiation complex. This process is controlled with three initiation factors IF1, IF2, and IF3. Joining of the 50S subunit leads to formation of the 70S initiation complex, and now the ribosome is ready to enter elongation cycle. In each elongation cycle, elongation factor Tu (EF-Tu). GTP complex delivers an aminoacylated tRNA (aa-tRNA) to the A-site of the ribosome. After the correct identity of aminoacyl-tRNA is established, aminoacyl-tRNA is accommodated to the A-site. Next, the ribosome catalyzes the peptide bond formation by joining the C-terminal amino acid of the peptide that is esterified to the P-site bound tRNA and the aminoacyl moiety of the A-site bound tRNA. In the process of the new peptide bond formation, the growing peptide is transferred from the P-site bound peptidyl-tRNA to the A-site bound tRNA and is extended by one amino acid. In order to accommodate the next incoming aa-tRNA, the A- and P- site tRNAs are shifted to the P- and E-sites, respectively, and the mRNA is moved by one codon which is facilitated by EF-G in a process known as translocation. These cycles continue until the ribosome encounters the mRNA stop codon. Release factors (RFs) 1 or 2 recognize the stop codon, bind to the A site and hydrolyze the peptide-tRNA ester bond, releasing the newly made polypeptide chain from the ribosome. The ribosome is disassembled into individual 30S and 50S subunits with the help of ribosome-recycling factor (RRF) and EF-G to recycle them for another round of translation (10).

1.2 The ribosome as an important antibiotic target

Since the ribosome performs the essential protein synthesis function in the cell, it is not surprising that many classes of antibiotic target the bacterial ribosome. Despite the huge size of the ribosome relative to small molecule inhibitors, only a few sites are targeted by natural and semisynthetic antibiotics: primarily within the decoding center, PTC, and the NPET. Antibiotics can interfere with the ribosome function directly or indirectly by inhibiting activities of some

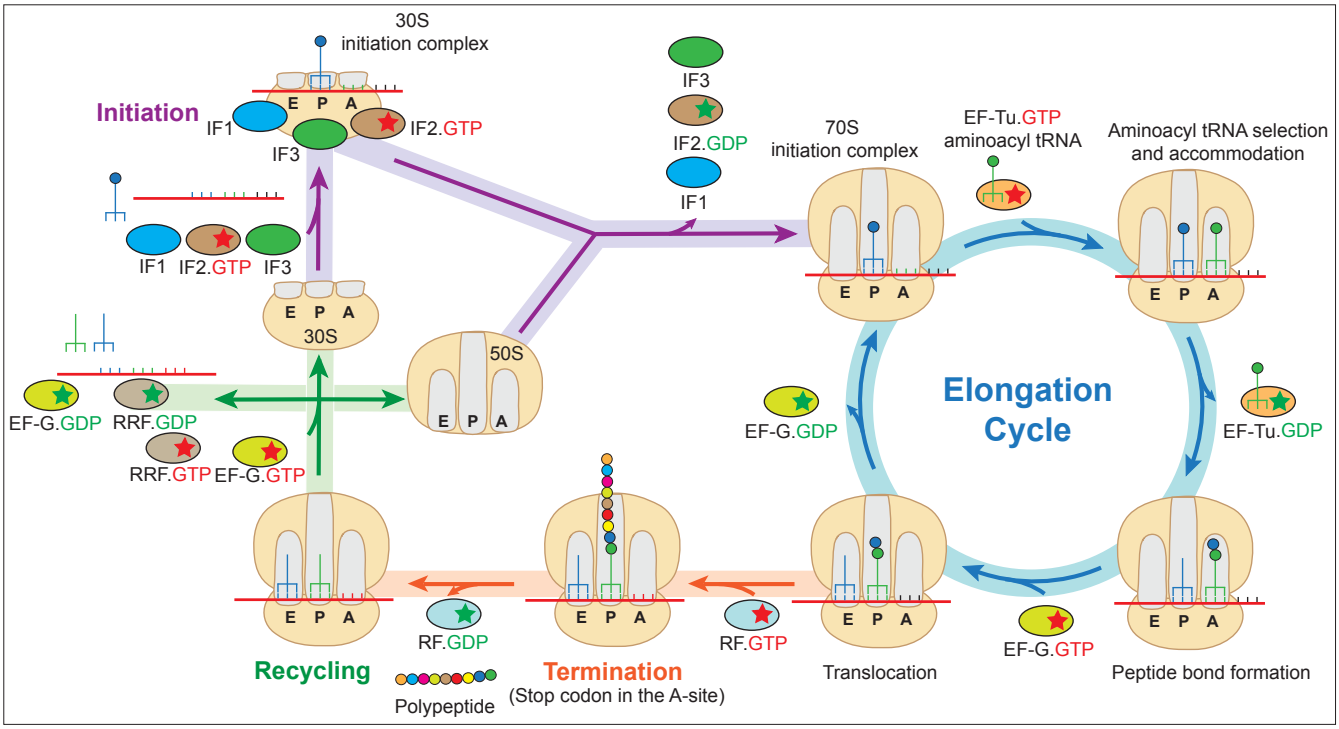

Figure 1.2: Overview of the bacterial translation (see the text for details).

proteins that involve in general protein synthesis (e.g. EF-G, aminoacyl synthetases, etc.) (11).

The ribosomal RNA is the main structural and functional component of the ribosome. Thus, antibiotics must interact with rRNA to interfere with the ribosome's functions. Since the rDNA is usually present in more than one copy in bacteria, it is hard for bacteria to develop target site mutation-based resistance to ribosome-targeted antibiotics by mutating one rDNA gene copy. Such a cell will remain antibiotic-sensitive, because the majority of the ribosomes are still wild type (12).

1.3 Macrolide antibiotics

Macrolides are considered as a very safe and effective class of antibiotics. They target the ribosomes of sensitive bacteria. They are effective against many Gram-positive and some Gram-negative bacteria. Macrolides are usually considered as bacteriostatic antibiotics that are used to treat infections of the upper and lower respiratory tract as well as skin and soft tissue. The first appearance of macrolides in the clinical setting was in 1950s with the launch of erythromycin (ERY) (13) (14). ERY is a natural antibiotic isolated from *Saccharopolyspora erythraea*. ERY is active against many Gram-positive pathogen such as *Staphylococcus aureus*, *Streptococcus pyogenes, Streptococcus pneumoniae*, and *Enterococcus species*; even against some Gram-negative pathogenic bacteria that include *Neisseria gonorrhoeae*, *Haemophilus influenzae* and *Bordetella pertussis.* ERY has been wildly used as an alternative to β-lactam therapy in allergic patients.

Poor oral bioavailability and some gastrointestinal (GI) side effects of ERY prompted development of the second generation of macrolides. This generation includes clarithromycin, roxithromycin, dirithromycin, and azithromycin. The drugs of the second generation circumvented many of the ERY limitations and are characterized by enhanced pharmacokinetics

and pharmacodynamic properties as well as reduction in the GI side effects. However, the emergence and the rapid spread of resistance against macrolide antibiotics of the first and second generations stimulated the search for better macrolides. Such efforts resulted in development of the more recent generation of macrolides called ketolides. Ketolides exhibited improved potency against many sensitive bacteria and some macrolide-resistant strains. Ketolides also possess bactericidal activity against some bacteria (15).

1.3.1 Structure of macrolide antibiotics

Macrolides that target the bacterial ribosome are characterized by the presence of the macrolactone ring that ranges in the size from 12 to 16 atoms. Clinically important macrolides are defined by the presence of a 14-, 15-, or 16-member macrolactone ring, which is decorated with several neutral and/or amino sugars and other side chains (Fig. 1.3 and 1.5A). ERY is comprised of a core 14-member macrolactone ring that carries two sugars, cladinose (neutral sugar) at C3 position, and desosamine (amino sugar) at C5 position (Fig. 1.3A). In the second generation of macrolides, ERY was used as starting material to produce the semisynthetic derivative clarithomycin by methylation of the 6-OH (Fig. 1.3A). The 15-member macrolactone ring of azithromycin is made by extension of the ERY macrolactone ring by an additional nitrogen atom (Fig. 1.3B) (16, 17). In the newer macrolide generation, ketolides generated from ERY in which the C3 cladinose sugar was replaced by a keto group and hence its name. Also, ketolides can have an 11,12 cyclic carbamate and an extended alkyl-aryl side chain, which can be attached to different positions of the macrolactone ring (Fig. 1.3C).

The 16-membered macrolides of clinical or veterinary value includes josamycin, tylosin, carbomycin A, and spiramycin. This group contains an extended disaccharide that is attached at the C5 position and often possesses other additional side chains at different positions of the macrolactone ring (Fig. 1.5A). In the case of carbomycin A and josamycin, the disaccharide at

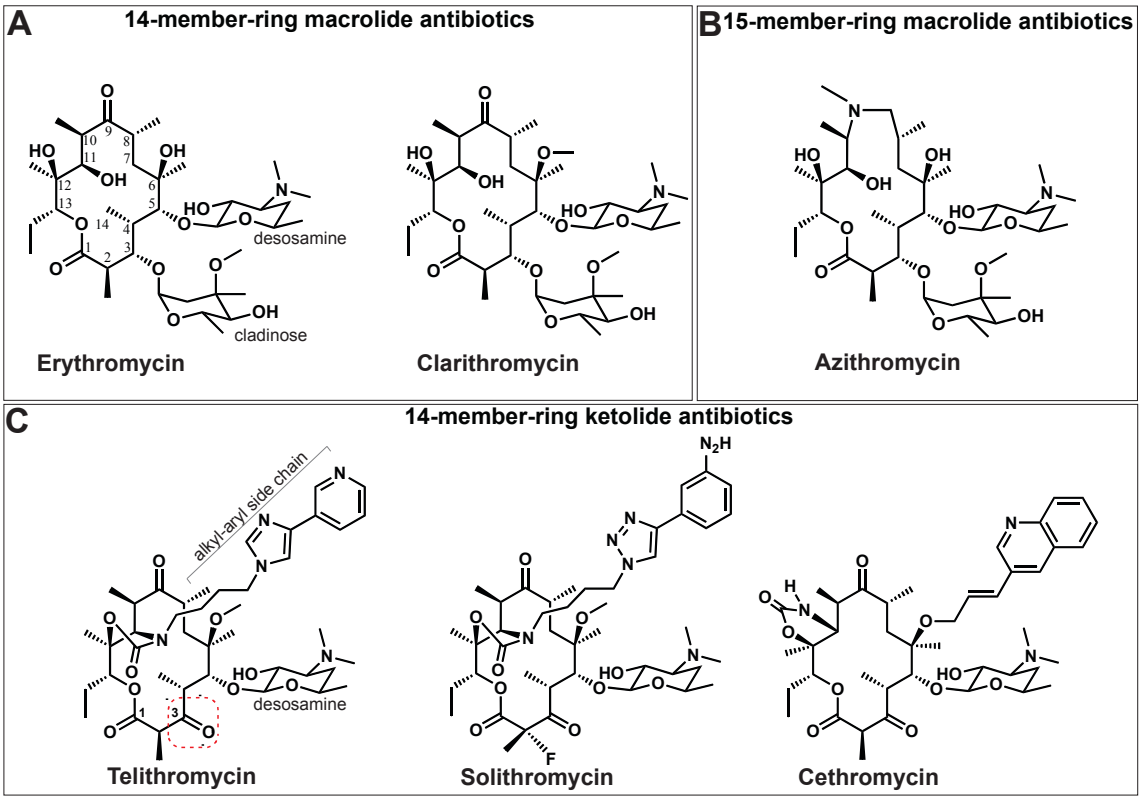

Figure 1.3: Chemical structures of different macrolide antibiotics. (A) 14-member-ring macrolides, erythromycin and clarithromycin. (B) 15-member-ring containing azithromycin. (C) Ketolides, telithromycin, solithromycin and cethromycin. Atoms of the macrolactone ring are numbered on erythromycin structure. Different sugars and side chains are labeled. Keto group in telithromycin is boxed.

C5 position is further extended by isobutyrate group (Fig. 1.5A and C) (18).

The macrolactone ring contributes to the binding affinity of the macrolides to the ribosome. However, since different sizes of macrolactone ring are found in active macrolides, variation in the structure of the core macrolactone can be tolerated. The contribution of the macrolides side chains is more pronounced. Side chains can influence the macrolides interactions with certain rRNA nucleotides, macrolides mode of action, and the ability of macrolides to activate resistance genes (19, 20).

1.3.2 Macrolide binding site

Macrolide antibiotics bind to the large subunit of the bacterial ribosome. They bind in the upper segment of the ribosomal tunnel, between the PTC and the constriction formed by extended loops of the ribosomal proteins L4 and L22 (Fig. 1.4A). Early biochemical and genetic analyses showed that macrolide-binding site is formed mainly by rRNA nucleotides that belong to domains II and V of the 23S rRNA. Recent crystallographic studies of macrolides complexed to the archeal and bacterial ribosomes confirmed this notion and helped to define their exact binding site. In these crystal structures, the macrolactone moiety lays flat against the wall of NPET and establishes hydrophobic interactions with the rRNA residues G2057, C2611, A2058, and A2059 (*Escherichia coli* numbering of rRNA nucleotides is used throughout the manuscript). However, the macrolides' side chains extend either up the tunnel toward the PTC or down the tunnel toward the constriction formed by L4 and L22 proteins (19-22). The C5-desosamine (in the 14- and 15-membered ring macrolides) and C5-mycaminose (in the 16-membered ring macrolides) extend in the PTC direction and on the way pass in very close proximity into a crevice between A2058 and A2059 adenine residues (Fig. 1.4B and C, Fig. 1.5B and C). A key interaction between macrolides and the ribosome is established between the A2058 and A2059 in 23S rRNA on one side and 2'-OH and 3'-*N*-dimethylamino groups of the desosamine and

mycaminose sugars on the side of the drug. Disruption of the C5 sugar-based interactions with A2058 and A2059 significantly reduces the affinity of all macrolides for the ribosome. For example, most of macrolide-resistant bacteria possess mutations or modifications in A2058 and A2059.

The C5-desosamine sugar of 14- and 15-member ring macrolides is too short to reach the PTC cavity. However, the existence of the mycaminose-mycarose disaccharide in case of spiramycin and tylosin is sufficient to closely approach the PTC active site where it is placed in the PTC A2451 and C2452 crevice (Fig. 1.5B). In carbomycin A and josamycin, the C5 disaccharide is further extended by an isobutyrate moiety that reaches directly into the PTC A-site, where it is penetrated deeper in the catalytic center (Fig. 1.5C).

The universal macrolides' contacts between the C5 side chains and the macrolactone ring with the tunnel nucleotides are supported by additional idiosyncratic interactions between side chains of some macrolides and the ribosome, which contribute to the ribosome-macrolide affinity. For example, tylosin has mycinose sugar at C14 position that projects down the tunnel and interacts with G748 and A752 that belong to the loop of helix 35 in domain II of 23S rRNA (Fig. 1.5B) (19). In the case of ketolides, they possess an extended alkyl-aryl side-chain that protrudes down the tunnel and stack with A752 and U2609 base pair formed by rRNA residues that belong to domains II and V of 23S rRNA, respectively (Fig. 1.4C) (12, 20, 23). Side chains of macrolides not only interact with rRNA components of the ribosome, but also make some contacts with the ribosomal proteins. For example, ketolide alkyl-aryl side chain and C9-linked forosamine sugar of spiramycin extend down the tunnel and come into close proximity to loops of L22 and L4 proteins, respectively (19). Mutations of these proteins confer resistance to macrolides, which could affect drug binding directly by interfering with drug-protein interaction (at least in case of ketolides and spiramyicn) or indirectly by allosterically rearranging the rRNA

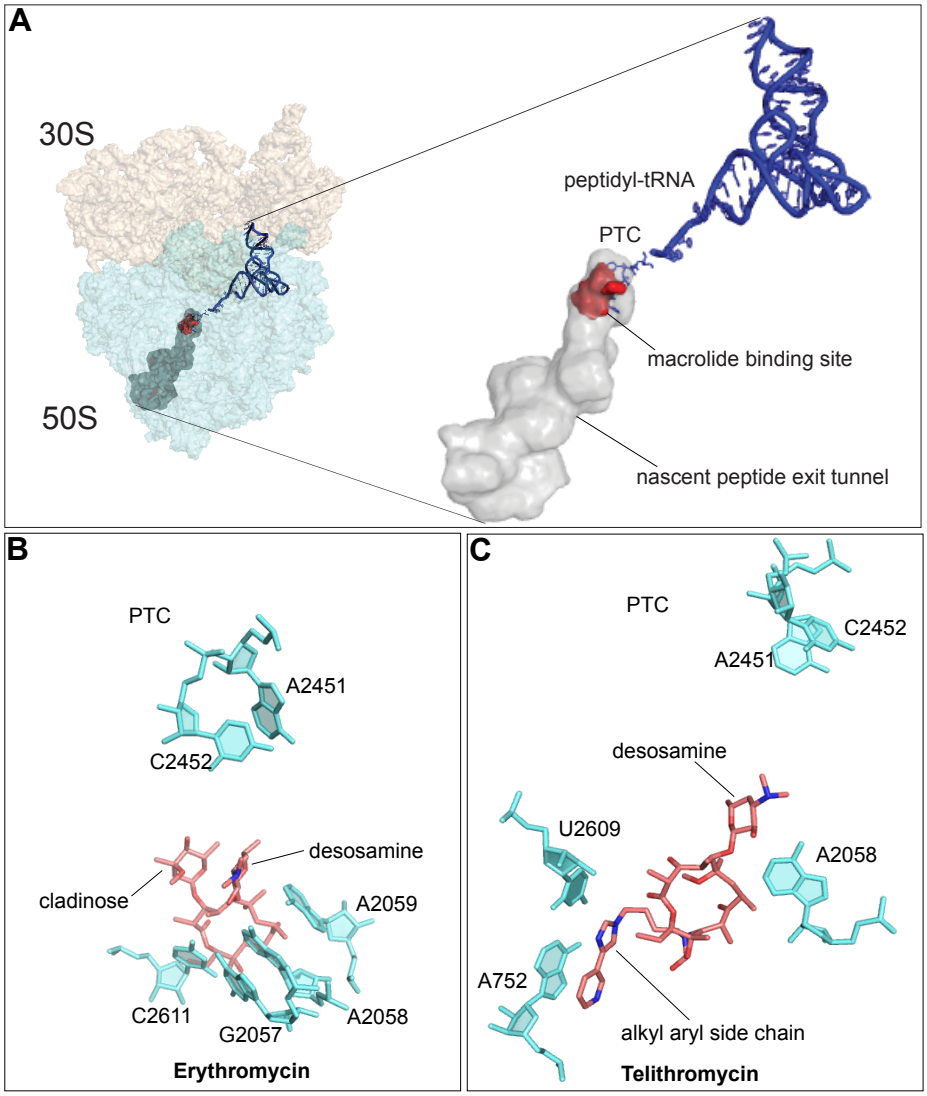

Figure 1.4: Binding site of macrolide antibiotics within the ribosomal tunnel. (A) ERY target site is located in the ribosomal tunnel close to the PTC. 30S and 50S ribosomal subunits are shown in wheat and cyan colors, respectively. The ribosomal tunnel surface is colored in grey and peptidyl-tRNA with a short nascent peptide in blue. ERY molecule is shown as red. (B) Binding of ERY (shown as salmon-colored sticks) in *E. coli* ribosome. Important rRNA residues within ERY binding site are indicated (PDB accession number 3OFR) (20). (C) Binding of TEL (shown as salmon-colored sticks) in the *E. coli* ribosome (PDB accession number 3OAT) (20). Alkyl-aryl side chain of TEL that stacks upon the A752-U2609 base pair is marked. In (B) and (C), the PTC residues A2451 and C2452 are marked for orientation.

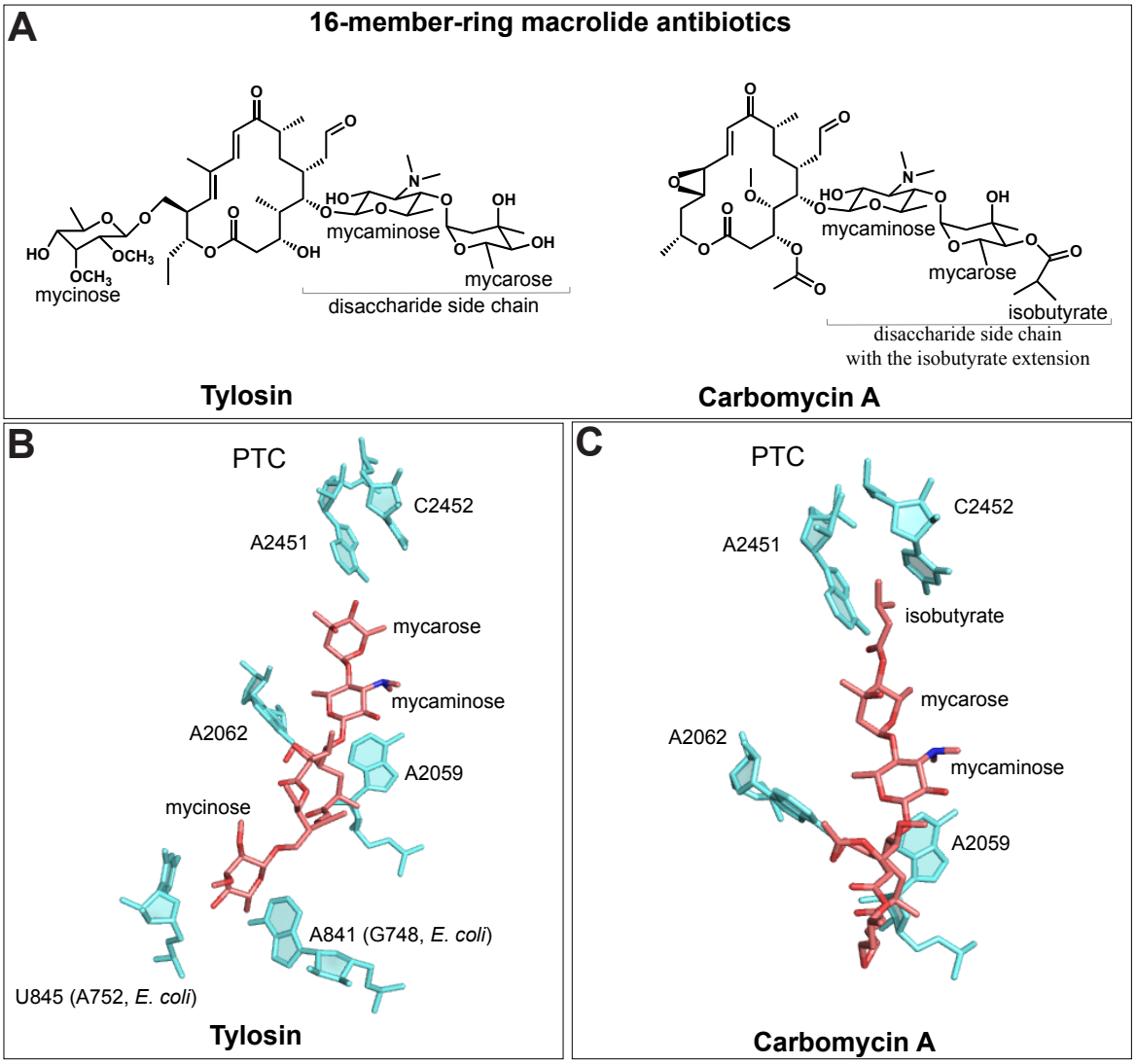

Figure 1.5: Structures and binding site of some 16-membered macrolide antibiotics. (A) Chemical structures of tylosin and carbomycin A. (B) Mycaminose-mycarose side chain of tylosin can reach into the PTC. Mycinose sugar of tylosin comes into close contact with the loop of helix 35 residues A752 and G748 (*H. marismortui* 50S subunit, PDB accession number 1K9M (19)). (C) The longer mycaminose-mycarose-isobutyrate side chain of carbomycin A is able to reach the heart of the PTC (*H. marismortui* 50S subunit, PDB accession number 1K8A (19)).

residues in the macrolide-binding site (24).

1.3.3 Mechanism of action of macrolides

In the previously popular model of macrolides action (plug-in-the-bottle model), macrolides are viewed as non-discriminating inhibitors of synthesis of all cellular polypeptides. This model is based on the observation that all macrolides interfere with the polypeptide's egress by working as blockers of the NPET. In case of 14- and 15-membered ring macrolides with short side chains, they lack the direct interference with the PTC and do not inhibit the first peptide bond formation; therefore, they do not affect the protein synthesis during the early rounds of translation. Their direct effect on the translation starts once the ribosome polymerized enough amino acids that enable the growing polypeptide to encounter the NPET-bound macrolide; this presumably prevents the subsequent progression of the peptide through the NPET. Macrolide hindering of the nascent peptide growth eventually leads to dissociation of the peptidyl-tRNA from the ribosome (25-27). The length of the peptide allowed to be synthesized on the macrolide-bound ribosome and thus carried by peptidyl-tRNA depends on the presence of the C3-cladinose sugar in the 14- and 15-memebred ring macrolides. In case of the cladinose-containing macrolides, the dissociated peptidyl-tRNAs carry 4-9 amino acid long peptides. On the other hand, ketolides, which lack the C3 cladinose, allow polymerization of 9-10 amino acids of several model polypeptides (27). The accumulation of peptidyl tRNAs leads to exhaustion of the pool of free tRNAs in the cell which could contribute to translation inhibition in macrolide-treated cells (26). This idea is further supported with the observation that cells deficient in peptidyl tRNA hydrolase activity exhibit hypersusceptibility to macrolide antibiotics (28).

Early biochemical and genetic studies of macrolides' action contributed significantly to the initial understanding of the mode of action of these antibiotics. More recent crystallographic studies helped to visualize the macrolides-ribosome interactions. All crystallographic studies

confirmed that macrolides obstruct the NPET, thus seemingly supporting plug-in the-bottle model (20-22, 29). However, at the same time, the structures showed that the bound macrolide molecule does not block the NPET completely; instead they narrow the NPET leaving considerable room in the tunnel lumen (29). The existence of this residual space provided important clues that nascent peptides possibly can bypass the macrolide obstruction. The recent work of Kannan et al. showed that indeed some proteins have the ability to bypass the tunnel-bound antibiotic (30). His work contradicted the view of macrolides as general protein synthesis inhibitors. In contrast, they showed that macrolides are protein specific inhibitors. According to the findings of Kannan et al., when macrolides are bound to the NPET, the newly synthesized nascent chain can undergo one of three fates: (1) it can be aborted, (2) stalled, or (3) continued to completion (Fig. 1.6A) (30). These scenarios depend on the amino acid sequence of the nascent chain, macrolides structure, and the tunnel architecture. In the first scenario, the protein synthesis is aborted as the result of blocking the growing of polypeptide by the macrolide molecule bound in the NPET, eventually resulting in peptidyl-tRNA drop-off. This phenomenon is compatible with the plug-in-the-bottle model. However, this model failed to explain the bypass mechanism, which will lead to either stalled or continued protein synthesis. Furthermore, recent genome-wide ribosome profiling analysis in *E. coli* supported this new view of the mode of macrolide action (31, 32).

In comparison with previous generations of macrolides, ketolides are viewed as more potent antimicrobials and sometimes even are bactericidal agents against some Gram-positive bacteria. Surprisingly, ketolides allow synthesis of far more proteins than other macrolides (Fig. 1.7). It appears that inhibiting synthesis of a limited subset of cellular proteins has a more detrimental effect upon cell growth or survival than complete or near-complete inhibition of translation (Fig. 1.7) (30).

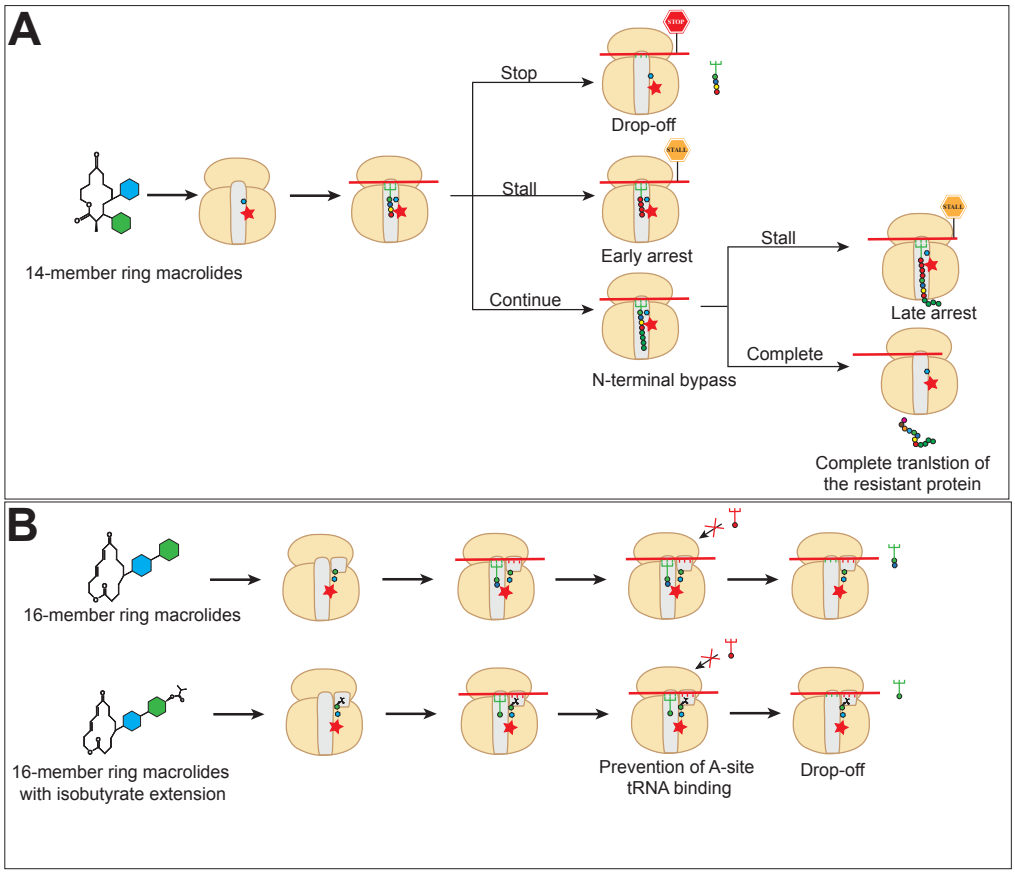

Figure 1.6: Mode of action of macrolide antibiotics. (A) The mode of action of 14-member ring macrolides and 15-member ring macrolides. (B) The mode of action of 16-member ring macrolides. (See text for details).

The mechanism of action of the 16-membered macrolides differs significantly from other types of macrolides. They contain an extended mycaminose-mycarose disaccharide side chain at the C5 position, which enables them to interfere with early rounds of translation. In spiramycin and tylosin, the mycaminose-mycarose side chain extends into the PTC and interferes with the first and second peptide bond formation (Fig. 1.6B) (33). In carbomycin A and josamycin, the disaccharide side chain is extended by an isobutyrate group which now reaches the A-site and inhibits the placement of the incoming aminoacyl-tRNA and effectively preventing the formation of the first peptide bond (Fig. 1.6B).

1.3.4 Mechanisms of resistance against macrolides

The development of resistance in pathogenic bacteria has curbed the clinical value of many antibiotics including macrolides. There are different mechanisms by which bacteria can become resistant to macrolide antibiotics. These mechanisms include macrolide-specific selection of spontaneous resistant mutants carrying specific point mutations and horizontal transfer of resistance genes. Resistance to macrolides can spontaneously arise in bacteria due to a mutation at ribosomal RNA (rRNA) or ribosomal protein residues within or near the macrolide-binding site. In horizontal gene transfer, the resistance can be acquired from other bacteria in the form of plasmids and transposons. The well characterized mechanisms mediated by acquisition of the resistance genes include: (1) membrane-bound efflux pumps that secrete the drug out of bacterial cells, (2) chemical modification of the drug into inactive form by modifying enzymes and (3) modification of the ribosomal target site leading to decreased macrolide binding site affinity. Among these resistance mechanisms, modification of the ribosomal target site is the most prevalent which not only confers resistance to macrolides, but also to other classes of antibiotics that share the same binding site such as lincosamides and streptogramin B (MLS_B resistance phenotype). In contrast, the efflux-pump and drug inactivation based mechanisms

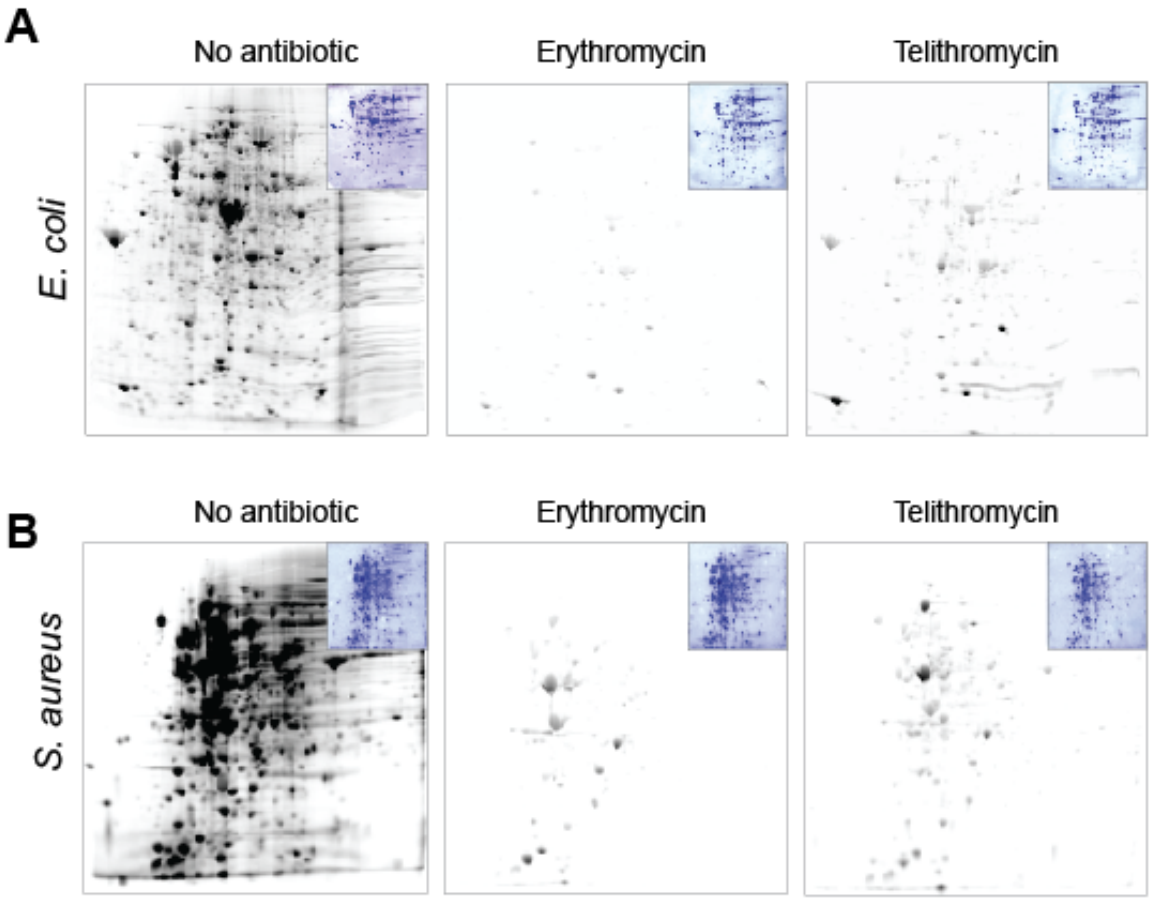

Figure 1.7: The selective proteins synthesis in cells exposed to macrolides. 2D gel electrophoresis analysis of proteins synthesized in *E. coli* (A) or *S. aureus* str. Newman (B) upon treatment the cells with 100-fold MIC of different macrolides (adapted from (16) with modifications).

provide more narrow spectra of resistance (34, 35).

The macrolide target site modification based resistance mechanism acts upon a crucial nucleotide A2058 in the 23S rRNA that is involved in important interactions with macrolides. A family of resistance enzymes known as the erythromycin resistance methyltransferases (Erm) catalyze this modification (36). Erms have been found in some macrolide-producing *Streptomyces* species, as well as in many pathogenic strains (37). These enzymes can monomethylate A2058 and confer low to intermediate resistance against ketolides and macrolides, respectively (but high resistance to lincosamides) (type I MLS_B phenotype). Most of Erms have dimethylase activity leading to dimethylation of A2058, elevating the resistance to MLS_B class of antibiotic to a much higher level (type II MLS_B resistance phenotype) (38). The expression of *erm* genes can be either constitutive or inducible. The inducible expression is activated by the presence of sub-inhibitory concentrations of ERY or some of its analogues, which is operated via translational attenuation mechanism (Fig. 1.8) (39, 40). In the uninduced state, the short upstream open reading frame (uORF) that precedes the resistance gene is translated, but the downstream resistance cistron is not translated because the mRNA secondary structure sequesters its ribosome-binding site (RBS) and start codon (Fig. 1.8B). In the presence of inducer macrolides, the ribosome stalls within the uORF leading to rearrangement of mRNA secondary structure, which exposes the translation initiation region of the resistance gene and activates its expression (Fig 1.8C and D) (41).

1.4 How antibiotic-producing bacteria avoid suicide?

Antibiotic-producing organisms must have intrinsic protection mechanisms in order to avoid suicide. These bacteria usually possess resistance genes that are commonly found in the vicinity of the antibiotic biosynthetic gene cluster. Because of the necessity of having antibiotic

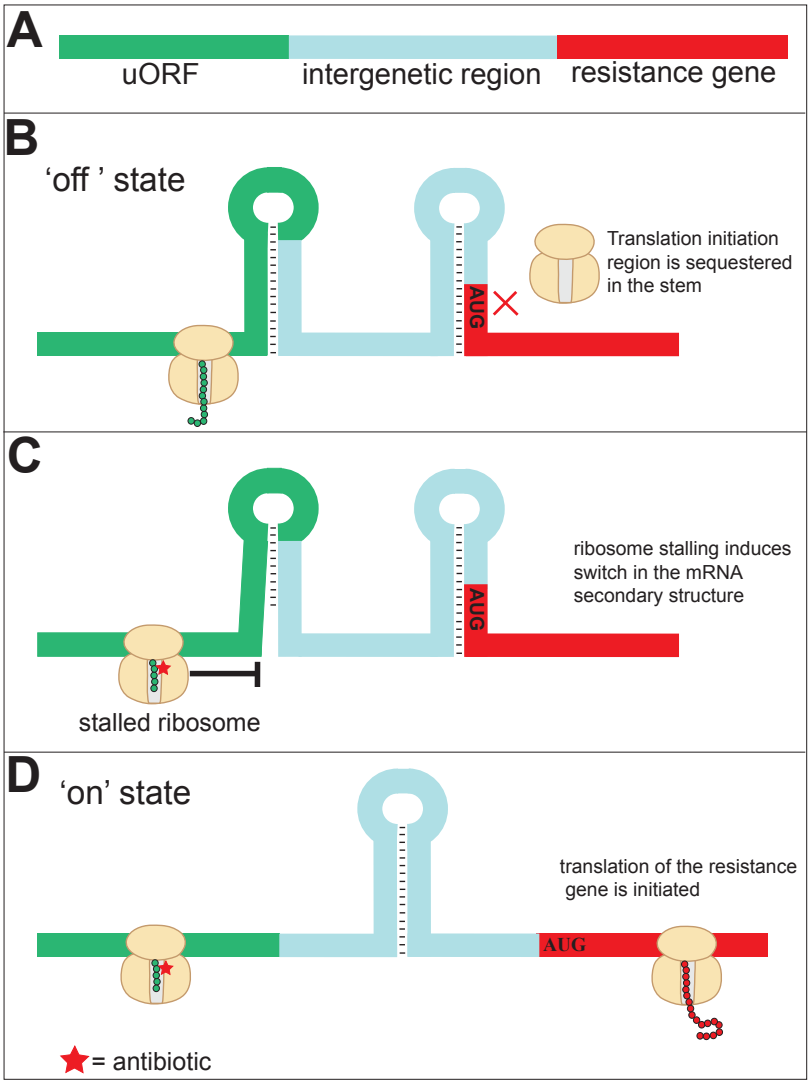

Figure 1.8: Regulation of bacterial resistance gene expression by programmed translation arrest. (A) The general organization of the resistance gene operon. The resistance gene (red-colored) is preceded by upstream open reading frame (uORF) (green-colored). Both are separated by intergenic space (cyan-colored). (B) In the 'off' state, presence of the secondary structure prevents translation of the resistance gene. (C), (D) In the 'on' state, ribosome stalling at the regulatory uORF triggers a switch in mRNA secondary structure that allows the expression of the downstream resistance gene.

resistance genes, antibiotic-producing bacteria are believed to be a reservoir of resistance genes that can be horizontally transferred into clinical microbial strains. Study of this reservoir could provide an early warning system for future clinically relevant antibiotic resistance mechanisms and improve our understanding of the resistance mechanisms in the producer.

Different resistance mechanisms exist in different macrolide-producing bacteria. In the ERY-producing *Saccharopolyspora erythraea*, the A2058 position is constitutively dimethylated by the action of ErmE and the ribosome from this bacterium is always resistant to ERY (42). The resistance strategy is more complicated in the tylosin producers *Streptomyces fradiae* due to the presence of four resistance genes. Tylosin makes general interactions with the ribosome similar to other macrolides, however, its ability to make idiosyncratic interactions especially with domain II due to the presence of mycinose at C12 makes the monomethylation of A2058 position is not enough to make the cells resistant to tylosin. Therefore, one way to make the cells resistant to tylosin is achieved by expressing of two monomethylases the constitutively expressed TlrD and the inducible TlrB that monomethylate A2058 and G748, respectively (43). Another mechanism involves dimethylation of the A2058 by the inducible TlrA dimethylase, which renders the *S. fradiae* completely resistant to tylosin (44). In addition, this organism has another resistance determinant, which is ATP Binding transporter TlrC. All of these resistance mechanisms are believed to act in concert at varying levels to make *S. fradiae* resistant to its own product tylosin (43). The producer of oleandomycin

Streptomyces antibioticus achieves self-protection of oleandomycin by harboring two resistance genes *oleI* and *oleD*, which both encode macrolide glycosyltransferases that inactivate oleandomycin. OleI and OleD differ by their specificities; OleI is specific to oleandomycin, whereas OleD has the ability to accept different macrolides as substrates (45).

Streptomyces venezuelae ATCC 15439 has two putative resistance genes *pikR1* and *pikR2*, which are located immediately upstream of the MTM/PKM biosynthetic gene cluster (Fig. 1.9A). These genes have been proposed to provide the producer with resistance to the antibiotics it makes (46). They are considerably similar to the *erm* genes (47). In addition, PikR1 and PikR2 are also very homologous to each other. In the Chapter 2, we addressed the following questions: Do PikR1 and PikR2 confer resistance to MTM and PKM? If so, what are their target sites and how are they regulated? And why does the MTM/PKM producer need to maintain two similar resistance genes? The answers for these questions helped us to understand how the ketolide-producing bacteria protect themselves during active antibiotic production. Importantly, the results revealed possible new ketolide resistance mechanisms, which can be disseminated among pathogenic bacterial strains upon the anticipated wild use of ketolide antibiotics in the clinical setting.

1.5 Methymycin/pikromycin biosynthetic pathway in *Streptomyces venezuelae* ATCC15439

The *Streptomyces* species are soil dwelling Gram-positive bacteria that have a complicated lifestyle. From the clinical perspective, they are famous for their potential ability to make antibiotics. Their large genomes allow them to dedicate a significant fraction of their genes for production of secondary metabolites. It is estimated that *Streptomyces* bacteria contributed up to 50% of the currently marketed antibiotics.

Most of the antibiotics producing-bacteria dedicate a specific biochemical pathway for synthesizing a single antibiotic. However, *Streptomyces venezuelae* ATCC15439 has a unique biosynthetic pathway due to its capacity to efficiently generate two distinct ketolide antibiotics, methymycin (MTM) and pikromycin (PKM) (Fig. 1.10) (48, 49) MTM is the smallest known macrolide antibiotic composed of a 12-member macrolactone ring while PKM is a 14-member

macrolactone ring which is structurally similar to other clinically used macrolides (Fig. 1.10B). The MTM/PKM biosynthetic operon comprises of 18 discreet genes, which can be classified into five separate loci: *pikA* locus, which is type-I modular polyketide synthase (PKS) that is required for assembling the macrolactone core, the *des* locus is responsible for biosynthesis of the desosamine sugar and attaching it to C-5 position of macrolactone, the *pikC* locus encodes a cytochrome P450 hydroxylase that decorates the macrolactone ring with hydroxyl groups at different positions, *pikD* is a positive transcriptional activator of this pathway, and lastly the *pikR* locus which contains two putative resistance genes (Fig. 1.10A) (48).

The unique ability of this system to branch and produce two ketolides is determined by choosing of one of the two start codons in the *pikAIV* gene (50).Translation of *pikAIV* from the first start codon generates PKM. If however, translation of *pikAIV* starts from second internal start codon, then MTM will become the end product.

Since MTM and PKM belong to ketolide class of macrolide antibiotics, studying their binding sites and modes of action may provide important insights to the general action of clinical ketolide antibiotics. Currently little is known about the binding site of PKM. However, based on its structural similarity to other macrolides, one can anticipate that PKM may bind to the 'conventional' macrolide site in the ribosomal tunnel. On the other hand, the MTM binding site is more mysterious partly due to the significant structural differences between MTM and other macrolides. To add to the puzzle, a recent report suggested that MTM is not binding to the tunnel, but instead, it binds in the PTC at a site that overlaps with the binding site of a classic PTC inhibitor chloramphenicol (CHL) (51). The chapter 3 focused on the investigation of the binding sites of MTM and PKM and their modes of action.

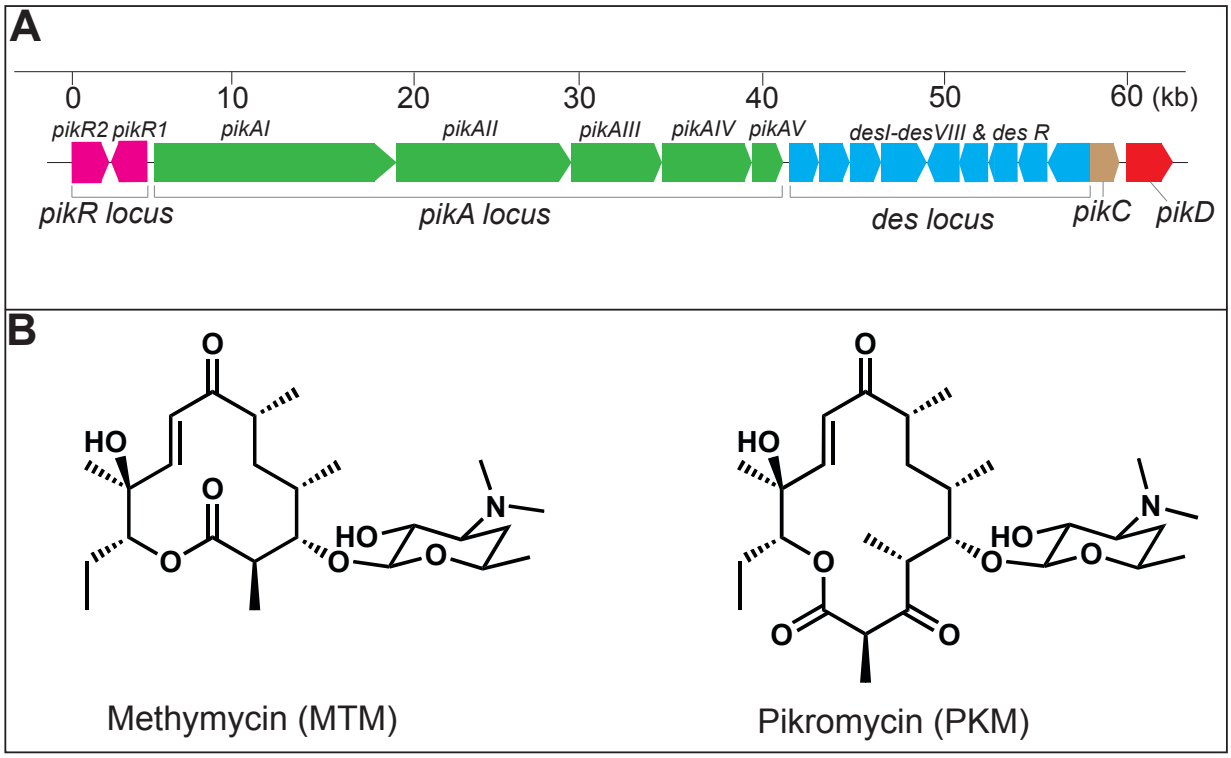

Figure 1.9: Methymycin/pikromycin biosynthetic pathway. (A) The MTM/PKM biosynthetic genes cluster. (B) The chemical structures of methymycin (MTM) and pikromycin (PKM).

1.6 Cited Literature

1. Schluenzen F*, et al.* (2000) Structure of functionally activated small ribosomal subunit at 3.3 angstrom resolution. *Cell* 102(5):615-623.

2. Wimberly BT*, et al.* (2000) Structure of the 30S ribosomal subunit. *Nature* 407(6802):327-339.

3. Demeshkina N, Jenner L, Yusupova G, & Yusupov M (2010) Interactions of the ribosome with mRNA and tRNA. *Curr Opin Struct Biol* 20(3):325-332.

4. Ban N, Nissen P, Hansen J, Moore PB, & Steitz TA (2000) The complete atomic structure of the large ribosomal subunit at 2.4 angstrom resolution. *Science* 289(5481):905-920.

5. Harms J*, et al.* (2001) High resolution structure of the large ribosomal subunit from a mesophilic eubacterium. *Cell* 107(5):679-688.

6. Yusupov MM*, et al.* (2001) Crystal structure of the ribosome at 5.5 angstrom resolution. *Science* 292(5518):883-896.

7. Polikanov YS, Steitz TA, & Innis CA (2014) A proton wire to couple aminoacyl-tRNA accommodation and peptide-bond formation on the ribosome. *Nature structural & molecular biology* 21(9):787-793.

8. Voss NR, Gerstein M, Steitz TA, & Moore PB (2006) The geometry of the ribosomal polypeptide exit tunnel. *Journal of molecular biology* 360(4):893-906.

9. Jenni S & Ban N (2003) The chemistry of protein synthesis and voyage through the ribosomal tunnel (vol 13, pg 212, 2003). *Curr Opin Struc Biol* 13(4):533-533.

10. Schmeing TM & Ramakrishnan V (2009) What recent ribosome structures have revealed about the mechanism of translation. *Nature* 461(7268):1234-1242.

11. Wilson DN (2009) The A-Z of bacterial translation inhibitors. *Critical reviews in biochemistry and molecular biology* 44(6):393-433.

12. Mankin AS (2001) Ribosomal Antibiotics. *Molecular Biology* 35.

13. Okuda K, Hirota T, Kingery DA, & Nagasawa H (2009) Synthesis of a fluorine-substituted puromycin derivative for Bronsted studies of ribosomal-catalyzed peptide bond formation. *The Journal of organic chemistry* 74(6):2609-2612.

14. McGuire JM*, et al.* (1952) [Ilotycin, a new antibiotic]. *Schweizerische medizinische Wochenschrift* 82(41):1064-1065.

15. Ackermann G & Rodloff AC (2003) Drugs of the 21st century: telithromycin (HMR 3647)--the first ketolide. *The Journal of antimicrobial chemotherapy* 51(3):497-511.

16. Kannan K & Mankin AS (2011) Macrolide antibiotics in the ribosome exit tunnel: species-specific binding and action. *Annals of the New York Academy of Sciences* 1241:33-47.

17. Gaynor M & Mankin AS (2003) Macrolide antibiotics: binding site, mechanism of action, resistance. *Current topics in medicinal chemistry* 3(9):949-961.

18. Katz L & Ashley GW (2005) Translation and protein synthesis: macrolides. *Chemical reviews* 105(2):499-528.

19. Hansen JL*, et al.* (2002) The structures of four macrolide antibiotics bound to the large ribosomal subunit. *Molecular cell* 10(1):117-128.

20. Dunkle JA, Xiong L, Mankin AS, & Cate JH (2010) Structures of the Escherichia coli ribosome with antibiotics bound near the peptidyl transferase center explain spectra of drug action. *Proceedings of the National Academy of Sciences of the United States of America* 107(40):17152-17157.

21. Schlunzen F*, et al.* (2001) Structural basis for the interaction of antibiotics with the peptidyl transferase centre in eubacteria. *Nature* 413(6858):814-821.

22. Bulkley D, Innis CA, Blaha G, & Steitz TA (2010) Revisiting the structures of several antibiotics bound to the bacterial ribosome. *Proceedings of the National Academy of Sciences of the United States of America* 107(40):17158-17163.

23. Gregory ST & Dahlberg AE (1999) Erythromycin resistance mutations in ribosomal proteins L22 and L4 perturb the higher order structure of 23 S ribosomal RNA. *Journal of molecular biology* 289(4):827-834.

24. Otaka T & Kaji A (1975) Release of (oligo) peptidyl-tRNA from ribosomes by erythromycin A. *Proceedings of the National Academy of Sciences of the United States of America* 72(7):2649-2652.

25. Menninger JR & Otto DP (1982) Erythromycin, carbomycin, and spiramycin inhibit protein synthesis by stimulating the dissociation of peptidyl-tRNA from ribosomes. *Antimicrob Agents Chemother* 21(5):811-818.

26. Tenson T, Lovmar M, & Ehrenberg M (2003) The mechanism of action of macrolides, lincosamides and streptogramin B reveals the nascent peptide exit path in the ribosome. *Journal of molecular biology* 330(5):1005-1014.

27. Menninger JR (1979) Accumulation of peptidyl tRNA is lethal to Escherichia coli. *J. Bacteriol.* 137:694-696.

28. Tu D, Blaha G, Moore PB, & Steitz TA (2005) Structures of MLSBK antibiotics bound to mutated large ribosomal subunits provide a structural explanation for resistance. *Cell* 121(2):257-270.

29. Kannan K, Vazquez-Laslop N, & Mankin AS (2012) Selective Protein Synthesis by Ribosomes with a Drug-Obstructed Exit Tunnel. *Cell* 151(3):508-520.

30. Kannan K, *et al.* (2014) The general mode of translation inhibition by macrolide antibiotics. *Proceedings of the National Academy of Sciences of the United States of America* 111(45):15958-15963.

31. Davis AR, Gohara DW, & Yap MN (2014) Sequence selectivity of macrolide-induced translational attenuation. *Proceedings of the National Academy of Sciences of the United States of America* 111(43):15379-15384.

32. Poulsen SM, Kofoed C, & Vester B (2000) Inhibition of the ribosomal peptidyl transferase reaction by the mycarose moiety of the antibiotics carbomycin, spiramycin and tylosin. *Journal of molecular biology* 304(3):471-481.

33. Subramanian SL, Ramu, H., Mankin, A. S. (2012) Inducible Resistance to Macrolide Antibiotics. *Antibiotic Discovery and Development* 1:455-484.

34. Leclercq R (2002) Mechanisms of resistance to macrolides and lincosamides: Nature of the resistance elements and their clinical implications. *Clinical Infectious Diseases* 34(4):482-492.

35. Weisblum B (1995) Erythromycin Resistance by Ribosome Modification. *Antimicrobial Agents and Chemotherapy* 39(3):577-585.

36. Cundliffe E & Demain AL (2010) Avoidance of suicide in antibiotic-producing microbes. *Journal of industrial microbiology & biotechnology* 37(7):643-672.

37. Liu MF & Douthwaite S (2002) Activity of the ketolide telithromycin is refractory to erm monomethylation of bacterial rRNA. *Antimicrobial Agents and Chemotherapy* 46(6):1629-1633.

38. Hahn J, Grandi G, Gryczan TJ, & Dubnau D (1982) Translational attenuation of ermC: a deletion analysis. *Molecular & general genetics : MGG* 186(2):204-216.

39. Horinouchi S, Byeon WH, & Weisblum B (1983) A complex attenuator regulates inducible resistance to macrolides, lincosamides, and streptogramin type B antibiotics in Streptococcus sanguis. *Journal of bacteriology* 154(3):1252-1262.

40. Ramu H, Mankin A, & Vazquez-Laslop N (2009) Programmed drug-dependent ribosome stalling. *Molecular microbiology* 71(4):811-824.

41. Skinner R, Cundliffe E, & Schmidt FJ (1983) Site of action of a ribosomal RNA methylase responsible for resistance to erythromycin and other antibiotics. *The Journal of biological chemistry* 258(20):12702-12706.

42. Liu MF & Douthwaite S (2002) Resistance to the macrolide antibiotic tylosin is conferred by single methylations at 23S rRNA nucleotides G748 and A2058 acting in synergy. *Proceedings of the National Academy of Sciences of the United States of America* 99(23):14658-14663.

43. Zalacain M & Cundliffe E (1989) Methylation of 23s Ribosomal-Rna Caused by Tlra (Ermsf), a Tylosin Resistance Determinant from Streptomyces-Fradiae. *Journal of bacteriology* 171(8):4254-4260.

44. Quiros LM, Aguirrezabalaga I, Olano C, Mendez C, & Salas JA (1998) Two glycosyltransferases and a glycosidase are involved in oleandomycin modification during its biosynthesis by Streptomyces antibioticus. *Molecular microbiology* 28(6):1177-1185.

45. Zhao L, Beyer NJ, Borisova SA, & Liu HW (2003) Beta-glucosylation as a part of self-resistance mechanism in methymycin/pikromycin producing strain Streptomyces venezuelae. *Biochemistry-Us* 42(50):14794-14804.

46. Park AK, Kim H, & Jin HJ (2010) Phylogenetic analysis of rRNA methyltransferases, Erm and KsgA, as related to antibiotic resistance. *FEMS microbiology letters* 309(2):151-162.

47. Xue YQ, Zhao LS, Liu HW, & Sherman DH (1998) A gene cluster for macrolide antibiotic biosynthesis in Streptomyces venezuelae: Architecture of metabolic diversity. *Proceedings of the National Academy of Sciences of the United States of America* 95(21):12111-12116.

48. Kittendorf JD & Sherman DH (2009) The methymycin/pikromycin pathway: a model for metabolic diversity in natural product biosynthesis. *Bioorganic & medicinal chemistry* 17(6):2137-2146.

49. Xue Y & Sherman DH (2000) Alternative modular polyketide synthase expression controls macrolactone structure. *Nature* 403(6769):571-575.

50. Tamar Auerbach IM, Anat Bashan,, Chen Davidovich HR, David H. Sherman, & Yonath aA (2009) Structural basis for the antibacterial activity of the 12-membered-ring mono-sugar macrolide methymycin. *biotechnologia* 84.

2. EFFICIENT RESISTANCE TO KETOLIDE ANTIBIOTICS THROUGH COORDINATED EXPRESSION OF METHYLTRANSFERASE PARALOGS IN A BACTERIAL PRODUCER OF NATURAL KETOLIDES

2.1 Introduction and rationale

The prototypes of most of the clinically useful antibiotics, including the large and diverse group of protein synthesis inhibitors, have been discovered among the secondary metabolites of various bacterial species (1, 2). These antibiotic-producing bacteria have developed an array of resistance genes to avoid committing suicide (3, 4). The wide medical use of antibiotics has created a strong selective pressure for such resistance genes to find their way into the genomes of bacterial pathogens, curbing the beneficial effects of the drugs and shortening their clinical lifespan (5). Consequently, antibiotic producers are not only our allies in providing useful drugs, but also play an adversary role by facilitating the spread of resistance.

Macrolides are among the most medically successful antibiotics originating from the secondary metabolites of actinomycetes (6). They inhibit translation by binding in the nascent peptide exit tunnel (NPET) close to the peptidyl transferase center (PTC) of the large ribosomal subunit (7-10). The most common mechanism of macrolide resistance involves modification of a specific nucleotide in the drug-binding site (A2058 in the *E. coli* 23S rRNA) by Erm methyltransferases (11). Expression of the *erm* genes is often inducible and is activated only when antibiotic is present. Such induction operates via antibiotic-controlled ribosome stalling at an upstream leader ORF (11, 12).

Clinically relevant macrolide antibiotics are built upon a 14-16 atom macrolactone ring decorated with various side chains. The prototype 14-atom ring macrolide erythromycin (ERY) and its second-generation derivatives carry cladinose at the C3-position of the ring (Fig. 1.3A).

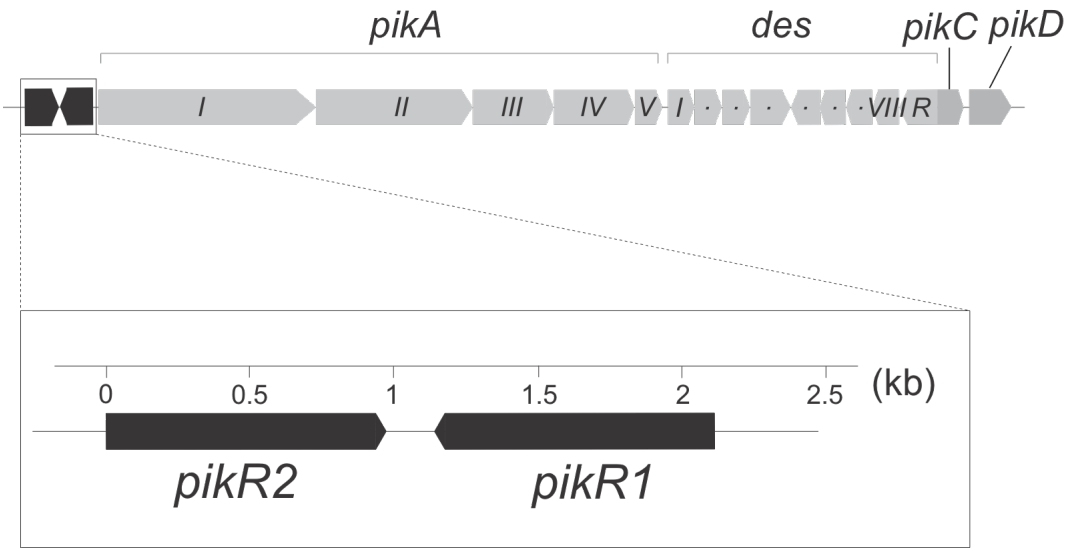

Figure 2.1. *S. venezuelae pikR* resistance genes. The structure of the MTM/PKM biosynthetic gene cluster in *S. venezuelae* ATCC 15439 (24). The polyketide synthase (*pikA*) and desosamine biosynthesis (*des*) gene operons along with the *pikC* and *pikD* genes required for production of the active MTM and PKM antibiotics are shown. The putative resistance genes *pikR1* and *pikR2* precede the MTM/PKM biosynthesis operon in a head-to-head arrangement.

In the newest generation of drugs, the ketolides, the C3-cladinose is replaced with a keto function (Fig. 1.3C) (13). Ketolides are viewed as one of the most promising classes of antibiotics presently under development, and offer broad medical application (14, 15). The first medically-useful ketolide telithromycin (TEL) and newer ketolides currently in clinical trials show dramatically improved antibacterial activity compared to earlier generations of macrolides, and to a large extent this is due to their reduced propensity to activate inducible resistance genes (16-18).

All the clinically relevant ketolides are synthetic or semi-synthetic derivatives of natural macrolides (19). The only naturally occurring 14-atom macrolactone ring ketolide that is presently known is pikromycin (PKM) (20) produced by *Streptomyces venezuelae* (strain ATCC 15439) (Fig. 1.9B). The biosynthesis pathway of PKM is unique due to a modular polyketide synthesis (PKS) skipping mechanism that can divert the pathway towards production of a second macrolide molecule, methymycin (MTM), which has a smaller macrolactone ring of 12 atoms (Fig. 1.9B) (21, 22). While both PKM and MTM possess antibacterial activity, their modes of binding to the ribosome and their mechanisms of action remain unclear.

The modular PKS genes *pikAI-pikAV* in the biosynthetic cluster of *S. venezuelae* ATCC 15439 are preceded by two putative resistance genes, *pikR1* and *pikR2,* arranged head-to-head (Fig. 2.1). The protein products PikR1 and PikR2 are 42% identical (Fig. 2.2) and show similarity to Erm-type rRNA methyltransferases (23, 24). Given the significant fitness cost associated with *erm*-based resistance (25), the duplication of PikR enzymatic function in *S. venezuelae* is puzzling. Besides being of general biological interest, the mechanism by which a natural producer of ketolides attains resistance is of significant medical importance. Not in the least, it can be envisioned that selective pressure imposed by broad medical use of ketolides could promote the transfer of natural ketolide resistance genes to clinical pathogens.

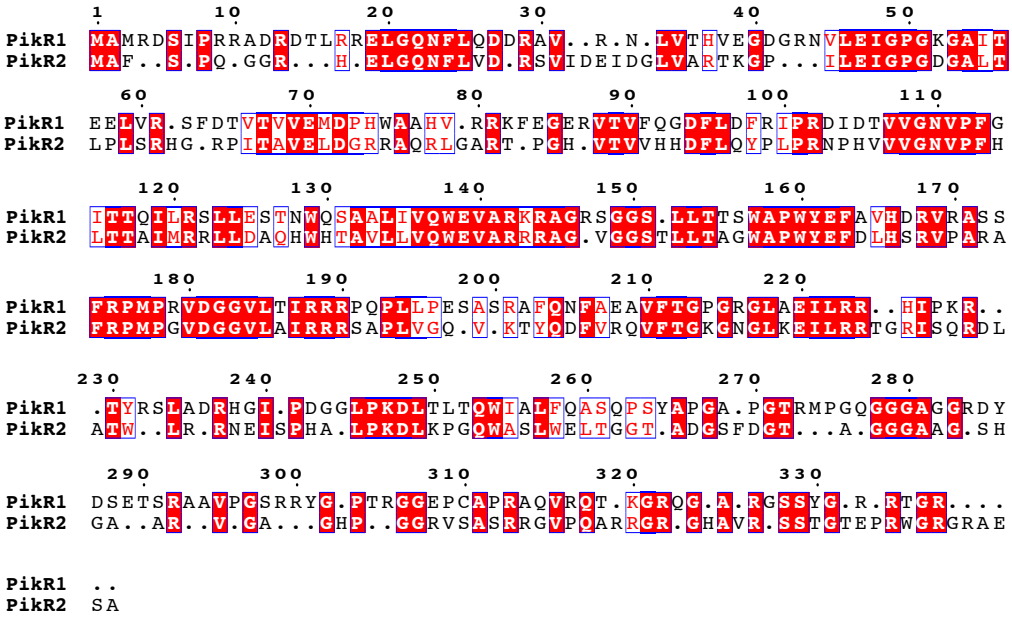

Figure 2.2. Similarity of proteins encoded in the *pikR1* and *pikR2* genes in *S. venezuelae* ATCC 15439.

Understanding the function and regulation of *pikR1*/*pikR2* and similar genes would facilitate their molecular surveillance and possibly curbing their dissemination. Study of *pikR1*/*pikR2*-like stimulates preemptive development of new drugs that retain antimicrobial activity against strains harboring these resistance mechanisms.

In this chapter, we demonstrate that the *pikR1* and *pikR2* genes render the ketolide-producing *S. venezuelae* cells resistant to PKM and MTM as well as to clinical ketolide antibiotics. Having determined the target, the mode of action, and the regulation of these genes, we reveal how *S. venezuelae* achieves ketolide resistance at a low fitness cost by balancing the activities of PikR1 and PikR2 and timing their expression.

We present evidence that the *pikR2* gene has been optimized through evolution to respond to ketolide antibiotics. Finally, we demonstrate that transfer of *pikR2* to other bacteria renders them resistant to high concentrations of ketolides, and this effect is accentuated in combination with *pikR1*. These findings illuminate resistance mechanisms that could potentially be acquired by clinical pathogens upon launching new ketolide antibiotics.

2.2 Materials and methods

Antibiotics, enzymes and chemicals. MTM and PKM were synthesized chemically as previously described (49), and repurified by preparatory HPLC using a Phenomenex Luna 5u C18 250 x 21.2mm column (serial 444304-4) monitored at 250 nm at a flow rate of 9 mL/min with an isocratic mobile phase of H_2O/MeCN (45/55) and a 0.1% NEt_3 modifier. Telithromycin, cethromycin and solithromycin were from Cempra, Inc., erythromycin, chloramphenicol and thiostrepton were from Sigma Aldrich. Enzymes used for DNA cloning were from Fermentas. [γ^{32}P]-ATP (specific activity 6000 Ci/mmol) was from MP Biomedicals. Other reagents and chemicals were purchased from either Fisher Scientific or Sigma Aldrich. All oligonucleotides used in the study were synthesized by IDT and are shown in Table II.I.

Strains and plasmids. The Δ*acrA* derivative of the *E. coli* strain JM109 (genotype: *end*A1, *rec*A1, *gyr*A96, *thi*, *hsd*R17(rk$^-$, ml$^+$), *rel*A1, *sup*E44, λ$^-$, Δ(*lac-pro*AB), [F', *tra*D36, *pro*AB, *lac*I^q, *lac*ZΔM15]) was constructed by recombineering (50) using DNA from the Keio collection strains JW0452 (51) as a PCR template for preparing donor DNA using the primers acrAup and acrAdown (Table II.I) (52). In order to generate *E. coli* strains constitutively expressing PikR1 and PikR2 methyltransferase enzymes, their corresponding genes were PCR amplified from the *S. venezuelae,* strain ATCC 15439, genomic DNA using the primers NdeI-pikR1-D2 and AflII-pikR1-R2 or NdeI-pikR2-D2 and AflII-pikR2-R2 (Table II.I), respectively, which introduced strong Shine-Dalgarno sequence upstream from the initiator AUG codons. The PCR products were digested with *Nde*I and *Afl*II and cloned in the corresponding sites of the plasmid pERMZα (33) (Table II.II), behind the Ptac promoter. The resulting plasmids pPikR1 and pPikR2 were used to transform the JM109 Δ*acrA* strain, and the transformants were used for MIC testing and RNA preparation.

In order to study the inducibility of *pikR1* and *pikR2* genes, their regulatory regions (including the putative leader ORFs, the intergenic region and the first five codons of the resistance genes) were PCR amplified from the DNA of *S. venezuelae* ATCC15439, using the primers ORF-PikR1-D-new and ORF-PikR1-R or ORF2-PikR2-D and ORF2-PikR2-R, respectively (Table II.I). The PCR products were digested with *Nde*I and *Afl*II and cloned in the corresponding sites of plasmid pERMZα. The JM109 Δ*acrB* strain was transformed with the resulting plasmids pRL1 and pRL2, and the transformants were used for antibiotic disk diffusion experiments (Table II.II).

For studying the expression of the individual resistance genes in *S. venezuelae*, strains that lack either *pikR1* or *pikR2* or both of them were engineered. To prepare the strain that had only *pikR1*, the *pikR2* gene in the *S. venezuelae* DHS2001 strain (Table II.III) was inactivated by in-frame deletion of 271 codons (codons 31-301) to avoid any polar effects. To achieve that, the plasmid pSRP112 (Table II.II), based on *E. coli-Streptomyces* shuttle vector pKC1139 (53), was constructed by amplifying and cloning left-and right-flanking regions of the *pikR2* genes using the genomic DNA of *S. venezuelae* DHS2001 as a template, primer pairs SR199-SR200 and SR201-SR202 and KOD Xtreme DNA polymerase (Novagen). The plasmid was assembled using Gibson assembly mix (New England Biolabs) according to the manufacturer's instructions. Briefly, the amplified PCR products of flanking regions of *pikR2* and linearized pKC1139 vector with *EcoR*I and *Hin*dIII were incubated at 50°C for 2 hr. Following incubation, the samples were transformed into *E. coli* DH5α. Restriction digestion and sequencing verified the isolated pSRP112 plasmid. The plasmid pSRP112 was then introduced into the *S. venezuelae* DHS2001 by protoplasts-based transformation. A strain in which a single crossover between the pSRP112 plasmid and *S. venezuelae* DHS2001 chromosome had occurred was selected by cultivation of antibiotic-resistant transconjugants at 37°C (the non-permissive temperature for the pSG5-based

replicon) in the presence of apramycin. Cells from one colony were subjected to second rounds of propagation in the absence of apramycin to allow for the second crossover. The desired double crossover mutant Δ*pikR2* was selected by its apramycin-sensitive phenotype and verified by PCR. The resulting *pikR2*-deletion mutant of *S. venezuelae* DHS2001 was designated R1 (DHS328) (Table II.III). The Δ*pikR1* and Δ*pikR1-pikR2* mutants were generated in the same way as described above using the primer pairs SR216- SR217 and SR218- SR219 for Δ*pikR1* and SR219- SR220 and SR221- SR222 for Δ*pikR1-pikR2*. The *pikR1* in-frame deletion encompassed codons 11-327 and the *pikR1-pikR2* deletion left intact the first 10 codons of *pikR1* and *pikR2* removing the entire DNA segment in between. The resulting *pikR1*- and *pikR1-pikR2*- deletion mutants of *S. venezuelae* DHS2001 were designated R2 (DHS330) and Δ (DHS332), respectively (Table II.III).

In order to check the resistance conferred by the *pikR2* gene in *M. smegmatis*, *pikR2* was PCR-amplified with its regulatory region (including the *pikR2L* and the intergenic region) from the DNA of *S. venezuelae* strain ATCC15439 using the primers pMIP12-R2-D2-short and pMIP12-R2-R-short. The PCR product was gel purified and used as a template for the second PCR using the primers pMIP12-R2-D2 and pMIP12-R2-R. The PCR product was gel purified and introduced by Gibson assembly into the pMIP12 plasmid (54) cut with *Bam*HI and *Spe*I restriction enzymes. The reaction mixture was transformed into *E. coli* JM109. The recombinant plasmid designated pMR2 (Table II.II) was isolated, sequenced and introduced into the Δ*erm38* strain of *M. smegmatis* (strain mc² 155 ermKO-4) (55) (Table II.III) by electroporation. The transformed cells were plated on 7H11/ADC/glycerol/tween plates (Milddlebrook 7H11, 10% [albumin, dextrose, catalase], 0.2% glycerol, 0.05% tween 80) containing 15μg/ml of kanamycin.

To clone the *pikR2-pikR1* tandem (that contains *pikR2* with its leader ORF and *pikR1* with it native promoter) a 3.25 kb DNA fragment from the genomic DNA of *S. venezuelae* was initially PCR-amplified using the primers pMIP12-R2-D2-short and pMIP12-R1-R-short. The purified PCR product was re-amplified using the primers pMIP12-R2-D2 and pMIP12-R1-R to introduce flanking regions suitable for cloning in the pMIP12 vector. The resulting PCR product was introduced into the *Bam*HI and *Spe*I cut plasmid pMIP12 by Gibson assembly as described above. The resulting plasmid, pMR1R2 (Table II-II), was eventually introduced into *M. smegmatis* strain mc² 155 ermKO-4.

Microbiological testing. MICs of antibiotics were determined by the broth microdilution assay (56). The MIC values were read after an overnight incubation (*E. coli* and *S. venezuelae*) or after 3 days incubation (*M. smegmatis*) at 37°C.

Disc diffusion assays for testing the inducibility of the pRL1 and pRL2 reporters (Table II.II) were carried out essentially as described previously (33) with the exception that the JM109 Δ*acrB* strain was used as the host. Briefly, cells transformed with reporter plasmids were grown overnight in the presence of 100 μg/ml ampicillin and 0.5 mM IPTG and then 1.5 ml of cell cultures were mixed with 8.5 ml soft agar (0.6% LB agar at 50°C) and overlaid on agar plates containing 100 μg/ml ampicillin, 0.5 mM IPTG and 80 μg/ml X-gal. After the soft agar solidified, Ø 5 mm Whatmann 3MM paper discs containing 32 μg of MTM, 32 μg of PKM, 32 μg of ERY, 32 μg TEL or 8 μg of CHL were placed on top of the agar; plates were incubated for 18 to 24 h at 37°C and were then photographed.

RNA preparation and primer extension. For isolation of the total RNA from *S. venezuelae*, cells were grown overnight in SGGP media, then diluted 1:100 in the SCM media (45) and grown for 5 days at 30°C with constant shaking. Cells were pelleted from 5 ml cultures,

resuspended in 1 ml TE buffer (10 mM Tris-HCl, pH 8.0, 1 mM EDTA) containing 5 mg/ml lysozyme, incubated for 10 min at room temperature and then shaken for 10 min in the mini-bead breaker (Biospec products) with 50 µl of glass beads (particle size ≤ 106 µm) (Sigma-Aldrich). Total RNA was isolated using RNeasy maxi kit (Qiagen).

The RNeasy Plus mini kit was used to prepare total RNA from exponentially growing *E. coli* following standard manufacturer's protocol. Primer extension analysis under the standard conditions suitable for detection of adenine N6 dimethylation was carried out as previously described (33). In experiments where detection of N6 monomethylation was required, the concentration of dTTP was reduced from 1 mM to 0.01 mM with extension for 15 min at 37°C instead of the standard 30 min at 42°C. Primers L2180, L2563 and L2667 (Table II.I) were used to examine domain V of 23S rRNA of *E. coli*. Primer L2405-R was used to check the modification status of A2058 in 23S rRNA of *S. venezuelae*.

Toe-printing Assay. Toe-printing was carried out as described previously (35). The templates containing genes coding for the putative PikR leader peptides under the control of the T7 promoter were generated by PCR using primers T7-pikR1-ORF1-fwd and pikR1-ORF1-rev-spacer-NVI (*pikR1L*), T7-SD-ORF2-pikR2, O2-R2-IL-R, T7, and O2-R2-NV1-R (*piKR2L*) (Table II.I). The reverse PCR primer replaced the penultimate *pikR2* Arg codon (CGC) with an Ile codon (ATC) in order to enable macrolide-independent translation arrest at this codon. The templates were translated in 5 µl of PURExpress cell-free translation reactions (New England Biolabs) for 30 min at 37°C. All the reactions contained 50 µM mupirocin, an Ile-RS inhibitor. When needed, other antibiotics (MTM, PKM, ERY, TEL or thiostrepton) were added to the final concentration of 50 µM. Following the addition of 5'-[^{32}P]-radiolabeled primer NV1, reverse transcription was carried out for 15 min at 37°C. Samples were then processed and analyzed as described in (35).

Mass-spectrometry analysis of rRNA modification. The status of rRNA modification in *E. coli* and *S. venezuelae* was analyzed using the approach described previously (46). Briefly, total RNA was extracted from cells (see above) and hybridized with the DNA oligonucleotides complementary to the 23S rRNA sequence C2035-C2084 (*E. coli*) or C2025-C2083 (*S. venezuelae*). rRNA regions that were not protected by hybridization were digested away with nucleases, and the protected rRNA fragments were isolated by gel electrophoresis. The purified material was digested with RNase T1 or RNase A and subjected to MALDI-ToF on a Bruker Daltronics Ultraflextreme spectrometer recording in reflector and positive ion modes (47). Spectra were analyzed using Flexanalysis software (Bruker).

TABLE II.I. PRIMERS USED IN THE STUDY

Name	Sequence
NdeI-pikR1-D2	TCGTTCCATATGGCAATGCGCGACTCCAT
AflII-pikR1-R2	CTTAAGCTTAAGCCAGACCAGCGGGAGGCGGA
NdeI-pikR2-D2	GACTCCATATGGCATTTTCCCCGCAGGGCGG
AflII-pikR2-R2	CCCACCTTAAGGGTCGGATCCGGCTCAGCAC
ORF-PikR1-D-new	CAGCTGCATATGGGTAACAGCCGATCCC
ORF-PikR1-R	TCTAGCTTAAGGTCGCGCATTGCCATGAACGATCCC
ORF2-PikR2-D	GACTATCATATGCAGTTCTGCCACTCTCAG
ORF2-PikR2-R	TACTAGCTTAAGCGGGGAAAATGCCATGAG
T7-pikR1-ORF1-fwd	ATTAATACGACTCACTATAGGGATATAAGGAGGAAAACATATGGGTAACAGCCGATCC
pikR1-ORF1-rev-spacer-NVI	GGTTATAATGAATTTTGCTTATTAACGATAGAATTCTATCACATTATGTCGGGGGTGAAATCAA
T7-SD-ORF2-pikR2	ATTAATACGACTCACTATAGGGATATAAGGAGGAAAACATATGCAGTTC
O2-R2-IL-R	TTAACGATAGAATTCTATCACGGACGCGCGAGGATCGAGACGCGTGAGGAGGGGCCCGCCGCTAGGAGATGCGCAGCCTCATGTAACGGG
T7	ATTAATACGACTCACTATAGGG
O2-R2-NV1-R	GGTTATAATGAATTTTGCTTATTAACGATAGAATTCTATCACG
NV1	GGTTATAATGAATTTTGCTTATTAAC
L2405-R	AGAGTGGTATTTCAACGGCGA
L2563	TCGCGTACCACTTTA
L2667	GGTCCTCTCGTACTAGGAGCAG
L2180	GGGTGGTATTTCAAGGTCGG
SR199	GCTATGACATGATTACGATTCGTCCCGGAGCGCCACACG
SR200	ACCGCATGCACCAGGCCGTCGATCTCG
SR201	GCCTGGTGCATGCGGTACGGAGCTCC
SR202	CGACGGCCAGTGCCAAGCTTGCGGCGGAAATTCGAAGG
SR216	GCTATGACATGATTACGAATTCGGAGTACTGGCCATCCGGC
SR217	CGAGGCGATCGTCGTACGGACGCCGC
SR218	TACGACGATCGCCTCGGTATGGAGTCG
SR219	CGACGGCCAGTGCCAAGCTTGTCTCCGGAAGCCGCGCT
SR220	GCTATGACATGATTACGAATTCCCACGACCCGACGCAG

SR220	GCTATGACATGATTACGAATTCCCACGACCCGACGCAG
SR221	CGAGGCGAGGAAAATGCCATGAGTCTGCTCC
SR222	GCATTTTCCTCGCCTCGGTATGGAGTCG
pMIP12-R2-D2	ATGGATTAGAAGGAGAAGTACCGATGGGATTCTGCCACTCTCAGGCCCGTTACA
pMIP12-R2-R	TCGCCCGATCCCGTGTTTCGCTATTTCACGCGCTCTCCGCCCGCC
pMIP12-R2-D2-short	TTCTGCCACTCTCAGGCCCGTTACA
pMIP12-R2-R-short	TCACGCGCTCTCCGCCCGCC
pMIP12-R1-R	TCGCCCGATCCCGTGTTTCGCTATTACGAATTCCTCGGACTCACTCTTGGAC
acrAup	CATATGTTCGTGAATTTACAG
acrAdown	GCAATCGTAGGATATTGCG

TABLE II.II. PLASMIDS USED IN THE STUDY

Plasmid Name	Notes	Reference
pERM*Za*	The reporter plasmid containing the regulatory region of the macrolide-inducible *ermC* gene in which codons 3-244 of the *ermC* gene are replaced with 57 codons of *lacZa* gene	(33)
pPikR1	pERM*Za* derivative constitutively expressing the *pikR1* gene under the control of the Ptac promoter and optimized Shine-Dalgarno sequence	This study
pPikR2	pERM*Za* derivative constitutively expressing the *pikR1* gene under the control of the Ptac promoter and optimized Shine-Dalgarno sequence	This study
pRL1	pERM*Za* derived reporter plasmid containing the regulatory region of the *pikR1* gene in which codons 6-331 of the *pikR1* gene are replaced with 57 codons of *lacZa*. The transcription is driven by the Ptac promoter.	This study
pRL2	The reporter plasmid containing the regulatory region of the *pikR1* gene in which codons 6-317 of the *pikR2* gene are replaced with 57 codons of *lacZa*. The transcription is driven by the Ptac promoter.	This study
pRL2R2	pERM*Za* derived plasmid containing the *pikR2* gene and 208 bp of the upstream regulatory region including the *pikR2L* regulatory ORF. The transcription is driven by the Ptac promoter.	This study
pKC1139	*E. coli* - *Streptomyces* shuttle vector pKC1139 containing a temperature-sensitive replicon	(53)
pSRP112	pKC1139-derived plasmid containing flanking regions of the *pikR2* gene; used for inactivation of *pikR2* in the genome of *S. venezuelae* DHS2001	This study
pSRP113	pKC1139-derived plasmid containing flanking regions of the *pikR1* gene; used for deletion of *pikR1* from the genome of *S. venezuelae* DHS2001	This study
pSRP114	pKC1139 containing flanking regions of the *pikR1-pikR2* gene cluster; used for deletion of *pikR1-pikR2* cluster from the genome of *S. venezuelae* DHS2001	This study
pMIP12	*E. coli – M. smegmatis* shuttle vector containing kanamycin resistance gene	(54)

pMR2	pMIP12-derivative containing *pikR2* with its regulatory region under the control of the PBlaF* promoter.	This study
pMR1R2	pMIP12-derivative containing *pikR2* with its regulatory region under the control of the PBlaF* promoter.	This study

TABLE II.III. STRAINS USED IN THE STUDY

Strain	Genotype	Reference
E. coli JM109	*F′ (traD36, proAB+ lacIq, Δ(lacZ)M15) endA1 recA1 hsdR17(rk -, mk+) mcrA supE44 λ- gyrA96 relA1 Δ(lac- proAB) thi-1*	(58)
E. coli JM109 Δ*acrA*	JM109, Δ*acrA*	This study
E. coli JM109 Δ*acrB*	JM109, Δ*acrB*	(52)
E. coli BW25113	*F-, Δ(araD-araB)567, ΔlacZ4787(::rrnB-3), λ-, rph-1, Δ(rhaD-rhaB)568, hsdR514*	(50)
E. coli JW3466	BW25113, Δ *rlmJ*::kan	(51)
S. venezuelae ATCC15439	Wild type	(21)
WT* (DHS2001)	*S. venezuelae* ATCC15439, Δ*pikAI-pikAIV*	(29)
DHS8708	*S. venezuelae* ATCC15439, Δ*desI*	(59)
R1 (DHS328)	DHS2001, Δ*pikR2*	This study
R2 (DHS330)	DHS2001, Δ*pikR1*	This study
Δ (DHS332)	DHS2001, Δ*pikR1*- Δ*pikR2*	This study
ermKO-4	*M. smegmatis* mc^2155 Δ*erm38*	(55)

2.3 Results

2.3.1 *pikR1* and *pikR2* confer resistance to MTM and PKM

We first assessed whether *pikR1* and *pikR2*, which show similarity to macrolide resistance *erm* genes (26), confer resistance to the natural ketolides MTM and PKM produced by *S. venezuelae*. The *pikR* ORFs were individually expressed from plasmids pPikR1 and pPikR2 (Table II.II) in an *Escherichia coli* strain that is hyper-susceptible to macrolides. While cells lacking these genes were completely inhibited by 4 μg/ml of MTM or 8 μg/ml of PKM, expression of *pikR1* or *pikR2* rendered *E. coli* resistant to >512 μg/ml of either of the compounds. This indicates that, when expressed, *pikR1* and *pikR2* confer resistance to natural ketolides and thus have evolved to protect *S. venezuelae* from its endogenous protein synthesis inhibitors.

2.3.2 PikR1 and PikR2 modify the same 23S rRNA nucleotide

The presence of two resistance genes of potentially similar function may suggest that one of them is redundant, and thus prompted us to dissect their individual functions, and to determine whether there are significant differences in their modes of action. The sites of action of MTM and PKM in the bacterial ribosome have not been biochemically defined previously, although structural evidence from the *Deinococcus radiodurans* large ribosomal subunit suggests that the MTM binding site is in the PTC (27) rather than in the NPET where all conventional 14-membered ring macrolides and ketolides bind (7-10). Therefore, the site of action and the nature of the modifications introduced by PikR1 and PikR2 could not be predicted with any certainty. The majority of the investigated Erm-type enzymes confer resistance to macrolides by dimethylating the exocyclic amine of the 23S rRNA nucleotide A2058 (*E. coli* numbering throughout) (11). A2058 dimethylation (but not monomethylation) stalls the progress of reverse transcriptase (RT) on the RNA template, and can thus be readily detected by primer extension

(28). A strong band corresponding to RT pausing at A2058 on rRNA extracted from *E. coli* cells expressing PikR2 indicated that it probably dimethylates this nucleotide (Fig. 2.3A). In contrast, under the standard primer extension conditions, no reverse transcriptase stop was detected at either A2058 or any other site within the PTC and the adjacent NPET regions on rRNA from cells with pPikR1 (Fig. 2.3A). However, when we optimized primer extension conditions for detecting N6-monomethylation of adenosine (see Materials and Methods and the legend to Fig. 2.2B), RT pausing at A2058 was observed on rRNA from cells expressing PikR1 (Fig. 2.3B, lane 2) supporting the hypothesis that PikR1 monomethylates A2058. No additional modifications were detected under these conditions.

The nature of the reactions catalyzed by PikR1 and PikR2 was corroborated by mass spectrometry. A 50 nt-long 23S rRNA fragment encompassing A2058 was isolated from rRNA extracted from *E. coli* cells expressing PikR1 or PikR2 and subjected to RNase A digestion and MALDI-ToF mass spectrometric analysis. In the PikR1 sample, the peak corresponding to the unmodified RNA fragment $GGA_{2058}AAGAC$ (*m/z* 2675) was almost absent and a new peak at *m/z* 2689 appeared (Fig. 2.3C) indicating a methyl group had been added. In the corresponding 23S rRNA fragment from the PikR2 sample, the unmethylated peak was also absent and replaced by a peak at *m/z* 2703 showing addition of two methyl groups (Fig. 2.3D). Combined with the results of primer extension analysis, the mass spectrometry data demonstrate that PikR1 and PikR2 target the same rRNA nucleotide but generate two different products: PikR1 monomethylates A2058 whereas PikR2 dimethylates this nucleotide.

2.3.3 *pikR1* is constitutively expressed in the native host, whereas *pikR2* is activated only when antibiotics are produced

Why does a ketolide-producer that is equipped with the A2058 dimethyltransferase gene *pikR2* also need the *pikR1* gene, whose product merely monomethylates the same nucleotide?

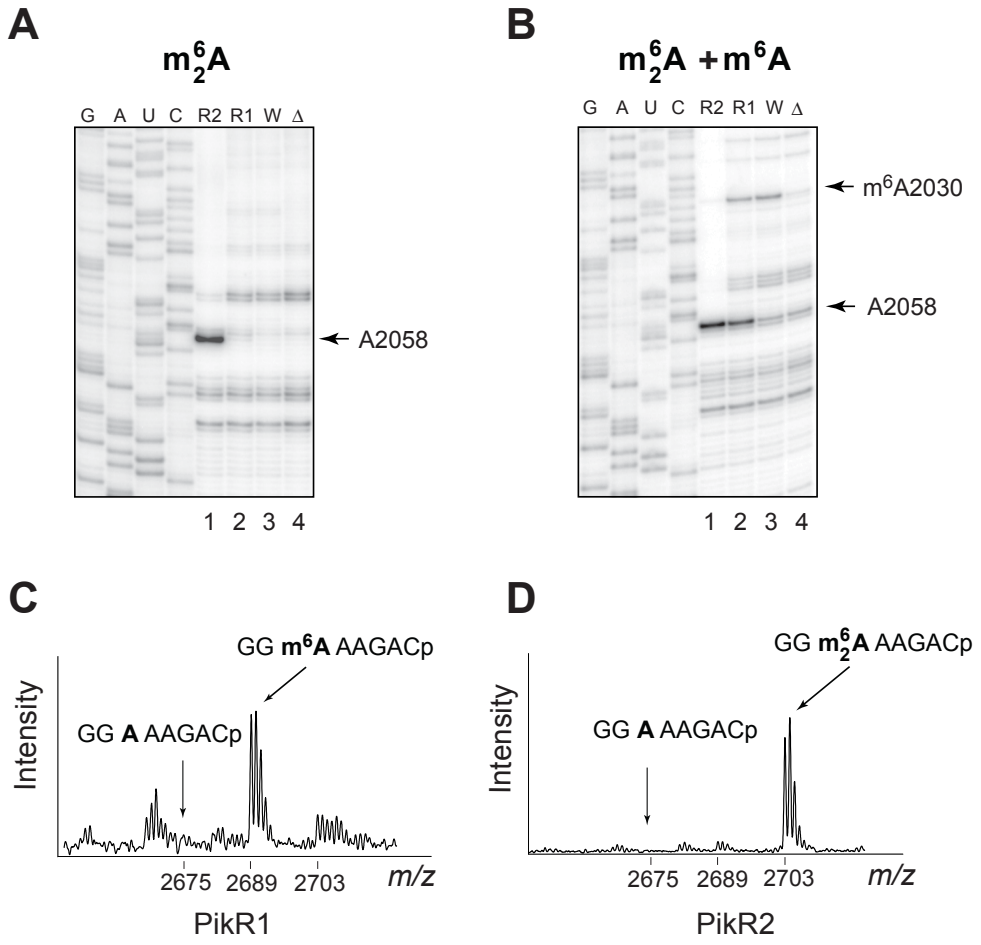

Figure 2.3: PikR1 and PikR2 RNA methyltransferases target A2058 in the 23S rRNA. (A) Primer extension analysis of m_2^6A modification of rRNA extracted from wild type *E. coli* cells (W, lane 3) or those constitutively expressing *pikR1* (R1, lane 2) and *pikR2* (R2, lane 1) genes. (*B*) Primer extension analysis of the same samples as in (A) but carried out under conditions optimized for detection of m^6A modification (see materials and methods). The *E. coli* Δ*rlmJ* mutant, which lacks the native m^6 modification of A2030 (48) was used as a control (Δ, lane 4). (C) and (D), MALDI-ToF analysis of the RNase A - generated 23S rRNA fragment encompassing nucleotide A2058. rRNA samples were prepared from cells expressing PikR1 (C) or PikR2 (D).

To address this question, we examined the regulation of expression of *pikR1* and *pikR2* in *S. venezuelae* ATCC 15439. When production of functional antibiotics was inactivated in *S. venezuelae* by deletion of either the *pikAI-pikAIV* genes (Δ*pikA*) or the *desI* gene (Δ*desI*) in thebiosynthetic operon (leaving the *pikR1* and *pikR2* resistance genes intact), A2058 in the 23S rRNA was found to be fully monomethylated (Fig. 2.4), but there was essentially no dimethylation of A2058 in these strains (Fig. 2.4 A, D, E). This result indicated that *pikR1* is constitutively expressed, whereas *pikR2* remains inactive when no antibiotic is produced. In contrast, the antibiotic-producing wild type *S. venezuelae* ATCC 15439, converted a significant fraction (ca. 30%) of A2058 to m_2^6A (Fig. 2.4A and C), showing that *pikR2* is activated when MTM and/or PKM are present in the cell. Because dimethylation of A2058 is known to reduce cell fitness (25), the inducible nature of *pikR2* is consistent with an evolutionary adaptation by the antibiotic-producing host to achieve secure protection against endogenously produced ketolides while maintaining a low fitness cost for this service.

2.3.4 Expression of *pikR2* is activated in the natural host by clinically relevant ketolides

Induction of *pikR2* by natural ketolides in its native host suggested that the gene could also be activated by medically relevant ketolides. Therefore, we tested whether pre-incubation with the clinical ketolide TEL could activate *pikR2* expression in *S. venezuelae.* Derivative strains containing only *pikR1* (DHS328), only *pikR2* (DHS330), or lacking both *pikR* genes (DHS332) (designated in this manuscript as R1, R2 or Δ, respectively) were prepared from the Δ*pikA* strain (DHS2001, designated here as WT*) (29). Without pre-incubation, the WT* and R1 cells showed an intermediate level of resistance to TEL (MIC 8 μg/ml) whereas R2 and Δ were highly sensitive (MIC 0.25 μg/ml) (Table II.IV). Pre-incubation of the WT* and R2 strains with

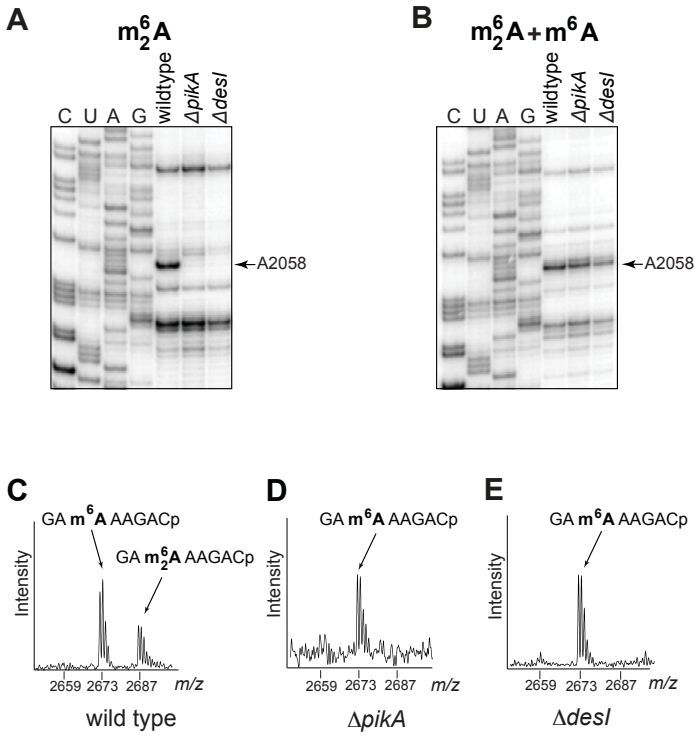

Figure 2.4: Expression of *pikR2* in *S. venezuelae* is activated during antibiotic production. (A) and (B), primer extension analysis of rRNA extracted from different *S. venezuelae* strains, carried under conditions specific for detection of m_2^6A (A) or m_2^6A and m^6A (B) modification. RNA was extracted from the wild type cells or from mutants that are unable to produce active antibiotics due to knock-out of the *pikAI- pikAIV* (Δ*pikA*) or *desI* (Δ*desI*) genes. (C, D, E), MALDI-ToF analysis of 23S rRNA fragments from the wild type or the Δ*pikA* and Δ*desI* knock-out mutants of *S. venezuelae*; the fragments were generated with RNase A and encompass nucleotide A2058.

TEL concentrations of one-fourth the MICs raised their respective resistance levels 8- and 64-fold (Table II.IV). The higher resistance of the WT* and R2 cells upon exposure to sub-inhibitory concentrations of TEL correlated with increased dimethylation at nucleotide A2058 (Fig. 2.5).

The microbiological and biochemical data thus demonstrate that although constitutive expression of *pikR1* provides some protection from the clinical ketolide, TEL, resistance is dramatically increased by drug-mediated activation of *pikR2*.

2.3.5 Molecular mechanism of *pikR2* induction

Macrolide resistance genes are activated via programmed ribosome stalling at the upstream leader ORFs (30-32). Many of the resistance genes are induced exclusively or preferentially by cladinose-containing macrolides, whereas ketolides are poor inducers (18,12). Indeed, ketolides owe their high activity against many clinical isolates to their low propensity for activation of inducible resistance genes. No resistant genes induced specifically by ketolides are currently known.

We were interested in elucidating the molecular mechanism of ketolide-dependent induction of the *pikR2* gene. Examination of the *pikR2* upstream regions revealed the presence of a 16-codon ORF (*pikR2L*), 157 bp upstream of *pikR2* (Fig. 2.6A). The role played by *pikR2L* in ketolide-mediated inducibility was investigated using a plasmid construct containing the *pikR2L* ORF, the intergenic region, and the first five codons of *pikR2* fused to the *lacZα* reporter gene (Fig. 2.6B). An *E. coli* Ptac promoter drives transcription of the reporter system. Induction of the *pikR2-lacZα* chimera was tested in *E. coli* by a disk-diffusion assay (33). Natural and semi-synthetic clinical ketolide antibiotics, but notably not the cladinose-containing macrolide ERY, activated expression of the *pikR2L*-based reporter system (Fig. 2.6B). These data demonstrate that ketolide-specific induction of *pikR2* occurs at the level of translation and is likely controlled

TABLE II.IV: MIC (µg/ml) OF TEL OR CHLORAMPHENICOL (CHL) FOR *S. venezuelae* Δ*pikA* STRAINS CONTAINING DIFFERENT *pikR* RESISTANCE GENES.

Strains [a)]	Antibiotics					
	TEL			CHL		
	no pre-incubation	pre-incubated [b)]	**fold change**	no pre-incubation	pre-incubated [b)]	**fold change**
WT*	8	64	**8**	8	8	**1**
Δ (Δ*pikR1*/Δ*pikR2*)	0.25	0.25	**1**	8	8	**1**
R1 (Δ*pikR2*)	8	16	**2**	8	8	**1**
R2 (Δ*pikR1*)	0.25	16	**64**	8	8	**1**

[a)] The Δ*pikA* strain, which contained both *pikR1* and *pikR2* resistance genes but was unable to produce antibiotics (DHS2001) was designated 'WT*' control. Formal names of the other strains are DHS332 (Δ), DHGS328 (R1) and DHS330 (R2).

[b)] Cells were grown for 10 h in CRM medium (containing the following components (grams per liter): glucose, 10; sucrose, 103; $MgCl_2.6H_2O$, 10.12; tryptic soy broth, 15; and yeast extract, 5) supplemented with one-fourth the MIC of TEL (0.0625 µg/ml for Δ and R2 strains or 2 µg/ml for WT* and R1 strains) prior to MIC testing.

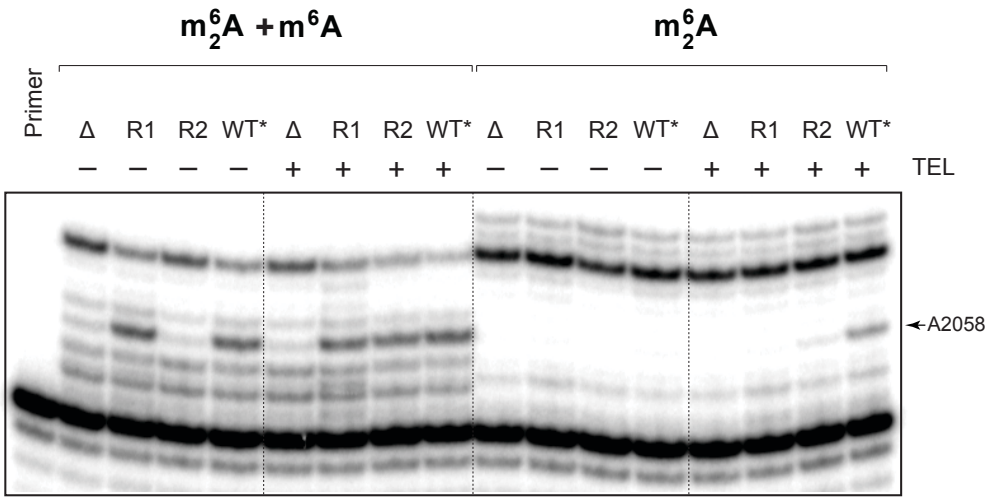

Figure 2.5: The expression of *pikR2* is induced in the host by TEL. Primer extension analysis of mono- and di-methylation of A2058 in 23S rRNA extracted from different *S. venezuelae* mutants without (-) and with (+) preincubation for 10 h with 1/4 fold MIC of TEL. All the strains used in the experiment were derivatives of the Δ*pikA* strain (WT*) containing only *pikR1* (R1), only *pikR2* (R2), or lacking both of the *pikR* genes (Δ).

by the upstream sequence, which includes a putative leader ORF.

The mechanism of translational induction was investigated in a cell-free transcription-translation system using a primer extension assay (toeprinting) (34, 35) to test for ketolide- and macrolide- induced stalling of the ribosome on the *pikR2L* mRNA. Both of the natural ketolides MTM and PKM induced strong translation arrest at the Leu13 codon of *pikR2L* where they stalled approximately 50% of the ribosomes (Fig. 2.6C, lanes 2 and 3). Unexpectedly, the clinical ketolide TEL was even more potent in arresting the ribosome at the Leu13 codon (Fig. 2.6C, lane 4). In contrast, ERY failed to induce ribosome stalling (Fig. 2.6C, lane 5) and this was consistent with the lack of *in vivo* induction of the *pikR2L* reporter system by this macrolide (Fig. 2.6B). Taken together, the results suggest that *pikR2* has been evolutionary optimized for specific activation by natural ketolide antibiotics and that semi-synthetic clinical ketolides can serve as even more potent inducers.

Computational prediction of the mRNA secondary structure suggests that a stable stem-loop configuration in the *pikR2L-pikR2* intergenic region may sequester the *pikR2* ribosome-binding site (Fig. 2.7A). In a model that parallels that of macrolide resistance genes (30), ketolide-induced ribosome stalling at the Leu13 codon of *pikR2L* would destabilize the proximal mRNA stem and promote an alternative conformation in which the initiation region of *pikR2* is accessible for translation (Fig. 2.7B).

2.3.6 Inducible expression of *pikR2*, alone or in combination with *pikR1*, confers high level of ketolide resistance in a clinically-relevant host

After establishing that the natural resistance mechanisms conferred by *pikR1* and *pikR2* in the *Streptomyces* ketolide-producer remain operational upon transfer to *E. coli*, we extended the investigation to a heterologous Gram-positive model because treatment of Gram-positive infections is the primary clinical application of macrolides and the newer ketolides. The Gram-

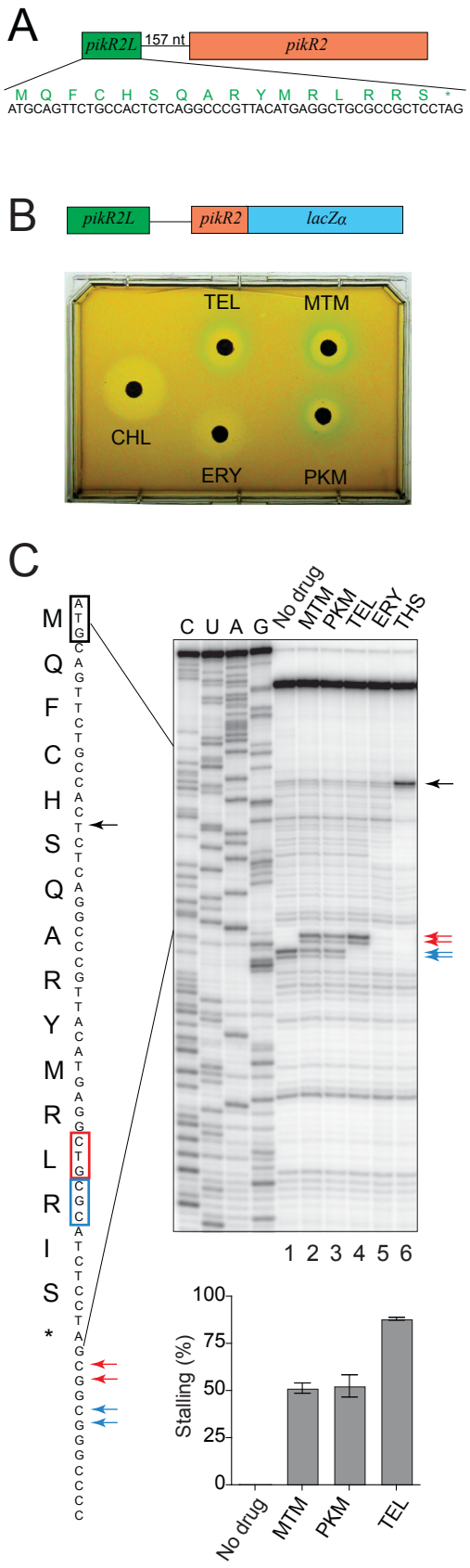
A
pikR2L
157 nt
pikR2
M Q F C H S Q A R Y M R L R R S *
ATGCAGTTCTGCCACTCTCAGGCCCGTTACATGAGGCTGCGCCGCTCCTAG
B
pikR2L
pikR2
lacZα
TEL
MTM
CHL
ERY
PKM
C
M Q F C H S Q A R Y M R L R I S *
C U A G No drug MTM PKM TEL ERY THS
1 2 3 4 5 6
Stalling (%)
100
75
50
25
0
No drug
MTM
PKM
TEL

Figure 2.6: The *pikR2* regulatory region controls the inducible expression of the *pikR2* resistance gene. (*A*) The putative leader ORF *pikR2L* precedes the *pikR2* resistance gene. The nucleotide sequence of the ORF and the amino acid sequence of the encoded leader peptide are shown. (*B*) Antibiotic disk-diffusion assay reveals inducibility of *pikR2* in *E. coli*. In the reporter construct in *E. coli* cells, the *pikR2* regulatory region controls expression of the *lacZ*α reporter. The antibiotic disks contained TEL, MTM, PKM, ERY or chloramphenicol (CHL). The clear areas around the disks contain antibiotic concentrations that inhibited cell growth. Blue halos around the ketolide-containing disks indicate drug-dependent induction of the reporter. (*C*) (Top) Toeprinting analysis shows ketolide-induced ribosome stalling at the Leu13 codon of the *pikR2L* ORF. The band of the ribosomes stalled by the control antibiotic thiostrepton (THS) at the initiation codon is indicated by a black arrow. The ribosomes arrested with the Leu13 codon in their P-site are shown by the red arrows. The ribosomes that reached the *pikR2L* 13th codon but failed to arrest translation were captured at the next Arg14 codon (blue arrows) due to the depletion of Ile-tRNA from the translation reaction by the presence of the Ile-RS inhibitor, mupirocin. (Bottom) Stalling efficiency was calculated from the ratios of the intensity of the bands representing ketolide-dependent arrest (codon 13) *vs*. readthrough (codon 14). Error bars indicate data spread in two independent experiments.

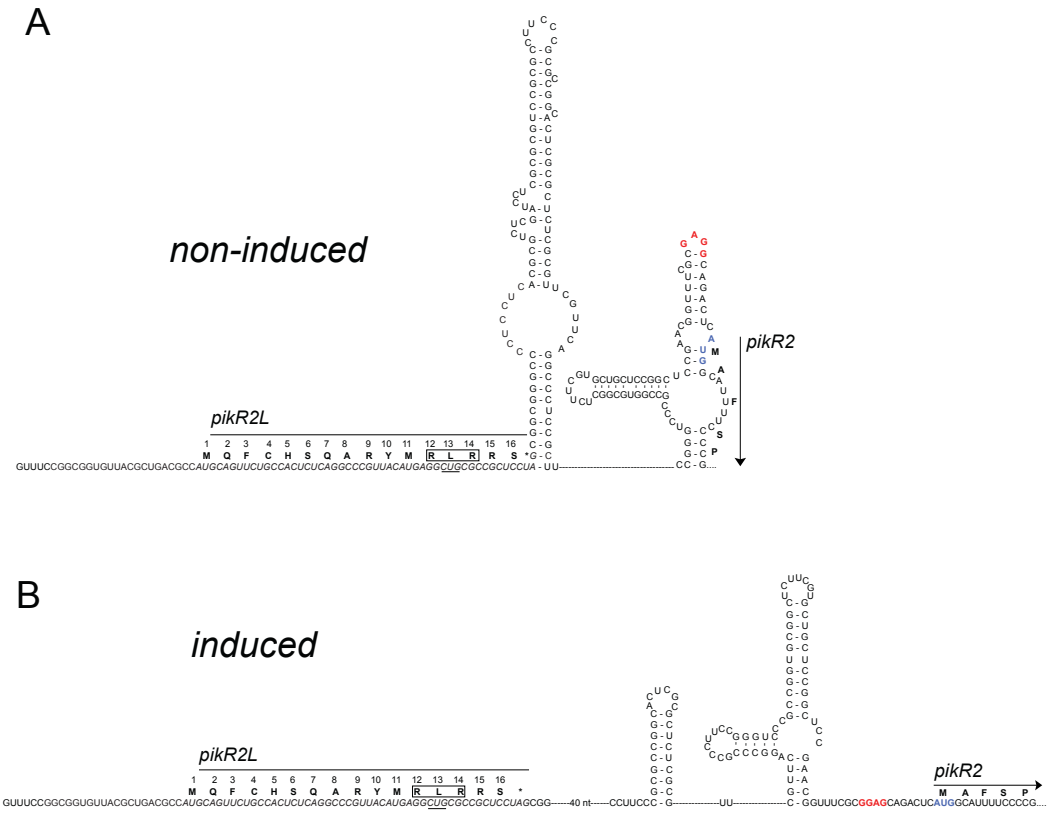

Figure 2.7: The predicted *pikR2* mRNA secondary structures. The models of the secondary structure of *pikR2* mRNA in the non-induced (*A*) and induced (*B*) states. The nucleotide sequence of the leader ORF *pikR2L* is italicized. The RLR sequence in the PikR2L leader peptide, encompassing the Leu13 stalling codon is boxed and the codon is underlined. Shine-Dalgarno region of the *pikR2* gene is shown in red and the initiator codon is blue. The models are based on mfold predictions (57).

positive bacterium *Mycobacterium tuberculosis* is the etiological agent of tuberculosis, and is considered a suitable target for ketolide therapy (36). We constructed strains of *M. smegmatis*, a laboratory model closely related to pathogenic mycobacteria, with either the *pikR2* gene controlled by its regulatory region or with the entire *pikR1-pikR2* cluster (Fig. 2.1A). The presence of *pikR2* alone elevated the resistance of *M. smegmatis* to several clinically relevant ketolides by 16-32 fold without preincubation with the drug (Table II.V). Under the same experimental conditions, the combination of *pikR1* and *pikR2* conferred a much higher level of resistance (exceeding 1 mg/ml for TEL). Constitutive monomethylation of A2058 by PikR1 most likely facilitates continued ribosome activity and expression of *pikR2* upon abrupt exposure of the cells to high concentrations of ketolides. When *M. smegmatis* cells with *pikR2* or *pikR1-pikR2* were pre-incubated with subinhibitory concentrations of TEL, ketolide resistance reached even higher levels exceeding that of the control cells by several hundred fold (Table II.V). Thus the resistance genes originating in the producer of natural ketolides can render heterologous bacteria resistant to high concentrations of clinical ketolide antibiotics.

TABLE II.V: MIC (µg/ml) OF CLINICALLY RELEVANT KETOLIDES [a] FOR *M. smegmatis* [b] HARBORING *pikR1* GENE ALONE OR THE COMBINATION OF *pikR1* AND *pikR2* GENES

Plasmids	TEL		SOL		CET	
	no pre-incubation	pre-incubated [c]	no pre-incubation	pre-incubated [c]	no pre-incubation	pre-incubated [c]
pMIP12 (empty vector)	2	2	1	1	1	2
pMR2	64	2048	16	1024	32	512
pMR1R2	1024	2048	256	1024	256	512

[a] Antibiotics used: telithromycin (TEL), solithromycin (SOL), and cethromycin (CET).

[b] The *M. smegmatis* strain used in MIC testing was a derivative of the strain mc^2 155 in which the endogenous macrolide resistance gene *erm38* was inactivated by allelic exchange (55).

[c] Cells were grown for 72 h in 7H9/ADC/glycerol/tween medium (Milddlebrook 7H11, 10% [albumin, dextrose, catalase], 0.2% glycerol, 0.05% tween 80) supplemented with 1/8 MIC of TEL (0.25 µg/ml for cells transformed with the empty vector, 8 µg/ml for cells transformed with pMR2 or 128 µg/ml for cells transformed with pMR1R2) prior to MIC testing.

2.4 Discussion

In this study, we present evidence that the genes *pikR1* and *pikR2* have been evolutionary optimized to confer resistance to ketolide antibiotics. The *pikR1* and *pikR2* genes not only render *S. venezuelae* ATCC 15439 resistant to its endogenous ketolides, but also confer appreciable resistance to clinical ketolides. The resistance conferred by *pikR1* and *pikR2* can also be transferred to heterologous Gram-negative and Gram-positive hosts. We further show that the fitness cost of resistance is economized to inducible expression of *pikR2* being activated specifically by ketolides. Taking these factors into account, acquisition of the *pikR1* and *pikR2* genes is expected to confer a marked selective advantage upon bacteria undergoing repeated exposure to ketolides, which could promote the horizontal transfer of these genes to pathogens when ketolides become more widely used in a clinical setting.

Our studies provide insights into the important biological question of why *Streptomyces venezuelae*, the producer of the natural ketolide antibiotic MTM and PKM, maintains two resistance genes with seemingly overlapping functions. We found that the constitutively expressed PikR1 monomethylates 23S rRNA nucleotide A2058 located at the site of ketolide action, and this confers an intermediate level of resistance. Higher levels of resistance are attained with the inducible PikR2 methyltransferase, which adds a second methyl group to the same nucleotide. The combined action of two differentially regulated genes would ensure active protein synthesis in the ketolide-producing cells across a broad range of the inhibitor concentrations.

The inducibility of the *pikR2* gene is significant for the operation of the resistance mechanism in the MTM/PKM producer and in heterologous Gram-positive and Gram-negative hosts. While dimethylation of A2058 is known to significantly reduce cell fitness due to aberrant expression of several cellular genes (25), the presence of only one methyl group at the A2058

exocyclic amine is expected to have less of a deleterious effect. Thus, with a small toll in fitness cost for the constitutive expression of the PikR1 monomethyltransferase, *S. venezuelae* easily tolerates low concentrations of MTM and/or PKM. However, when *S. venezuelae* augments its production of these drugs, activation of the more costly PikR2 enzyme is necessitated, and results in A2058 dimethylation and higher resistance levels. Producers of other natural antibiotics, whose genomes encode more than one resistance gene, may use a similar strategy for achieving the most cost-effective protection from protein synthesis inhibitors (37).

In contrast to other inducible resistance genes, which respond primarily to cladinose-containing macrolide inhibitors, the mechanism of the *pikR2* regulation has been evolutionary selected for specific activation by ketolides (Fig. 2.6). Ketolide-specific induction of *pikR2* is most likely determined by programmed translation arrest site within the upstream *pikR2L* leader ORF. Cladinose-containing macrolides are prone to promoting early peptidyl-tRNA drop-off occurring within the first 6-10 codons (38) (39). Consistently, the sites of programmed macrolide-dependent arrest within the leader ORFs of the known resistant genes are located within the first 10 codons of the leader ORFs, so that the drug-bound ribosome is able to reach the arrest site without prematurely dissociating from the mRNA (11, 35, 40-42). Ribosomes translating *pikR2L* have to travel slightly further and polymerize 13 amino acids prior to reaching the stalling codon from which expression of the downstream resistance gene is activated. Because ketolides are less prone to promoting peptidyl-tRNA drop-off (43), it is apparently easier for ketolide-bound ribosomes than for ERY-bound ribosomes to polymerize the 13 amino acid-long nascent PikR2L chain. Indeed, the ERY-bound ribosome fails to reach the stalling site (Fig. 2.6), and thus also fails to initiate the structural isomerization of the mRNA, which is critical for expression of the downstream *pikR2* gene. Ketolide-induced stalling in the *pikR2L* ORF occurs within the sequence $RL_{13}R$, which is also present in the leader ORFs preceding a

variety of resistance genes (41, 44) and represents one of the most problematic motifs for translation by ketolide-bound ribosomes (43, 44). We note that a short ORF is also found in front of the *pikR1* gene, although this ORF does not promote macrolide- or ketolide-dependent stalling and thus plays no role in the constitutive expression of *pikR1* (Fig. 2.8).

Both the properties and regulation of the *pikR1* and *pikR2* genes are principally important for tolerating the broad range of inhibitor concentrations experienced by *S. venezuelae*. Constitutive monomethylation of A2058 by PikR1 renders ribosomes moderately resistant to ketolides, affording protection to *S. venezuelae* at the early stages of antibiotic production. Monomethylation of A2058 is thus a critical step towards acquisition of high level of resistance, facilitating efficient translation of *pikR2* despite the presence of a ketolide inhibitor. Indeed, upon abrupt exposure of the *S. venezuelae pikR1*-null mutant (Δ*pikR1*) to TEL, the lone *pikR2* gene was unable to provide any significant protection (Table II.IV), but when both *pikR* genes were present and cells were pre-incubated with low concentrations of a ketolide (mimicking the onset of antibiotic production) a high level of resistance was achieved.

The synergy between the *pikR1* and *pikR2* genes was observed to an even greater extent in *M. smegmatis*, which was used to model the expression of the *pikR* genes in clinical pathogens. Here the *pikR2* gene alone conferred considerable resistance to clinical ketolides. However, it was the simultaneous presence of both *pikR1* and *pikR2* genes that provided the highest resistance to the ketolide antibiotics (Table II.V). The inducibility of *pikR2*, which lowers the fitness cost of the two-gene resistance mechanism, may facilitate not only its acquisition by a new host through horizontal gene transfer but also its maintenance upon discontinuation of the antibiotic treatment. Horizontal transfer of the *pikR1/pikR2* gene pair may be further facilitated by their close physical proximity in the *S. venezuelae* chromosome (Fig. 2.1). Despite the high GC content of *pikR1* and *pikR2*, our results strongly suggest that their transfer into some clinical

strains would not hinder their expression and would render the strains highly resistant to ketolide therapy. These findings thus provide further justification for renewed drug-discovery efforts to identify novel variants of macrolides and other antibiotics capable of overcoming resistance rendered by *pikR1* and *pikR2,* as well as by other ribosome-targeting resistance genes that exist in nature.

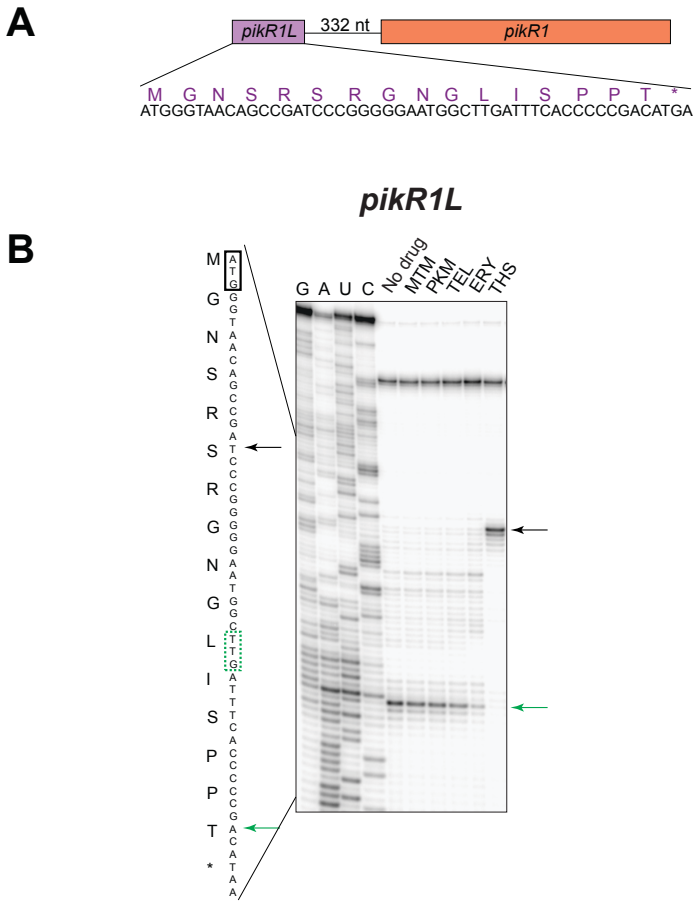

Figure 2.8: In contrast to the mechanism seen for *pikR2*, regulation of the *pikR1* gene does not occur via stalling at its putative upstream ORF. (*A*) The sequence of the putative upstream ORF (*pikR1L*) and the encoded protein sequence. (*B*) Toeprinting analysis does not show any ketolide- or macrolide-specific stops during in vitro translation of the *pikR1L* ORF. The black arrow indicates the toeprinting band corresponding to the ribosome stalled by the control antibiotic thiostrepton (THS) at the *pikR1L* initiator codon (boxed). The green arrow shows the band representing the ribosomes that were captured at the *pikR1L* 11th codon (boxed) due to the depletion of Ile-tRNA from the translation reaction by the presence of the Ile-RS inhibitor, mupirocin.

2.5 Cited literature

1. Watve MG, Tickoo R, Jog MM, & Bhole BD (2001) How many antibiotics are produced by the genus Streptomyces? *Arch Microbiol* 176(5):386-390.

2. Newman DJ & Cragg GM (2012) Natural products as sources of new drugs over the 30 years from 1981 to 2010. *J Nat Prods* 75(3):311-335.

3. Cundliffe E (1989) How antibiotic-producing organisms avoid suicide. *Annu Rev Microbiol.* 43:207-233.

4. Cundliffe E & Demain AL (2010) Avoidance of suicide in antibiotic-producing microbes. *J Ind Microbiol Biotechnol* 37(7):643-672.

5. D'Costa VM, McGrann KM, Hughes DW, & Wright GD (2006) Sampling the antibiotic resistome. *Science* 311(5759):374-377.

6. Iacoviello VR, Zinner, S. H. (2002) Macrolides: a clinical overview. *Macrolide Antibiotics*, ed Parnham MJ, Bruinvels, J. (Birkhäuser Verlag, Bael), pp 15-24.

7. Schlunzen F*, et al.* (2001) Structural basis for the interaction of antibiotics with the peptidyl transferase centre in eubacteria. *Nature* 413(6858):814-821.

8. Tu D, Blaha G, Moore PB, & Steitz TA (2005) Structures of MLSBK antibiotics bound to mutated large ribosomal subunits provide a structural explanation for resistance. *Cell* 121(2):257-270.

9. Bulkley D, Innis CA, Blaha G, & Steitz TA (2010) Revisiting the structures of several antibiotics bound to the bacterial ribosome. *Proc Natl Acad Sci USA* 107(40):17158-17163.

10. Dunkle JA, Xiong L, Mankin AS, & Cate JH (2010) Structures of the *Escherichia coli* ribosome with antibiotics bound near the peptidyl transferase center explain spectra of drug action. *Proc Natl Acad Sci USA* 107(40):17152-17157.

11. Weisblum B (1995) Erythromycin resistance by ribosome modification. *Antimicrob Agents Chemother* 39(3):577-585.

12. Vázquez-Laslop N, Ramu, H., Mankin, A.S. (2011) Nascent peptide–mediated ribosome stalling promoted by antibiotics. *Ribosomes: Structure, Function, and Dynamics*, ed Rodnina MV, Green, R., Wintermeyer, W. (Springer-Verlag, Vienna).

13. Bryskier A (2000) Ketolides-telithromycin, an example of a new class of antibacterial agents. *Clin Microbiol Infect* 6(12):661-669.

14. Bush K (2012) Improving known classes of antibiotics: an optimistic approach for the future. *Curr Opin Pharmacol* 12(5):527-534.

15. Sutcliffe JA (2011) Antibiotics in development targeting protein synthesis. *Ann N Y Acad Sci* 1241:122-152.

16. Clarebout G & Leclercq R (2002) Fluorescence assay for studying the ability of macrolides to induce production of ribosomal methylase. *Antimicrob Agents Chemother* 46(7):2269-2272.

17. Rosato A, Vicarini H, Bonnefoy A, Chantot JF, & Leclercq R (1998) A new ketolide, HMR 3004, active against streptococci inducibly resistant to erythromycin. *Antimicrob Agents Chemother* 42(6):1392-1396.

18. Bonnefoy A, Girard AM, Agouridas C, & Chantot JF (1997) Ketolides lack inducibility properties of MLS(B) resistance phenotype. *J Antimicrob Chemother* 40(1):85-90.

19. Brown P & Dawson MJ (2015) A perspective on the next generation of antibacterial agents derived by manipulation of natural products. *Progr Med Chem* 54:135-184.

20. Brockman H, Henkel, W. (1950) Pikromycin, ein neues Antibiotikum aus Actinomyceten. *Naturwissenschaften* 37:138-139.

21. Lambalot RH & Cane DE (1992) Isolation and characterization of 10-deoxymethynolide produced by Streptomyces venezuelae. *J Antibiot*45(12):1981-1982.

22. Xue Y, Wilson D, & Sherman DH (2000) Genetic architecture of the polyketide synthases for methymycin and pikromycin series macrolides. *Gene* 245(1):203-211.

23. Xue Y, Zhao L, Liu HW, & Sherman DH (1998) A gene cluster for macrolide antibiotic biosynthesis in Streptomyces venezuelae: architecture of metabolic diversity. *Proc Natl Acad Sci USA* 95(21):12111-12116.

24. Kittendorf JD & Sherman DH (2009) The methymycin/pikromycin pathway: a model for metabolic diversity in natural product biosynthesis. *Bioorg Med Chem* 17(6):2137-2146.

25. Gupta P, Sothiselvam S, Vazquez-Laslop N, & Mankin AS (2013) Deregulation of translation due to post-transcriptional modification of rRNA explains why erm genes are inducible. *Nat Commun* 4:1984.

26. Roberts MC (2008) Update on macrolide-lincosamide-streptogramin, ketolide, and oxazolidinone resistance genes. *FEMS Microbiol Lett* 282(2):147-159.

27. Auerbach T, Mermershtain, I., Bashan, A., Davidovich, C., Rozenberg, C. H., Sherman, D. H., Yonath, A. (2009) Structural basis for the antibacterial activity of the 12-membered-ring mono-sugar macrolide methymycin. *Biotechnologia* 1:24-35.

28. Vester B & Douthwaite S (1994) Domain V of 23S rRNA contains all the structural elements necessary for recognition by the ErmE methyltransferase. *J Bacteriol* 176:6999-7004.

29. Jung WS, *et al.* (2006) Heterologous expression of tylosin polyketide synthase and production of a hybrid bioactive macrolide in Streptomyces venezuelae. *Appl Microbiol Biotechnol* 72(4):763-769.

30. Weisblum B (1995) Insights into erythromycin action from studies of its activity as inducer of resistance. *Antimicrob Agents Chemother* 39(4):797-805.

31. Ramu H, Mankin A, & Vazquez-Laslop N (2009) Programmed drug-dependent ribosome stalling. *Mol Microbiol* 71(4):811-824.

32. Subramanian SL, Ramu H, & Mankin AS (2011) Inducible resistance to macrolide antibiotics. *Antibiotic Drug Discovery and Development*, ed Dougherty TJ, Pucci, M. J. (Springer Publishing Company, New Yoork, NY).

33. Bailey M, Chettiath T, & Mankin AS (2008) Induction of ermC expression by 'non-inducing' antibiotics. *Antimicrob Agents Chemother* 52:866-874.

34. Hartz D, McPheeters DS, Traut R, & Gold L (1988) Extension inhibition analysis of translation initiation complexes. *Methods Enzymol* 164:419-425.

35. Vazquez-Laslop N, Thum C, & Mankin AS (2008) Molecular mechanism of drug-dependent ribosome stalling. *Mol Cell* 30(2):190-202.

36. Falzari K, *et al.* (2005) In vitro and in vivo activities of macrolide derivatives against Mycobacterium tuberculosis. *Antimicrob Agents Chemother* 49(4):1447-1454.

37. Memili E & Weisblum B (1997) Essential role of endogenously synthesized tylosin for induction of ermSF in Streptomyces fradiae. *Antimicrob Agents Chemother* 41(5):1203-1205.

38. Otaka T & Kaji A (1975) Release of (oligo) peptidyl-tRNA from ribosomes by erythromycin A. *Proc Natl Acad Sci USA* 72(7):2649-2652.

39. Tenson T, Lovmar M, & Ehrenberg M (2003) The mechanism of action of macrolides, lincosamides and streptogramin B reveals the nascent peptide exit path in the ribosome. *J Mol Biol* 330(5):1005-1014.

40. Ramu H, *et al.* (2011) Nascent peptide in the ribosome exit tunnel affects functional properties of the A-site of the peptidyl transferase center. *Mol Cell* 41:321-330.

41. Sothiselvam S, *et al.* (2014) Macrolide antibiotics allosterically predispose the ribosome for translation arrest. *Proc Natl Acad Sci USA* 111(27):9804-9809.

42. Arenz S, *et al.* (2014) Molecular basis for erythromycin-dependent ribosome stalling during translation of the ErmBL leader peptide. *Nat Communs* 5:3501.

43. Kannan K, *et al.* (2014) The general mode of translation inhibition by macrolide antibiotics. *Proc Natl Acad Sci USA* 111(45):15958-15963.

44. Davis AR, Gohara DW, & Yap MN (2014) Sequence selectivity of macrolide-induced translational attenuation. *Proc Natl Acad Sci USA* 111(43):15379-15384.

45. Zhang Q & Sherman DH (2001) Isolation and structure determination of novamethymycin, a new bioactive metabolite of the methymycin biosynthetic pathway in Streptomyces venezuelae. *J Nat Prod* 64(11):1447-1450.

46. Douthwaite S & Kirpekar F (2007) Identifying modifications in RNA by MALDI mass spectrometry. *Methods Enzymol* 425:1-20.

47. Kirpekar F, Douthwaite S, & Roepstorff P (2000) Mapping posttranscriptional modifications in 5S ribosomal RNA by MALDI mass spectrometry. *RNA* 6:296-306.

48. Golovina AY, *et al.* (2012) The last rRNA methyltransferase of E. coli revealed: the yhiR gene encodes adenine-N6 methyltransferase specific for modification of A2030 of 23S ribosomal RNA. *RNA* 18(9):1725-1734.

49. Hansen DA, *et al.* (2013) Biocatalytic synthesis of pikromycin, methymycin, neomethymycin, novamethymycin, and ketomethymycin. *J Am Chem Soc* 135(30):11232-11238.

50. Datsenko KA & Wanner BL (2000) One-step inactivation of chromosomal genes in Escherichia coli K-12 using PCR products. *Proc Natl Acad Sci USA* 97(12):6640-6645.

51. Baba T, *et al.* (2006) Construction of Escherichia coli K-12 in-frame, single-gene knockout mutants: the Keio collection. *Mol Syst Biol* 2:2006 0008.

52. Vazquez-Laslop N, Ramu, H., Klepacki, D., Kannan, K., Mankin, A. S. (2010) The key role of a conserved and modified rRNA residue in the ribosomal response to the nascent peptide. *EMBO J.* 29:3108-3117.

53. Bierman M, *et al.* (1992) Plasmid cloning vectors for the conjugal transfer of DNA from Escherichia coli to Streptomyces spp. *Gene* 116(1):43-49.

54. Le Dantec C, Winter N, Gicquel B, Vincent V, & Picardeau M (2001) Genomic sequence and transcriptional analysis of a 23-kilobase mycobacterial linear plasmid: evidence for horizontal transfer and identification of plasmid maintenance systems. *J Bacteriol* 183(7):2157-2164.

55. Nash KA (2003) Intrinsic macrolide resistance in Mycobacterium smegmatis is conferred by a novel erm gene, erm(38). *Antimicrob Agents Chemother* 47(10):3053-3060.

56. CLSI (2006) Methods for dilution antimicrobial susceptibility tests for bacteria that grow aerobically. *Approved standard. CLSI document M7-A7* 26(2).

57. Zuker M (2003) Mfold web server for nucleic acid folding and hybridization prediction. *Nucleic Acids Res* 31(13):3406-3415.

58. Yanisch-Perron C, Vieira J, & Messing J (1985) Improved M13 phage cloning vectors and host strains: nucleotide sequences of the M13mp18 and pUC19 vectors. *Gene* 33:103-119.

59. Hansen DA, Koch AA, & Sherman DH (2015) Substrate controlled divergence in polyketide synthase catalysis. *J Am Chem Soc* 137(11):3735-3738.

3. THE SITE OF ACTION OF METHYMYCIN AND PIKROMYCIN, THE NATURAL KETOLIDE ANTIBIOTICS

3.1 Introduction and rationale

The ribosome-targeting macrolide antibiotics are among the most successful antibiotics because they actively inhibit the growth of a broad range of Gram-positive and even some Gram-negative pathogens. While producing very few adverse effects, they have been widely used in clinical practice for decades. The prototype macrolide erythromycin (ERY) is comprised of a 14-member macrolactone ring with two sugars cladinose and desosamine attached at positions C3 and C5, respectively (Fig. 1.3A). ERY structure served as a template for semi-synthetic macrolide antibiotics of the second generation (e.g. clarithromycin, azithromycin, and roxithromycin) with improved stability and pharmacological properties. The spread of clinical strains resistant to macrolides of the first and second generations stimulated the development of the newest version of macrolides, called ketolides. Semisynthetic ketolide antibiotics such as telithromycin (TEL), certhromycin (CET), and solithromycin (SOL) lack a C3 cladinose sugar, which in ketolides, is replaced with a keto function (hence the name of the class) (Fig. 1.3C). In addition, medically useful ketolides carry an extended alkyl-aryl side chain attached either to the 11,12 carbamate ring (in TEL or SOL) or at other sites. Ketolides exhibit superior activity against both macrolide-sensitive and many macrolide-resistant strains.

Macrolides inhibit protein synthesis by binding in the nascent peptide exit tunnel (NPET) in the large ribosomal subunit (Fig. 3.1). NPET starts at the peptidyl transferase center (PTC) where the ribosome polymerizes amino acids into the polypeptide chain and serves as a passageway for the newly made protein on its way out of the ribosome. The macrolide-binding site within the NPET is located at a short distance from the PTC (Fig. 3.1). Association of these

drugs with the ribosome results in several effects, which mostly depends on the amino acid sequence of the synthesized polypeptide. Firstly, by narrowing the NPET, macrolides obstruct progression of the nascent protein chain. At the early rounds of translation such obstruction may result in dissociation of peptidyl-tRNA from the ribosome (25-27). Secondly, binding of macrolides in the NPET allosterically affects the properties of the PTC, inhibiting its ability to catalyze peptide bond formation between a certain combination of the donor and acceptor substrates (31). Proteins that lack such sequences remain largely unaffected by the antibiotics (31, 32). Importantly, the nature of problematic sequences, and thus the spectrum of the resistant proteins in the cell, critically depend on the structure of the drug molecule bound in the NPET (30). Finally, macrolides can induce translation errors by stimulating misincorporation of amino acids or promoting ribosome frameshifting (52, 53).

All ribosome-targeting macrolides, including ketolides, bind to overlapping sites in the ribosome, which are comprised primarily of rRNA. However, the mode of binding and action of ketolides is significantly different from the macrolides of the previous generations. While ketolides lack cladinose-specific contacts, their extended side chain forms additional idiosyncratic interactions in the NPET (20, 23, 54-56). Furthermore, due to the lack of a bulky C3 cladinose, ketolides leave more room in the NPET and are less prone to inhibit translation at its early rounds (30, 31). As a consequence, more proteins continue to be synthesized in the ketolide-treated cells (30, 31). It has been suggested that more selective inhibition of cellular proteins accounts for the stronger antibacterial activity of ketolides (30).

The prototype macrolide ERY is a natural antibiotic originally isolated from *Saccharopolyspora erythraea* (14). Many other biologically active macrolides are produced by various actinomycetes where they are generated via dedicated polyketide biosynthesis pathways (49). The natural 14-member macrolactone ring macrolides usually carry C3 side chains

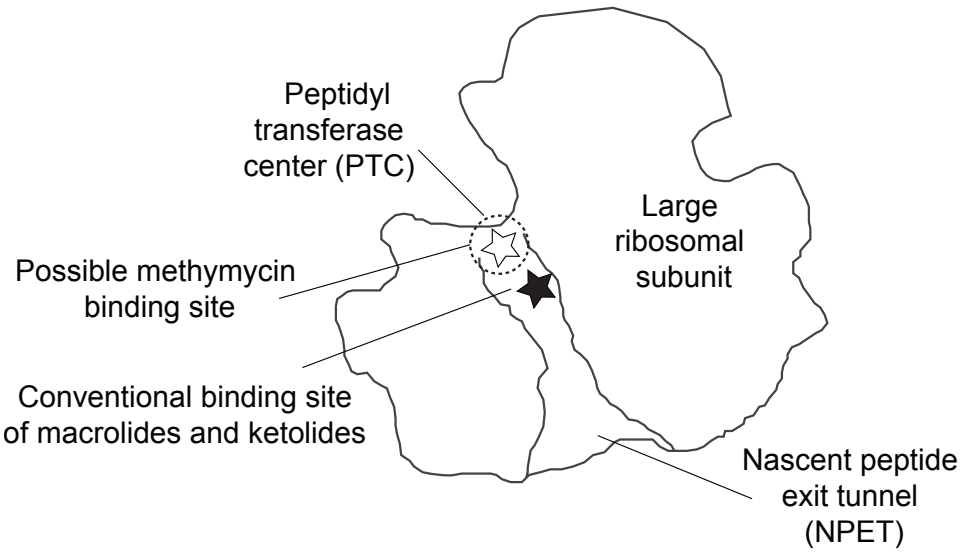

Figure 3.1: The macrolides-binding site(s) in the large ribosomal subunit. The conventional macrolide/ketolide-binding site in the NPET is shown by a black star. Putative methymycin-binding site in the PTC is shown by a white star.

(cladinose or other sugars) (57). The macrolides produced by the *Streptomyces venezuelae* strain ATCC 15439 are a notable exception. Pikromycin (PKM), the main 14-member macrolactone compound secreted by this strain, carries a C3 keto group and thus represents the only currently known natural ketolide (Fig. 1.9B). Due to an alternative translation initiation site in the modular polyketide synthase gene *pikAIV*, the second rather unusual 12-member macrolactone compound methymycin (MTM) is generated by the same biochemical pathway (Fig. 1.9B) (48, 49). Both PKM and MTM possess inhibitory activity against selected bacterial strains. While it remains unclear why *S. venezuelae* has evolved to generate two antibiotics PKM and MTM via the same biochemical pathway, it is well documented that producing two different ribosome-targeting antibiotics could endow the producer with a much more potent weapon. The producers of natural streptogramin antibiotics secrete two compounds (A and B), which both bind to the ribosome at the neighboring sites the PTC and NPET, respectively (29). Cooperative binding of streptogramins accounts for their strong synergistic action (58). Similar ribosomal sites are occupied by two other natural synergistic antibiotics lankamycin and lankacidin. Lankamycin, a 14-membered ring macrolide, binds in the conventional macrolide site in the NPET, whereas the 17-membered polyketide lankacidin binds in the PTC (59, 60). It has been proposed that the neighboring antibiotic sites in the PTC and NPET used by streptogramins or lankamycin/lankacidine are specifically suited for synergistic protein synthesis inhibitors (59). It is conceivable that the pair of natural ketolide compounds MTM and PKM produced by *S. venezuelae* follow the same trend. Moreover, preliminary crystallographic studies suggest that MTM bind to the PTC of the *Deinococcus radiodurans* large ribosomal subunit at the site overlapping that of the classic PTC inhibitor chloramphenicol (CHL) (51).

The unusual biology of producing two related but distinct antibiotics, and the unconventional chemical structure of MTM prompted us to investigate the binding sites and

modes of action of MTM and PKM in the bacterial ribosome within the living cell and in vitro. Biochemical and genetic evidences showed that both antibiotics produced by *S. venezuelae* ATCC 15439 bound to overlapping sites in the NPET. However, the binding site of MTM differs from that of PKM and, as a result, some mutations afford MTM-specific resistance. Due to the differences in their structures and their interactions with the ribosome, MTM and PKM somewhat inhibit the synthesis of different subsets of cellular proteins. Such a differential effect on protein synthesis may provide rationale for the production of two distinct inhibitors via the same biochemical pathway.

3.2 Materials and Methods

Antibiotics, enzymes and chemicals. MTM and PKM were synthesized chemically as previously described (61-63), and repurified by HPLC using a Phenomenex Luna 5u C18 250 x 21.2mm column (serial 444304-4) monitored at 250 nm at a flow rate of 9 mL/min with an isocratic mobile phase of H_2O/MeCN (45/55) and a 0.1% NEt_3 modifier. TEL and SOL were from Cempra, Inc., ERY, CHL and thiostrepton were from Sigma Aldrich. Enzymes used for DNA cloning were from Fermentas. [γ^{32}P]-ATP (specific activity 6000 Ci/mmol) was from MP Biomedicals. Other reagents and chemicals were purchased from either Fisher Scientific or Sigma Aldrich. All oligonucleotides used in the study were synthesized by IDT.

Testing whether PTM and MKM exhibit synergistic activity. Putative synergistic inhibition of cell growth by PTM and MTM was tested by checkerboard MIC experiment using MTM and PKM sensitive strain *S. pyogenes* NZ131. After the pilot MIC determination for each antibiotic individually, the 96-well checkerboard plate was set up with the two fold dilutions of MTM in columns B-H (0.25 –16 μg/ml) and of PKM in the rows 2-12 (0.03125 – 32 μg/ml). The well (A1) did not contain any antibiotic. The starting optical density of the bacterial cells was OD_{600} = 0.004. The plate was incubated overnight at 30°C for 18 hours and the cell growth was visualized by alamar blue staining.

Selection and characterization of resistant mutants. The *E.coli* SQ110DTC strain was used for selection of resistant mutants (64). The SQ110DTC strain was grown overnight at 37°C in LB medium containing 50 μg/ml of spectinomycin and 50 μg/ml of kanamycin. Cells were then diluted 100-fold and grown at 37°C in the presence of spectinomycin and kanamycin until they reached mid-log phase (OD_{600} = 0.4 to 0.7). At 1.25 A_{600} (ca. 10^9) cells of the cell culture were plated onto the LB agar plate supplemented with a 128 μg/ml of MTM, 64 μg/ml of PKM

or 1 μg/ml of CHL. Plates were incubated for two days at 37°C. The 23S rRNA domains V and VI were amplified either directly from the resistant colonies or isolated genomic DNA using the primer pairs L2020 (CCCGAGACTCAGTGAAATTGAACTC) and L2750 (CAAGTTTCGTGCTTAGATGC), L1880D (TCTTGATCGAAGCCCCGGTAA) and L2081 (GGGTGGTATTTCAAGGTCGG). The PCR products were purified and sequenced at the UIC DNA sequencing facility using the same primers.

Ribosome preparation. *S. aureus* RN4220 cells, grown to exponential phase in 1 L BHI medium, were collected by centrifugation and flash frozen. Cell pellets were thawed, resuspended in 25 ml of buffer containing 10 mM Hepes–KOH (pH 7.6), 50 mM KCl, 10 mM $Mg(OAc)_2$, 7 mM β-mercaptoethanol, 0.1 mg/ml lysostaphin and disrupted by two passes through French press at 20,000 psi. Cell debris was removed by centrifugation at 20,000 g for 30 min. Ribosomes were then purified from the cell lysates by chromatography on the HiTrap Butyl FF resin (GE Healthcare) following the published protocol (65).

E. coli ribosomes were prepared from the SQ110DTC (parental strain or the A2503C mutant) following the standard protocol (65).

Chemical probing. rRNA probing was performed following the published protocols, with minor modifications (66). Briefly, ribosomes (200 nM) were incubated without or with antibiotics in 50 μl of buffer B (400 mM HEPES-KOH, pH 7.8, 50 mM $MgCl_2$, 500 mM NH_4Cl) supplemented with 20 U Ribolock RNase inhibitor (40U/μl, Sigma) at 37°C for 10 min, followed by 10 min at 20°C. Antibiotics were present at the final concentration of 50 μM. In MTM titration experiments, the antibiotic was added to the final concentrations of 0.4, 2 and 10 μM. After antibiotic binding, modifying reagent (DMS, kethoxal, or 1-cyclohexyl-3-(2-morpholinoethyl) carbodiimide metho-p-toluene sulfonate) was added and tubes were incubated 10 min at 37°C. The reactions were stopped, ribosomes were ethanol-precipitated and rRNA was

extracted as described (66). The extent of *E. coli* 23S rRNA nucleotide modifications was assessed by primer extension using the primers L2081 (GGGTGGTATTTCAAGGTCGG), L2563 (TCGCGTACCACTTTA), L2667 (GGTCCTCTCGTACTAGGAGCAG), or L2750 (CAAGTTTCGTGCTTAGATGC). The primer SaL2230 (TAGTATCCCACCAGCGTCTC) was used in experiments with the *S. aureus* ribosome.

Toe-printing Assay. Toe-printing was done as described previously (67). The *ermBL* and *ermDL* templates were generated by overlapping PCR as described previously (64, 68). The DNA templates contained the T7 promoter and optimized ribosome-binding sites. The templates were translated in 5 µl of PURExpress cell-free translation reactions (New England Biolabs) without or with 50 µM of antibiotic (MTM, PKM, TEL or thiostrepton) for 30 min at 37°C. Following the addition of 5'-[^{32}P]-radiolabeled primer NV1, reverse transcription reactions were carried out for 15 min at 37°C. Samples were then processed and analyzed in the sequencing gel as described in (67).

2D-gel electrophoresis analysis of the radiolabeled proteins. Pulse labeling of proteins was carried out as described (30). Specifically, *E. coli* strain BWDK was grown overnight at 37°C in the M9 minimal medium containing 0.003 mM thiamine and supplemented with 40 µg/mL of 19 amino acids except methionine (M9AA-M) (69). The cells were diluted 1:200 in fresh M9 medium and grown to exponential phase ($OD_{600}\approx$ 0.2). One ml aliquots of exponential cultures were incubated with either no drug or 50-fold MIC of MTM (400 µg/ml), PKM (400 µg/ml) or SOL (50 µg/ml) for 10 min. Ten µCi of [^{35}S] Methionine (specific activity 1,175 Ci/mmol) was then added, and the cells were incubated for 3 min followed by the addition of unlabeled L-methionine to the final concentration of 80 µg/ml and further incubation for 7min. The cells were pelleted by centrifugation at 3000 rpm for 15 min at 4°C. Pellets were washed

twice with 1.5 ml of M9 medium and flash-frozen in liquid nitrogen. 2D-gel electrophoresis analysis was performed by Kendrick Labs, Inc. (Madison, WI).

TABLE III.I. STRAINS USED IN THIS STUDY

Strain	Genotype	Reference
E. coli SQ110DTC	Δ(*rrsH-aspU*)794(::*FRT*) Δ(*rrfG-rrsG*)791(::*FRT*) Δ(*rrfF-rrsD*)793(::*FRT*) Δ(*rrsC-trpT*)795(::*FRT*) Δ(*rrsA-rrfA*)792(::*FRT*)Δ(*rrsB-rrfB*)790(::*FRT*) Δ(*tolC*) (::*kana*) *rph-1* λ-; ptRNA67	(64)
SQ110DTC- A2503C	SQ110DTC, A2503C	This study
SQ110DTC- A2503G	SQ110DTC, A2503G	This study
SQ110DTC- A2057U	SQ110DTC, A2057U	This study
SQ110DTC- A2058G	SQ110DTC, A2058G	This study
SQ110DTC- A2058C	SQ110DTC, A2058C	This study
SQ110DTC- A2059G	SQ110DTC, A2059G	This study
SQ110DTC- C2611A	SQ110DTC, C2611A	This study
SQ110DTC- C2611G	SQ110DTC, C2611G	This study
SQ110DTC- C2611U	SQ110DTC, C2611U	This study
SQ171DTC	Δ*rrn*GADEHBC(pKK3535,ptRNA67)	(70)
SQ171DTC- A2058G	SQ171DTC, A2058G	(71)
S. pyogenes NZ131	Wild-type *S. pyogenes* M49 strain	(72)

3.3 Results

3.3.1 Resistance mutations point to the binding of MTM and PKM to overlapping but possibly distinct sites in the ribosomal exit tunnel

One of the most straightforward approaches for identifying the site of antibiotic action is to isolate resistant mutants with alterations in the drug target site. We used this approach to determine the MTM and PKM site(s) of action. For that, we exploited the recently developed *E. coli* strain SQ110DTC, which possesses a single chromosomal *rrn* allele and is also hypersusceptible to many inhibitors due to inactivation of the TolC multidrug transporter (64).

Plating of ca. 10^9 SQ110DTC cells on LB/agar plates supplemented with 4-fold MIC of PKM and MTM (64 μg/ml and 128 μg/ml, respectively) resulted in appearance of several resistant clones. The 23S rRNA gene was PCR-amplified directly from the resistant colonies and sequenced. Given that the PKM structure closely resembles that of the known 14-member ring macrolides, it was not surprising that mutations of nucleotides 2057, 2058, 2059 and 2611, previously implicated in macrolide-binding site (73), were identified in the PKM resistant mutants (Fig. 3.2). Unexpectedly, however, the independently isolated MTM resistant mutants also contained mutations at two of the same positions (2058 and 2059) (Fig. 3.2). Testing the MIC of PKM and MTM for the isolated mutants showed that the mutations in the macrolide binding site in the NPET conferred high level of resistance to both of the *S. venezuelae*-produced antibiotics, but not to the control PTC-targeting CHL (Table III.II). These results suggest that both inhibitors bind in the NPET at or near the conventional macrolide-binding site.

To ascertain whether MTM and PKM resistance can be specifically conferred by rRNA mutation in the macrolide-binding site without a possible contribution of a secondary mutation in the chromosome, the A2058G mutation was engineered by site- directed mutagenesis on the plasmid pAM552 carrying the *E. coli* rRNA operon *rrnB* (75). The engineered plasmid was

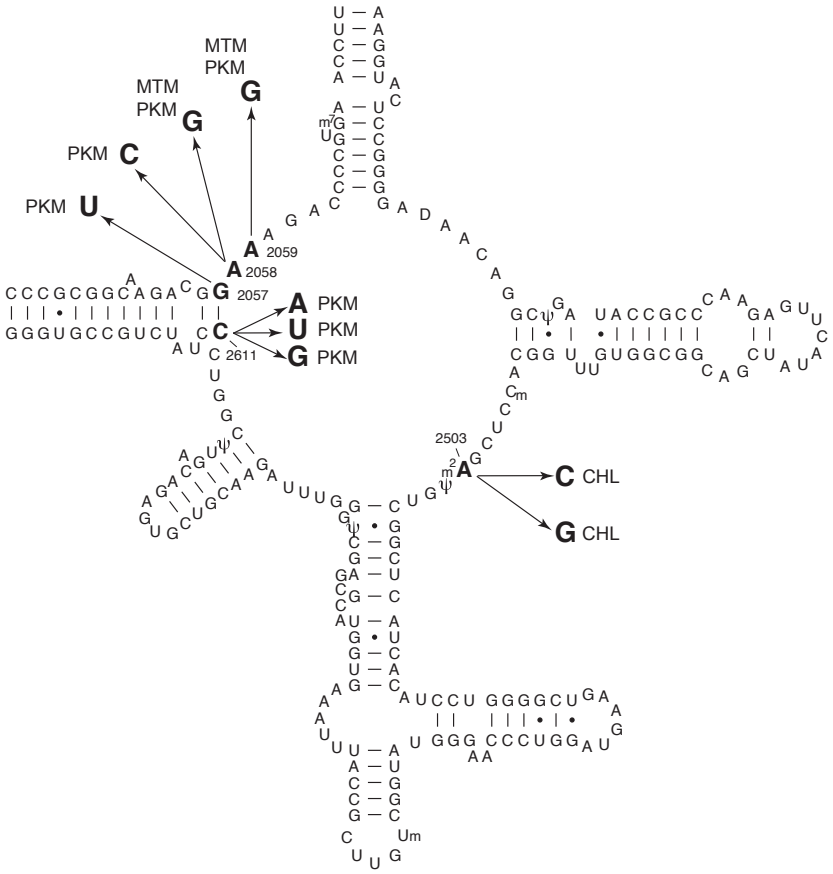

Figure 3.2: The mutations selected in the *E. coli* SQ110DTC strain using MTM, PKM or CHL. The mutated nucleotides are shown in bold and numbered. The types of mutations are indicated along with the antibiotic for which the corresponding mutant was selected. The 23S rRNA secondary structure was modeled following (74).

introduced into the *E. coli* SQ171DTC strain, where all the chromosomal *rrn* alleles are deleted and the resident plasmid pCSacB serves as a sole source of rRNA genes (70, 76). After elimination of the resident pCSacB plasmid by sucrose-based counter selection (77), the cells, which now expressed a pure population of the mutant A2058G ribosomes but were never exposed to MTM or PKM, were subjected to MIC testing. The MIC results confirmed that the ribosomal tunnel mutations are sufficient to confer high resistance to both MTM and PKM arguing thereby that both protein synthesis inhibitors bind in the NPET (Table III.II).

The finding that NPET mutations conferred resistance to MTM conflicted with the results of crystallographic results, which suggested that MTM could bind to PTC of the *D. radiodurans* large ribosomal subunit (51). The lack of PTC-specific mutations in our selection could reflect either the low frequency of such mutations under our experimental conditions or the MIC of PTC-mutants is not sufficiently high. Therefore, we decided to directly test whether a mutation conferring resistance specifically to PTC inhibitors could influence sensitivity of MTM in *E. coli*. Previously, using the SQ110DTC strain, we have isolated a mutant A2503C that is resistant to the classic PTC-targeting antibiotic CHL (64). A more extensive screening allowed us now to isolate another CHL resistant mutation A2503G (Fig. 3.2). As expected, none of the A2503 mutations had any significant effect on PKM or ERY MIC. In contrast, the MIC of MTM increased quite significantly (8 fold) in the A2503C mutant (although not in the A2503G mutant) (Table III.II). Because A2503 is located in the PTC very close to the entrance of the NPET, this result was generally compatible with two scenarios: i) MTM could be binding exclusively in the NPET, but in comparison with other macrolides its binding site could be shifted closer to the PTC, or ii) two MTM molecules could be binding to the ribosome with one in the NPET and another one in the PTC.

TABLE III.II: MIC (µg/ml) OF MTM, PKM, ERY AND CHL AGAINST WILD TYPE AND MUTANT *E. coli* STRAINS.

Strain	Mutation	MTM	PKM	ERY	CHL
SQ110DTC	WT	32	16	2	1
	G2057U	>256	>256	>256	1
	A2058G	>256	>256	>256	1
	A2059G	>256	>256	>256	1
	C2611U	>256	>256	>256	1
	A2503C	128	64	2	8
	A2503G	16	16	2	8
SQ171DTC	WT	4	4	2	0.25
	A2058G	>256	>256	>256	1

3.3.2 RNA probing confirms binding of MTM and PKM in the NPET

In order to gain more direct insights to PKM and MTM binding sites, we examined interactions of both compounds with the ribosome by rRNA chemical probing (footprinting) (66). Antibiotic-free or antibiotic-bound ribosomes were modified with dimethylsulfate (DMS), kethoxal, or 1-cyclohexyl-(2-morpholinoethyl) carbodiimide metho-p-toluene sulfonate. Then the rRNA bases accessible for chemical modifications were identified by primer extension. Similar to known footprints of other macrolides (23, 54, 78), MTM and PKM protected two adenines A2058 and A2059 in the *E. coli* ribosome from DMS modification, which indicated that they bound to the site identical to or overlapping the conventional macrolide-binding site (Fig. 3.3). Similarly, in ribosomes from Gram-positive *Staphylococcus aureus*, MTM and PKM protected the same two 23S rRNA residues from DMS modification (Fig. 3.4). Importantly, neither PKM nor MTM protected any other nucleotide in the domain V of 23S rRNA, encompassing the PTC and the adjacent section of the NPET, from chemical modification. These results were consistent with our genetic results showing that mutations in the macrolide binding site confer resistance to both MTM and PKM. Although the footprinting data cannot completely exclude binding of MTM at the PTC, we could safely conclude that chemical probing of the ribosome revealed that PKM and MTM bind in the NPET but does not provide support for binding of MTM in the PTC.

In order to understand why the PTC mutation A2503C confers resistance to MTM, which upon binding protects only the NPET nucleotides A2058 and A2059 from chemical modification, we compared the MTM-dependent protection of the two NPET adenosines in the wild type and A2503C ribosome. Titration of MTM showed that higher concentrations of the drug were required to achieve protection of A2058 and A2059 in the wild type ribosome compared to the A2503C mutant (Fig. 3.5). This result is compatible with either the A2503C mutation

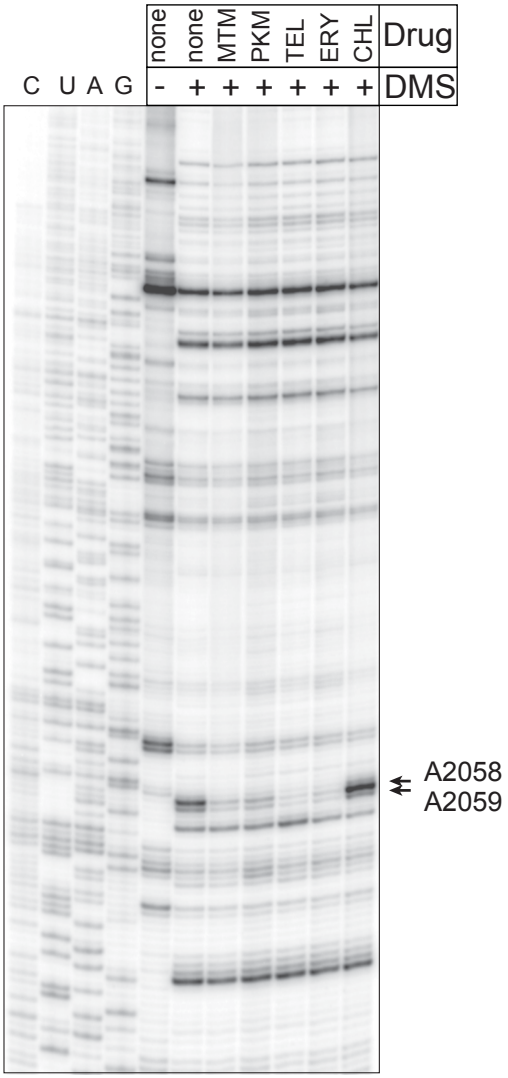

Figure 3.3: MTM and PKM protect *E.coli* 23S rRNA nucleotides located in the macrolide-binding site in the NPET from DMS modification. Footprinting of MTM, PKM, TEL, ERY and CHL on the *E. coli* ribosome. The 23S rRNA residues A2058 and A2059 located in the macrolide binding site are indicated by the arrows.

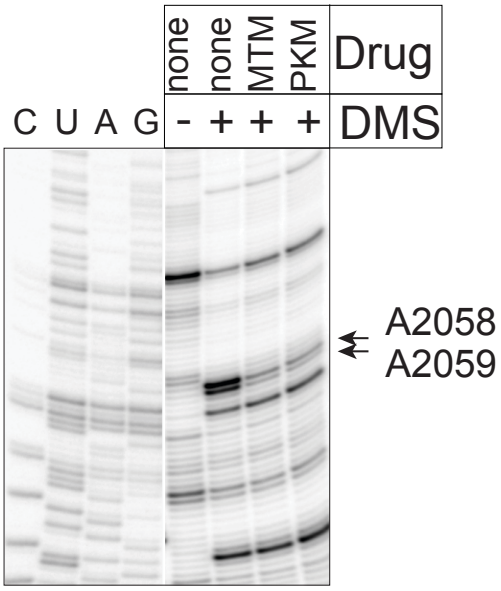

Figure 3.4: MTM and PKM protect *S. aureus* 23S rRNA nucleotides located in the macrolide-binding site in the NPET from DMS modification. Footprinting of MTM and PKM on the *S. aureus* ribosome. The 23S rRNA residues A2058 and A2059 located in the macrolide binding site are indicated by the arrows.

allosterically weakens the binding of MTM in the conventional macrolide site in the NPET or positioning of MTM in the NPET is somewhat closer to the PTC so that the A2503C mutation can directly interfere with its binding.

3.3.3 MTM and PKM do not exhibit synergy in their antibacterial action

The simultaneous binding of two different ribosome inhibitors to the neighboring sites in the NPET and PTC could produce a strong synergistic effect. This strategy is used by some antibiotic producers that secrete two different antibiotics (e.g. streptogramins A and B) that bind in the PTC and NPET, respectively, and can attain stronger inhibition of translation in the target organisms. The possibility that MTM binding to the PTC could be potentiated by PKM binding to the NPET prompted us to investigate if this combination exhibits synergy. We used the checkerboard MIC assay to test whether the combination of MTM and PKM is more potent than individual compounds in inhibiting the growth of a macrolide-susceptible strain *Streptococcus pyogenes*. The results were plotted as a fraction of inhibitory concentration (FIC) of individual compounds (Fig. 3.6). On such plot, the experimental points for the antibiotics with additive effect tended to align to the diagonal, whereas the synergistic antibiotics produce a strongly concave curve.

As anticipated, the control synergistic antibiotics of the streptogramin class (quinupristin and dalfopristin) were notably more potent inhibitors of *S. pyogenes* growth when present in combination compared to the individual components. In contrast, the experimental points for the MTM and PKM combination lay much closer to the diagonal revealing the lack of any significant synergy between the two compounds. Thus, the results of synergy testing did not provide support for PKM-stimulated binding of MTM to the PTC.

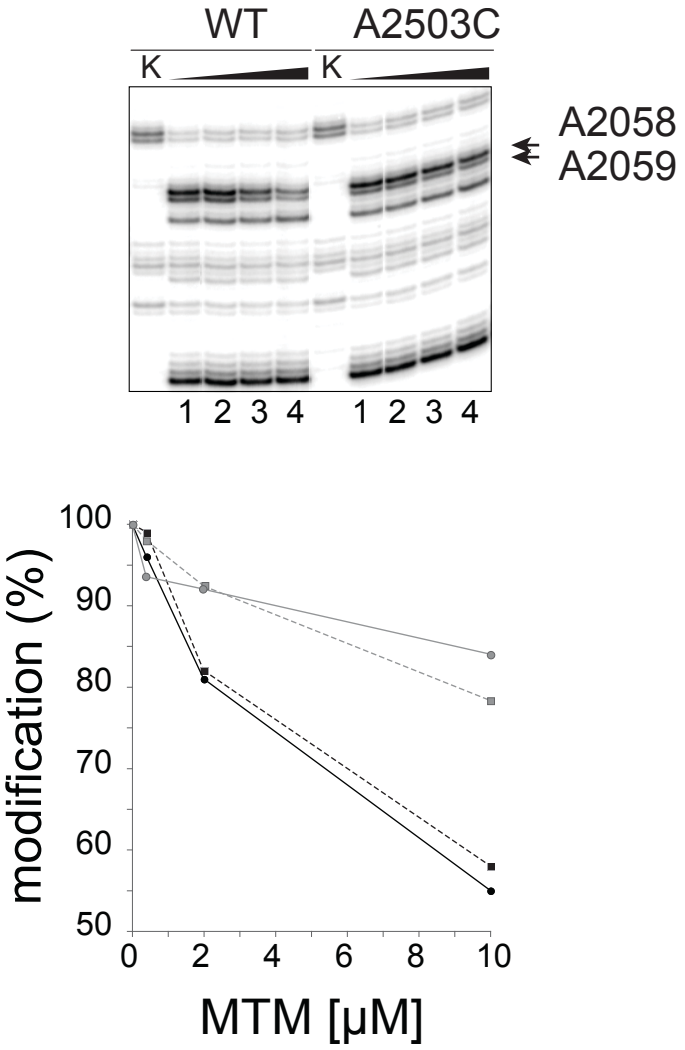

Figure 3.5: The A2503C mutation weakens interaction of MTM with the NPET. Top: Footprinting of varying concentrations of MTM on the ribosome isolated from the parental *E. coli* SQ110DTC strain or the A2503C mutant. The DMS-modified samples in the lanes 1, 2, 3 and 4 contained 0, 0.4, 2 and 10 μM of MTM. Bottom: quantification of the gel shown above. Black lines – parental strain (solid-A2058, dotted-A2059), gray lines – A2503C mutant (solid-A2058, dotted-A2059). The intensity of the A2058 and A2059 bands in the 'no antibiotic' control was taken as 100%.

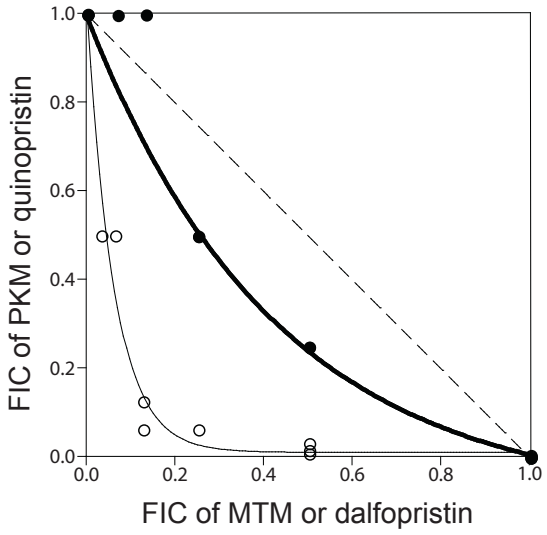

Figure 3.6: Testing synergy of MTM and PKM. The results of checkerboard MIC experiment carried out with *S. pyogenes*. The plots show the changes in fractional inhibitory concentration (FIC) of individual drugs when both drugs are present in combination. The dotted diagonal line indicated a hypothetical curve corresponding to the additive drug action. Black circles (and thick line) show FIC values for MTM and PKM. Open circles (and thin line) show the FIC curve for the control synergistic streptogramin antibiotics quinupristin and dalfopristin.

3.3.4 Context-specificity of translation inhibition by MTM and PKM resembles that of the NPET-bound antibiotics rather than the PTC-targeting antibiotics

The NPET-bound macrolide antibiotics (e.g. TEL) and PTC-targeting inhibitors like CHL, exhibit context-specific action (30-32, 64). In the presence of antibiotic, translation of a protein is not inhibited uniformly throughout the length of mRNA, but is arrested at specific codons (64). The idiosyncratic pattern of codon-specific arrests is antibiotic-specific and can be used to determine the primary mode of antibiotic action (64). In order to investigate whether inhibition of translation by MTM (and PKM) resembles that of the tunnel-binding TEL or the PTC-binding CHL, we carried out primer extension inhibition (toeprinting) analysis of the drug-induced arrest during translation of several model bacterial genes. We used the leader ORFs *ermDL* and *ermBL* of the inducible macrolide resistance genes and the leader ORF of the inducible CHL resistance gene *catL,* where the respective antibiotics induced translation arrest at well-defined codons (79, 80).

The results show that the translation arrest promoted by MTM and PKM at the leader ORFs of the macrolide resistance genes matches that induced by TEL (Fig. 3.7, red dots). In contrast, while CHL induces a strong and specific arrest at the 5th codon of the *catL* ORF, neither MTM nor PKM stimulated ribosome stalling at this codon (Fig. 3.7, green dots). These results argue that the mode of action of MTM (and PKM) matches that of the NPET-bound ketolide rather than the PTC-bound CHL.

Noteworthy, the intensities of the toeprint bands representing MTM- or PKM-induced ribosome stalling at the 10th codon of the *ermBL* gene were significantly different (Fig. 3.7, red dots). Thus, while the modes of inhibition of translation by MTM and PKM are qualitatively similar, these two drugs may differ in quantitative aspects of their site-specific inhibition effects.

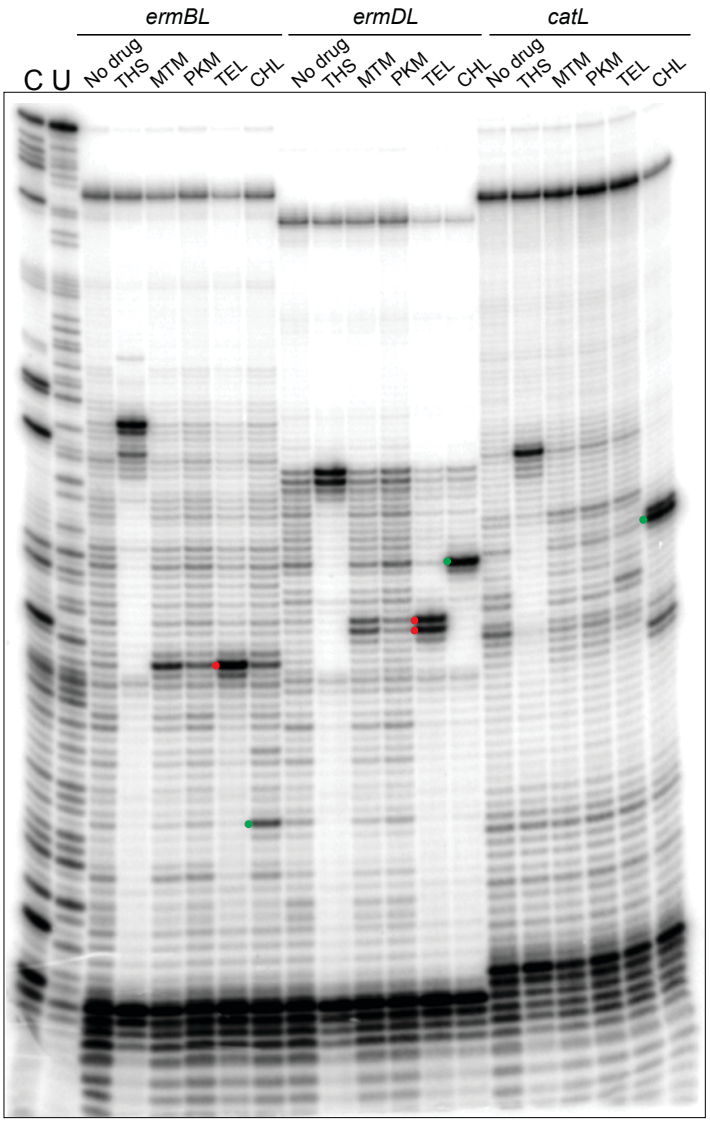

Figure 3.7: Toe-printing analysis of protein synthesis inhibitors. Toe-printing patterns were generated by THS, MTM, PKM, TEL and CHL with *ermBL*, *ermDL*, and *catL* templates. The ketolides and CHL toe-print bands are marked with red dots or green dot, respectively, on the gel.

3.3.5 PKM and MTM inhibit synthesis of small but specific subsets of cellular proteins

Context-specificity of macrolide antibiotics action results in synthesis inhibition of a defined subset of cellular polypeptides. Different macrolides prevent the production of different subsets of cellular polypeptides (30). Because of the differences between MTM and PKM in the chemical structure of the core macrolactone rings and their binding to the NPET, it was interesting to test whether the spectra of proteins inhibited by MTM and PKM are different. To investigate this, we exposed *E. coli* cells for 10 min to 50-fold MIC of MTM and PKM, pulse labeled the proteins that continue to be synthesized with [^{35}S] methionine, and resolved them by 2D-gel electrophoresis (Fig. 3.8). A clinically relevant ketolide SOL used in our previous experiments served as a control (30).

While cladinose-containing macrolides were shown previously to inhibit production of the majority of cellular proteins, clinical ketolides like SOL inhibited a much smaller subset of proteins (30). Supporting our previous results, a number of proteins also escaped SOL inhibition (Fig. 3.8B). Strikingly, even more proteins escaped PKM and MTM inhibition with only a small subset of cellular polypeptides inhibited by these antibiotics (black and red arrowheads in Fig. 3.8 A, C and D). Even despite a relatively small subset of proteins was affected by MTM and PKM, the spectra of the affected polypeptides were somewhat different for the two inhibitors (red arrows in Fig. 3.8 A, C and D). Thus, regardless of binding to overlapping sites in the ribosome, MTM and PKM produce differential effects on protein synthesis in the sensitive cells.

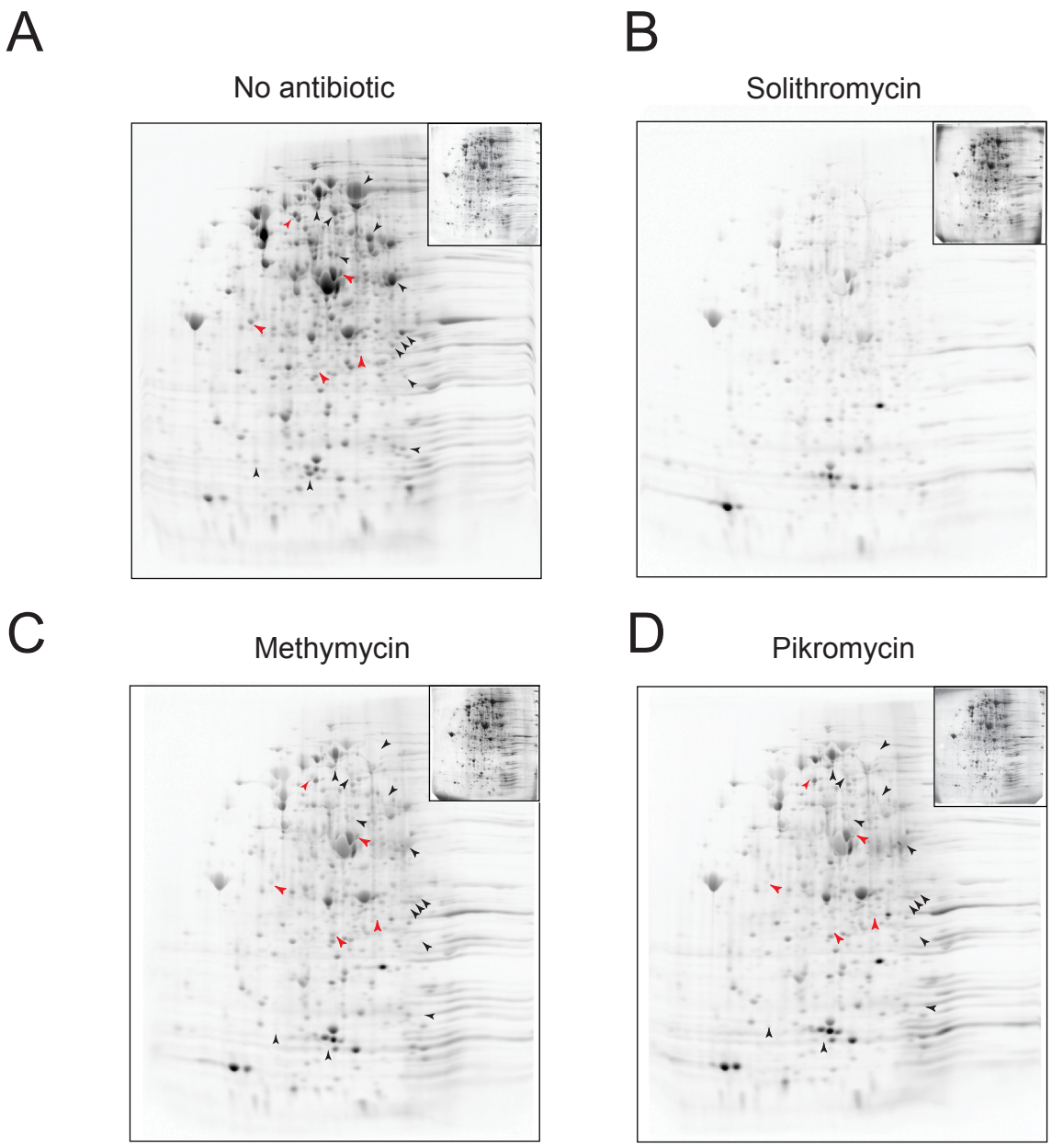

Figure 3.8: Two-dimensional gel electrophoresis analysis of proteins synthesized in *E. coli* cells treated with ketolides. Untreated *E. coli* cells (A) or cells treated with 50 fold MIC of SOL (B), MTM (C) or PKM (D). The Coomassie-stained gels are shown in insets.

3.4 Discussion

Prompted by the unusual structure of MTM, its purported binding to the PTC, and the fact that *S. venezuelae* ATCC 15439 secretes two related but distinct macrolide antibiotics, we here examined the mode of binding and action of these protein synthesis inhibitors. Our results indicate that both compounds bind to overlapping binding sites in the NPET, which overlap with the binding sites of other macrolide antibiotics. Yet the differential effect of some of the resistance mutations and the difference in the spectra of proteins inhibited by these antibiotics suggest that the binding of MTM, which possesses an unusual 12-atom macrolactone ring, differs from that of the 14-member macrolactone ring PKM.

The isolation of the resistance mutants with alterations of the 23S rRNA nucleotides in the macrolide binding site (e.g. 2057, 2058, 2059, and 2611), and protection of the two rRNA residues (A2058 and A2059) from DMS modification by MTM and PKM clearly showed that their primary site of binding and action is located in the NPET. Since the structure of PKM generally matches that of ERY and other 14-member ring macrolides, and because the spectrum of resistance mutations for PKM and ERY as well as their ribosomal footprints were indistinguishable, it is likely that the common parts of both antibiotics (the 14 atom macrolactone and desosamine sugar) establish very similar interactions within the ribosome. MTM, which is a 12-member macrolactone counterpart of PKM, protected the same set of nucleotides in the NPET from DMS modification. The mutations that rendered cells resistant to PKM or ERY also conferred resistance to MTM. Taken together, these results strongly argue that the primary site of binding of not only PKM, but also MTM, overlaps with the binding site of macrolide and ketolide antibiotics in the NPET. This conclusion was further supported by the activity assay, in which the pattern of context specific-translation arrests induced by PKM or MTM closely matched that of TEL, a clinical ketolide.

None of our results provided strong support for MTM binding in the PTC, as was originally suggested by crystallographic studies carried out with the *D. radiodurans* 50S subunit (51). We did not observe either MTM-specific protections of the PTC nucleotides in the footprinting experiments and also did not detect context-specific inhibition pattern that would match that of PTC-targeting antibiotics in the toeprinting assay. Furthermore, MTM and PKM did not show significant synergy in their action as could be expected from antibiotics targeting neighboring ribosomal sites exploited by the pairs of known synergistic inhibitors. Although the MTM resistance conferred by the A2503C mutation could be viewed as supporting the drug binding at the PTC, we disfavored this hypothesis. Binding of MTM exclusively in the NPET is compatible with the protection of A2058 and A2059 from DMS modification. Therefore, the only possible scenario to consider is simultaneous binding of two MTM molecules to the ribosome, one in the NPET and another one in the PTC. The mutations of the tunnel nucleotides conferring high resistance to MTM clearly showed that the primary site of drug binding and action is in the NPET. Although the A2503C mutation also affords 8-fold increase in MIC, resistance is less pronounced than that afforded by the tunnel mutations. If the A2503C mutation specifically interferes with the binding of MTM in the PTC, the interaction of the drug within the tunnel should remain unaffected and consequently, no changes in MIC would be observed. However, if the mutation decreases the affinity of the drug to its tunnel site, one would expect to observe an increase of MIC. This is exactly what we observed experimentally.

In spite of the general similarity of binding and action of MTM and PKM, these two compounds exhibit specific and important differences. The fact that the A2503C mutation has a different effect upon MTM compared to PKM or other macrolide antibiotics suggests that the placement of MTM in the NPET site could be somewhat shifted bringing the drug into closer contact with the A2503 residue. Therefore, the A2503C mutation may destabilize interaction of

MTM with its NPET binding site either directly or allosterically. This conclusion is compatible with a reduced protection of the tunnel nucleotides A2058 and A2059 by MTM in the A2503C mutant (Fig. 3.5). Possibly, as a result of such differential binding of MTM or due to the difference in the macrolactone structure, MTM and PKM exhibit somewhat different effects on protein synthesis. Although the general patterns of toeprint signals observed in our in vitro experiments were similar between MTM and PKM and closely matched those of TEL, the intensity of some MTM- and PKM-induced toeprint bands differed significantly (Fig. 3.7). Furthermore, MTM and PKM inhibited synthesis of slightly different subsets of proteins in the living cell (Fig. 3.8). The differential mode of protein inhibition may provide a biological rationale for producing two similar yet distinct antibiotics by *S. venezuelae* ATCC 15439.

It was originally tempting to think that production of the two antibiotics via the same complex polyketide biosynthetic pathway is advantageous, because the drugs could be binding to different ribosomal sites. Possible synergy in the action of the pair of secreted antibiotics would provide a strong evolutionary pressure for maintaining the programmed switched in the polyketide synthase gene *pikAIV,* which accounts for generation of two distinct macrolide molecules (50). However, our experimental results strongly argue against simultaneous binding of MTM and PKM to the ribosome, because the sites of action of these two inhibitors clearly overlap. This raises the question of what is the advantage for the producer to generate two seemingly redundant inhibitors?

We propose that this advantage lies in the effect of antibiotics on translation in different bacterial species. The growth retardation effect of the ribosome-targeting antibiotic is likely linked to the spectrum of the inhibited proteins. Because we observed that PKM and MTM exhibited differential protein specificity, it may be possible be that each compound could preferentially target different *S. venezuelae* competitors in the environment. In fact, we observed

such species-specificity experimentally because MTM failed to inhibit the growth of *Staphylococcus aureus*, *Bacillus subtilis, Bacillus cereus* or *Enterococcus feacalis,* which were all sensitive to PKM. Although at the moment we do not have sufficient data to distinguish differential inhibition of translation from differential uptake of MTM and PKM in these species, it is conceivable that species-specific action could serve as a sufficient evolutionary pressure for the producer to maintain this dual-antibiotic biosynthesis pathway.

3.5 Cited literature

1. Schluenzen F*, et al.* (2000) Structure of functionally activated small ribosomal subunit at 3.3 angstrom resolution. *Cell* 102(5):615-623.

2. Wimberly BT*, et al.* (2000) Structure of the 30S ribosomal subunit. *Nature* 407(6802):327-339.

3. Demeshkina N, Jenner L, Yusupova G, & Yusupov M (2010) Interactions of the ribosome with mRNA and tRNA. *Curr Opin Struct Biol* 20(3):325-332.

4. Ban N, Nissen P, Hansen J, Moore PB, & Steitz TA (2000) The complete atomic structure of the large ribosomal subunit at 2.4 angstrom resolution. *Science* 289(5481):905-920.

5. Harms J*, et al.* (2001) High resolution structure of the large ribosomal subunit from a mesophilic eubacterium. *Cell* 107(5):679-688.

6. Yusupov MM*, et al.* (2001) Crystal structure of the ribosome at 5.5 angstrom resolution. *Science* 292(5518):883-896.

7. Polikanov YS, Steitz TA, & Innis CA (2014) A proton wire to couple aminoacyl-tRNA accommodation and peptide-bond formation on the ribosome. *Nature structural & molecular biology* 21(9):787-793.

8. Voss NR, Gerstein M, Steitz TA, & Moore PB (2006) The geometry of the ribosomal polypeptide exit tunnel. *Journal of molecular biology* 360(4):893-906.

9. Jenni S & Ban N (2003) The chemistry of protein synthesis and voyage through the ribosomal tunnel (vol 13, pg 212, 2003). *Curr Opin Struc Biol* 13(4):533-533.

10. Schmeing TM & Ramakrishnan V (2009) What recent ribosome structures have revealed about the mechanism of translation. *Nature* 461(7268):1234-1242.

11. Wilson DN (2009) The A-Z of bacterial translation inhibitors. *Critical reviews in biochemistry and molecular biology* 44(6):393-433.

12. Mankin AS (2001) Ribosomal Antibiotics. *Molecular Biology* 35.

13. Okuda K, Hirota T, Kingery DA, & Nagasawa H (2009) Synthesis of a fluorine-substituted puromycin derivative for Bronsted studies of ribosomal-catalyzed peptide bond formation. *The Journal of organic chemistry* 74(6):2609-2612.

14. McGuire JM*, et al.* (1952) [Ilotycin, a new antibiotic]. *Schweizerische medizinische Wochenschrift* 82(41):1064-1065.

15. Ackermann G & Rodloff AC (2003) Drugs of the 21st century: telithromycin (HMR 3647)--the first ketolide. *The Journal of antimicrobial chemotherapy* 51(3):497-511.

16. Kannan K & Mankin AS (2011) Macrolide antibiotics in the ribosome exit tunnel: species-specific binding and action. *Annals of the New York Academy of Sciences* 1241:33-47.

17. Gaynor M & Mankin AS (2003) Macrolide antibiotics: binding site, mechanism of action, resistance. *Current topics in medicinal chemistry* 3(9):949-961.

18. Katz L & Ashley GW (2005) Translation and protein synthesis: macrolides. *Chemical reviews* 105(2):499-528.

19. Hansen JL*, et al.* (2002) The structures of four macrolide antibiotics bound to the large ribosomal subunit. *Molecular cell* 10(1):117-128.

20. Dunkle JA, Xiong L, Mankin AS, & Cate JH (2010) Structures of the Escherichia coli ribosome with antibiotics bound near the peptidyl transferase center explain spectra of drug action. *Proceedings of the National Academy of Sciences of the United States of America* 107(40):17152-17157.

21. Schlunzen F*, et al.* (2001) Structural basis for the interaction of antibiotics with the peptidyl transferase centre in eubacteria. *Nature* 413(6858):814-821.

22. Bulkley D, Innis CA, Blaha G, & Steitz TA (2010) Revisiting the structures of several antibiotics bound to the bacterial ribosome. *Proceedings of the National Academy of Sciences of the United States of America* 107(40):17158-17163.

23. Hansen LH, Mauvais P, & Douthwaite S (1999) The macrolide-ketolide antibiotic binding site is formed by structures in domains II and V of 23S ribosomal RNA. *Molecular microbiology* 31(2):623-631.

24. Gregory ST & Dahlberg AE (1999) Erythromycin resistance mutations in ribosomal proteins L22 and L4 perturb the higher order structure of 23 S ribosomal RNA. *Journal of molecular biology* 289(4):827-834.

25. Otaka T & Kaji A (1975) Release of (oligo) peptidyl-tRNA from ribosomes by erythromycin A. *Proceedings of the National Academy of Sciences of the United States of America* 72(7):2649-2652.

26. Menninger JR & Otto DP (1982) Erythromycin, carbomycin, and spiramycin inhibit protein synthesis by stimulating the dissociation of peptidyl-tRNA from ribosomes. *Antimicrob Agents Chemother* 21(5):811-818.

27. Tenson T, Lovmar M, & Ehrenberg M (2003) The mechanism of action of macrolides, lincosamides and streptogramin B reveals the nascent peptide exit path in the ribosome. *Journal of molecular biology* 330(5):1005-1014.

28. Menninger JR (1979) Accumulation of peptidyl tRNA is lethal to Escherichia coli. *J. Bacteriol.* 137:694-696.

29. Tu D, Blaha G, Moore PB, & Steitz TA (2005) Structures of MLSBK antibiotics bound to mutated large ribosomal subunits provide a structural explanation for resistance. *Cell* 121(2):257-270.

30. Kannan K, Vazquez-Laslop N, & Mankin AS (2012) Selective Protein Synthesis by Ribosomes with a Drug-Obstructed Exit Tunnel. *Cell* 151(3):508-520.

31. Kannan K*, et al.* (2014) The general mode of translation inhibition by macrolide antibiotics. *Proceedings of the National Academy of Sciences of the United States of America* 111(45):15958-15963.

32. Davis AR, Gohara DW, & Yap MN (2014) Sequence selectivity of macrolide-induced translational attenuation. *Proceedings of the National Academy of Sciences of the United States of America* 111(43):15379-15384.

33. Poulsen SM, Kofoed C, & Vester B (2000) Inhibition of the ribosomal peptidyl transferase reaction by the mycarose moiety of the antibiotics carbomycin, spiramycin and tylosin. *Journal of molecular biology* 304(3):471-481.

34. Subramanian SL, Ramu, H., Mankin, A. S. (2012) Inducible Resistance to Macrolide Antibiotics. *Antibiotic Discovery and Development* 1:455-484.

35. Leclercq R (2002) Mechanisms of resistance to macrolides and lincosamides: Nature of the resistance elements and their clinical implications. *Clinical Infectious Diseases* 34(4):482-492.

36. Weisblum B (1995) Erythromycin Resistance by Ribosome Modification. *Antimicrobial Agents and Chemotherapy* 39(3):577-585.

37. Cundliffe E & Demain AL (2010) Avoidance of suicide in antibiotic-producing microbes. *Journal of industrial microbiology & biotechnology* 37(7):643-672.

38. Liu MF & Douthwaite S (2002) Activity of the ketolide telithromycin is refractory to erm monomethylation of bacterial rRNA. *Antimicrobial Agents and Chemotherapy* 46(6):1629-1633.

39. Hahn J, Grandi G, Gryczan TJ, & Dubnau D (1982) Translational attenuation of ermC: a deletion analysis. *Molecular & general genetics : MGG* 186(2):204-216.

40. Horinouchi S, Byeon WH, & Weisblum B (1983) A complex attenuator regulates inducible resistance to macrolides, lincosamides, and streptogramin type B antibiotics in Streptococcus sanguis. *Journal of bacteriology* 154(3):1252-1262.

41. Ramu H, Mankin A, & Vazquez-Laslop N (2009) Programmed drug-dependent ribosome stalling. *Molecular microbiology* 71(4):811-824.

42. Skinner R, Cundliffe E, & Schmidt FJ (1983) Site of action of a ribosomal RNA methylase responsible for resistance to erythromycin and other antibiotics. *The Journal of biological chemistry* 258(20):12702-12706.

43. Liu MF & Douthwaite S (2002) Resistance to the macrolide antibiotic tylosin is conferred by single methylations at 23S rRNA nucleotides G748 and A2058 acting in synergy. *Proceedings of the National Academy of Sciences of the United States of America* 99(23):14658-14663.

44. Zalacain M & Cundliffe E (1989) Methylation of 23s Ribosomal-Rna Caused by Tlra (Ermsf), a Tylosin Resistance Determinant from Streptomyces-Fradiae. *Journal of bacteriology* 171(8):4254-4260.

45. Quiros LM, Aguirrezabalaga I, Olano C, Mendez C, & Salas JA (1998) Two glycosyltransferases and a glycosidase are involved in oleandomycin modification during its biosynthesis by Streptomyces antibioticus. *Molecular microbiology* 28(6):1177-1185.

46. Zhao L, Beyer NJ, Borisova SA, & Liu HW (2003) Beta-glucosylation as a part of self-resistance mechanism in methymycin/pikromycin producing strain Streptomyces venezuelae. *Biochemistry-Us* 42(50):14794-14804.

47. Park AK, Kim H, & Jin HJ (2010) Phylogenetic analysis of rRNA methyltransferases, Erm and KsgA, as related to antibiotic resistance. *FEMS microbiology letters* 309(2):151-162.

48. Xue YQ, Zhao LS, Liu HW, & Sherman DH (1998) A gene cluster for macrolide antibiotic biosynthesis in Streptomyces venezuelae: Architecture of metabolic diversity. *Proceedings of the National Academy of Sciences of the United States of America* 95(21):12111-12116.

49. Kittendorf JD & Sherman DH (2009) The methymycin/pikromycin pathway: a model for metabolic diversity in natural product biosynthesis. *Bioorganic & medicinal chemistry* 17(6):2137-2146.

50. Xue Y & Sherman DH (2000) Alternative modular polyketide synthase expression controls macrolactone structure. *Nature* 403(6769):571-575.

51. Tamar Auerbach IM, Anat Bashan,, Chen Davidovich HR, David H. Sherman, & Yonath aA (2009) Structural basis for the antibacterial activity of the 12-membered-ring mono-sugar macrolide methymycin. *biotechnologia* 84.

52. Thompson J, Pratt CA, & Dahlberg AE (2004) Effects of a number of classes of 50S inhibitors on stop codon readthrough during protein synthesis. *Antimicrobial Agents and Chemotherapy* 48(12):4889-4891.

53. Gupta P, Kannan K, Mankin AS, & Vazquez-Laslop N (2013) Regulation of gene expression by macrolide-induced ribosomal frameshifting. *Molecular cell* 52(5):629-642.

54. Xiong L, Shah S, Mauvais P, & Mankin AS (1999) A ketolide resistance mutation in domain II of 23S rRNA reveals the proximity of hairpin 35 to the peptidyl transferase centre. *Molecular microbiology* 31(2):633-639.

55. Schlunzen F*, et al.* (2003) Structural basis for the antibiotic activity of ketolides and azalides. *Structure* 11(3):329-338.

56. Llano-Sotelo B*, et al.* (2010) Binding and action of CEM-101, a new fluoroketolide antibiotic that inhibits protein synthesis. *Antimicrob Agents Chemother* 54(12):4961-4970.

57. Vazquez D (1979) Inhibitors of protein biosynthesis. *Molecular biology, biochemistry, and biophysics* 30:i-x, 1-312.

58. Cocito C, Di Giambattista M, Nyssen E, & Vannuffel P (1997) Inhibition of protein synthesis by streptogramins and related antibiotics. *The Journal of antimicrobial chemotherapy* 39 Suppl A:7-13.

59. Auerbach T*, et al.* (2010) The structure of ribosome-lankacidin complex reveals ribosomal sites for synergistic antibiotics. *Proceedings of the National Academy of Sciences of the United States of America* 107(5):1983-1988.

60. Belousoff MJ*, et al.* (2011) Crystal structure of the synergistic antibiotic pair, lankamycin and lankacidin, in complex with the large ribosomal subunit. *Proceedings of the National Academy of Sciences of the United States of America* 108(7):2717-2722.

61. Oh HS & Kang HY (2012) Total synthesis of pikromycin. *The Journal of organic chemistry* 77(2):1125-1130.

62. Oh HS, Xuan R, & Kang HY (2009) Total synthesis of methymycin. *Organic & biomolecular chemistry* 7(21):4458-4463.

63. Hansen DA*, et al.* (2013) Biocatalytic synthesis of pikromycin, methymycin, neomethymycin, novamethymycin, and ketomethymycin. *Journal of the American Chemical Society* 135(30):11232-11238.

64. Orelle C*, et al.* (2013) Tools for characterizing bacterial protein synthesis inhibitors. *Antimicrob Agents Chemother* 57(12):5994-6004.

65. Ohashi H, Shimizu Y, Ying BW, & Ueda T (2007) Efficient protein selection based on ribosome display system with purified components. *Biochemical and biophysical research communications* 352(1):270-276.

66. Merryman C NH (1998) Footprinting and modification-interference analysis ofbinding sites on RNA. *RNA:Protein Interactions, A Practical Approach* ed CWJ Smith (Oxford University Press, Oxford).

67. Vazquez-Laslop N, Thum C, & Mankin AS (2008) Molecular mechanism of drug-dependent ribosome stalling. *Molecular cell* 30(2):190-202.

68. Vazquez-Laslop N, Ramu H, Klepacki D, Kannan K, & Mankin AS (2010) The key function of a conserved and modified rRNA residue in the ribosomal response to the nascent peptide. *Embo J* 29(18):3108-3117.

69. Hamilton-Miller JM & Shah S (1998) Comparative in-vitro activity of ketolide HMR 3647 and four macrolides against gram-positive cocci of known erythromycin susceptibility status. *The Journal of antimicrobial chemotherapy* 41(6):649-653.

70. Bollenbach T, Quan S, Chait R, & Kishony R (2009) Nonoptimal microbial response to antibiotics underlies suppressive drug interactions. *Cell* 139(4):707-718.

71. Martinez AK*, et al.* (2014) Interactions of the TnaC nascent peptide with rRNA in the exit tunnel enable the ribosome to respond to free tryptophan. *Nucleic acids research* 42(2):1245-1256.

72. McShan WM*, et al.* (2008) Genome sequence of a nephritogenic and highly transformable M49 strain of Streptococcus pyogenes. *Journal of bacteriology* 190(23):7773-7785.

73. Triman KL, Peister A, & Goel RA (1998) Expanded versions of the 16S and 23S ribosomal RNA mutation databases (16SMDBexp and 23SMDBexp). *Nucleic acids research* 26(1):280-284.

74. Cannone JJ*, et al.* (2002) The comparative RNA web (CRW) site: an online database of comparative sequence and structure information for ribosomal, intron, and other RNAs. *BMC bioinformatics* 3:2.

75. Polikanov YS*, et al.* (2014) Negamycin interferes with decoding and translocation by simultaneous interaction with rRNA and tRNA. *Molecular cell* 56(4):541-550.

76. Asai T*, et al.* (1999) Construction and initial characterization of Escherichia coli strains with few or no intact chromosomal rRNA operons. *Journal of bacteriology* 181(12):3803-3809.

77. Zaporojets D, French S, & Squires CL (2003) Products transcribed from rearranged rrn genes of Escherichia coli can assemble to form functional ribosomes. *Journal of bacteriology* 185(23):6921-6927.

78. Moazed D & Noller HF (1987) Chloramphenicol, erythromycin, carbomycin and vernamycin B protect overlapping sites in the peptidyl transferase region of 23S ribosomal RNA. *Biochimie* 69(8):879-884.

79. Sothiselvam S*, et al.* (2014) Macrolide antibiotics allosterically predispose the ribosome for translation arrest. *Proceedings of the National Academy of Sciences of the United States of America* 111(27):9804-9809.

80. Arenz S*, et al.* (2014) Molecular basis for erythromycin-dependent ribosome stalling during translation of the ErmBL leader peptide. *Nat Commun* 5:3501.

4. CONCLUSION

We started this project by asking why *Streptomyces venezuelae* produces two natural ketolides by the same biosynthetic pathway? Initially, we hypothesized that MTM and PKM in combination could exhibit synergism, like the known cases of streptogramins or lankacidin/Lankamycin, because of their putative binding to neighboring sites in the PTC and ribosomal tunnel, respectively. Our results showed, however, that these natural ketolides are not synergistic. Furthermore, we found that they both target the same ribosomal site, the conventional binding pocket for all antibiotics of the macrolide family, located within the nascent chain exit tunnel. Interestingly, our biochemical experiments revealed that MTM establishes idiosyncratic interactions with rRNA nucleotides of the PTC neighborhood not characteristic of other macrolides, including PKM. Such differential binding modes of MTM and PKM to the ribosomal tunnel may be one reason for the ability of these compounds to inhibit the translation of somewhat distinct subsets of cellular proteins. These findings show that defining the set of proteins affected by the presence of a macrolides is not only defined by the presence of particular side chains of the drug but also by the size of the core macrolactone ring and the binding mode of the antibiotic. Furthermore, we observed that MTM inhibits the growth of a narrower spectrum of bacterial species in comparison with PKM, a feature that probably benefits the producer by allowing it to adjust the type of antibiotic it produces to specifically target competitor bacteria according to its needs.

The second question we pursued in this study is why does *S. venezuelae* carry two highly similar paralogous resistance genes linked to the MTM/PKM common biosynthetic operon? Our results show that the resistance genes generate two RNA methyltransferase enzymes, PikR1 and PikR2, which modify the same rRNA nucleotide located in the ribosomal exit tunnel to block binding of the drugs, providing the ketolide-producer with a prime solution for avoiding suicide.

Although similar, the resistance mechanisms provided by the enzymes differ in the extent of tunnel modification: PikR1 is responsible for monomethylation of tunnel rRNA nucleotide A2058, whereas PikR2 activity leads to dimethylation of the same residue. The constitutive nature of *pikR1* expression results in monomethylated ribosomes that provide continuous protection of *S. venezuelae* cells at the onset of MTM and PKM production. Monomethylation of the ribosomal tunnel is expected to be a less costly and temporary solution. However, once the producer bacteria actively start manufacturing MTM and PKM, they need to increase the level of resistance. We discovered that this is achieved by the ketolide-driven induction of expression of rRNA dimethylase PikR2, which hence boosts the resistance level. Our laboratory has previously found that expression of A2058 dimethylase is disadvantageous for bacterial cells not threatened by the presence of antibiotic. The tight regulation of *pikR2* ensures expression of the enzyme only when strictly required, to avoid the unnecessary fitness cost. In addition to its role in providing low level of resistance, the constitutive, PikR1-catalyzed monomethylation of the ribosome helps with translation of the PikR2 dimethylase, which has to take place when the ribosome inhibitor is already present in the cell.

Finally, we explored the medically important possible scenario of expression of the *S. venezuelae pikR* genes in a model of pathogenic bacteria. We found that expression from a plasmid vector of *pikR2* in *Mycobacterium smegmatis*, results in production of fully functional enzyme and that its translation remains inducible by ketolides. These model pathogenic bacteria become highly resistant to not only clinically relevant antibiotics of the macrolide family but also to ketolides currently in clinical trials. Importantly, simultaneous expression of both *pikR1* and *pikR2* greatly stimulates expression of resistance upon abrupt exposure of *M. smegmatis* to high concentrations of clinical ketolides. The anticipated wide usage of ketolides in the clinical setting could create the selective pressure for these natural resistance genes to be acquired by pathogenic

bacteria, by horizontal gene transfer from the producer bacteria, which could curb the medical value of new ketolides. We suggest that surveillance of *pikR1*/*pikR2* and similar genes will be required upon broad launch of clinical ketolides because it could facilitate early detection of the resistance. We further suggest that our results should stimulate search for novel macrolide compounds lacking inducing capabilities and able to escape the natural resistance mechanisms.

VITA

Mashal M. Almutairi

EDUCATION

Bachelor degree in pharmaceutical sciences, King Saud University**,** College of Pharmacy, Saudi Arabia, 2006

PROFESSIONAL EXPERIENCE

Summer Internship (Infection Biosciences), AstraZeneca, Boston, 2014 Teaching Assistant,

College of Pharmacy, King Saud University, Saudi Arabia, 2008

Clinical Pharmacist**.** Saudi Ministry of Health, Saudi Arabia, 2007

Hospital Internship**,** Forces Hospital, Saudi Arabia, 2006

PUBLICATIONS

Cédric Orelle, Skylar Carlson, Bindiya Kaushal, **Mashal M. Almutairi**, Haipeng Liu, Anna Ochabowicz, Selwyn Quan, Van Cuong Pham, Catherine L. Squires, Brian T. Murphy, Alexander S. Mankin. "Tools for characterizing bacterial protein synthesis inhibitors." Antimicrobial Agents and Chemotherapy (2013). Vol. 57 no. 12 (5994-6004).

Mashal M. Almutairi, Sung Ryeol Park, Simon Rose, Douglas A. Hansen, Nora Vázquez-Laslop, Stephen Douthwaite, David H. Sherman and Alexander S. Mankin. "Efficient resistance to ketolide antibiotics through coordinated expression of methyltransferase paralogs in a bacterial producer of natural ketolides." (Submitted to PNAS).

Mashal M. Almutairi, Douglas A. Hansen, Dorota Klepacki, Nora Vazquez-Laslop, Han-Young Kang, David H. Sherman, and Alexander S. Mankin. "The site of action of methymycin and pikromycin, the natural ketolide antibiotics." (Manuscript in preparation).

Mashal M. Almutairi, Renu Singh, Maryann San Martin, April Chen, Jane Ambler. "Evaluation of ceftaroline pharmacokinetic/pharmacodynamic (PK/PD) Target against diverse characterized clinical Staphylococcus aureus isolates in an in vitro hollow-fibre infection model." (Manuscript in preparation).

POSTER PRESENTATIONS

Mashal M. Almutairi, Douglas A. Hansen, Simon Rose, Stephen Douthwaite, David H. Sherman and Alexander S. Mankin. *Function and Regulation of Resistance Genes in Ketolide-producing Bacteria*, ***ASBMB Annual Meeting 2015***, Boston.

Mashal M. Almutairi, Douglas A. Hansen, Simon Rose, Stephen Douthwaite, David H. Sherman and Alexander S. Mankin. *Function and Regulation of Resistance Genes in Ketolide-producing Bacteria*, ***UIC College of Pharmacy's Research Day 2015***, Chicago.

Mashal M. Almutairi, Douglas A. Hansen, David H. Sherman and Alexander S. Mankin. "How Ketolide-Producing Bacteria Avoid Suicide?", ***XXI Midwest Microbial Pathogenesis Conference 2014***, Chicago.

Mashal M. Almutairi, Douglas A. Hansen, Simon Rose, Stephen Douthwaite, David H. Sherman and Alexander S. Mankin. *Function and Regulation of Resistance Genes in Ketolide-producing Bacteria*, ***34th Midwest Enzyme Chemistry Conference 2014***, Chicago.

Almutairi, Mashal, Singh, Renu, San Martin, Maryann; Chen, April; Ambler, Jane. Evaluation of ceftaroline pharmacokinetic/pharmacodynamic (PK/PD) Target against diverse characterized clinical *Staphylococcus aureus* isolates in an *in vitro* hollow-fibre infection model. ***AstraZeneca 2014***, Boston.

Mashal M. Almutairi, Douglas Hansen, David H. Sherman and Alexander S. Mankin. *Methymycin and Pikromycin: a Potentially Synergistic Pair of Ketolide Antibiotics*. ***ICAAC 2013***, Denver.

Mashal M. Almutairi, Douglas Hansen, David H. Sherman and Alexander S. Mankin. *Why a Macrolide Producer Carries Two Similar Resistance Genes*. ***Ribosome Meeting, 2013***, Napa Valley.

Mashal M. Almutairi, Douglas Hansen, Brian T. Murphy, David H. Sherman and Alexander S. Mankin. *One Drug: Two Sites of Action. Can Methymycin Target Two Different Sites in the Bacterial Ribosome?* ***UIC College of Pharmacy's Research Day, 2013***, Chicago.

Mashal M. Almutairi and Alexander S. Mankin. *Multiple Resistance Mechanisms in a Multi-drug Producer*. ***RNA Meeting 2012***, Anna Arbor.

Mashal M. Almutairi and Alexander S. Mankin. *Multiple resistance mechanisms in a multi-drug producer*. ***UIC College of Pharmacy's Research Day, 2012***, Chicago.

Max Rutter, Hiten Gutka, **Mashal M. ALmutairi**, Farahnaz Movahedzadeh. *Overexpression and Purification of an Acyl Carrier Protein of Mycobacterium tuberculosis*. ***UIC Student Forum 2011***, Chicago.

AWARDS

Van Doren Scholar Award, UIC (2015)

The ASM Student and Post Doctoral Fellow Travel Grant. The American Society of Microbiology and the ICAAC Program Committee, Denver (2013)

UIC Graduate College Student Presenter Award, UIC (2012, 2013, and 2015)

UIC Graduate Student Council Travel Award, UIC (2012, 2013, and 2015)

Travel Fellowship for the RNA 2012 Meeting, RNA 2012 Organizing Committee, Anna Arbor (2012)

King Saud University Scholarship for Graduate studies, King Saud University, Riyadh, Saudi Arabia (2008-2015)

PROFESSIONAL AFFILIATION

American Society of Biochemistry and Molecular Biology (ASBMB)

American Association of Pharmaceutical Scientists (AAPS)

American Society of Microbiology (ASM)

Saudi Pharmaceutical Society (SPS)

RNA Society